Electrochemical Immunosensors for Rapid and Sensitive Detection of Mycotoxins in Grain

by

Lin Lu

A dissertation submitted in partial fulfillment of the requirements for the degree of

Doctor of Philosophy

(Biological Systems Engineering)

at the

University of Wisconsin-Madison

2018

Date of final oral examination: 01/11/2018

The dissertation is approved by the following members of the Final Oral Committee:
Sundaram Gunasekaran, Professor, Biological Systems Engineering
Jae-Hyuk Yu, Professor, Bacteriology
Xudong Wang, Professor, Materials Science and Engineering
Joel Pedersen, Professor, Soil Science
Eric Johnson, Professor, Bacteriology

ABSTRACT

Electrochemical sensing methods are highly attractive for the monitoring of biotoxins, infectious diseases, cancer, and other chemicals and biomarkers, due to their high sensitivity, low cost, simple operation, easy miniaturization by microfabrication, and biocompatibility. Give the chemical nature of mycotoxins and the low action levels in food and feed, the development of mycotoxin monitoring methods has been facing many challenges such as unsatisfactory sensitivity, insufficient specificity, time-consuming, food matrix interference, etc. Deficiencies in any of the above-mentioned aspects is generally considered unacceptable. In addition, random interfering signals arising from non-specific adsorption/ foreign chemicals can cause problems in detection reliability. Therefore, much effort has been put into the modification of working electrode surfaces to improve the electron transfer efficiency and the specific target recognition.

In this dissertation, to provide a user-friendly tool for quantitatively and effectively monitoring mycotoxins level in grains, special attention has been paid to the design and fabrication of electrochemical biosensors for the detection of mycotoxins aflatoxin B1 (AFB1), fumonisin B1 (FB1) and deoxylnivalenol (DON).

We started by designing and fabricating a novel electrochemical immunosensor on screen printed electrode (SPE) platform, with polydiallyldimethylammonium chloride (PDDA), carbon nanotubes (CNTs) and gold nanoparticles (AuNPs) enhanced working electrode surface, which showed excellent sensitivity toward the detection of AfB1. However, a performance stability issue was found with the developed biosensor, which may due to Unoptimized surface

modification. This drove us to further optimize the surface modification strategy based on the same underlying principle. To overcome the issues, we modified the working electrode surface of the SPE with new combinations of conducting polymer polypyrrole (ppy), carbon nanomaterial graphene oxide (GO) and AuNPs. The newly fabricated electrode was immobilized with anti-FB1 and anti-DON antibodies respectively, and tested with respective target toxins. The results for both toxins showed great sensitivity, specificity and reliability, as well as wide linear ranges. The sensitivity for the detection of DON was 8.6 ppb and for FB1 was 4.2 ppb. The linear range for the detection of DON was 0.05 to 1 ppm and for FB1 0.2 to 4.5 ppm, which are comparable to most published research results. The developed biosensor was further examined in real food matrix—spiked corn powder sample. Calibration curves with real corn samples were very similar to those obtained with buffer, for both toxins. The as-prepared electrode was able to maintain performance after being stored in buffer at 4 ˚C for two weeks.

Since in reality, multiple mycotoxins usually co-occur in grain, we proceeded to the next stage：developing a biosensor for simultaneous detection of multiple mycotoxins. ITO coated glass was used to replace SPE as the sensing platform for more convenient fabrication of multiple working electrodes on one single chip. The ITO sensor was incorporated with capillary based microfluidic method to achieve better sensing performance. The ITO immunosensor incorporated with microfluidic devices was capable of detecting two different mycotoxins FB1 and DON in one sample at very low detection limits (97 pg/mL for FB1 and 35 pg/mL for DON).

In summary, the electrochemical immunosensors developed in this PhD work demonstrated high sensitivity and great specificity for the detection of mycotoxins both individually and simultaneously. In particular, the developed double-channel ITO immunosensor

incorporated with microfluidic devices demonstrates a promising potential to be applied on site for rapid and simultaneous mycotoxins monitoring.

ACKNOWLEDGMENTS

First and foremost, I would like to extend my sincere gratitude and appreciation to my Ph.D. advisor and chair of the dissertation committee, Dr. Sundaram Gunasekaran for his guidance and support during the past five years. I thank him for his patient guidance, practical advice and consistent encouragement throughout the work. I am very proud and lucky to have him as my academic advisor.

Many thanks also go to my committee members, Dr. Jae-Hyuk Yu and Dr. Eric Johnson from Department of Bacteriology, Dr. Joel Pedersen from Department of Soil Science, and Dr. Xudong Wang from Department of Materials Science and Engineering, for their guidance and advise.

I would also like to acknowledge Dr. Jay Warrick, for training me with the photolithographic and microfluidic techniques and allowing me to use his lab facility. I would like to thank all my lab members past and present for helping me with my research and day-to-day lab activities. Mainly I like to thank Dr. Rajesh Seenivasan, who helped me with the biosensor design and many electrochemical problems. His inputs were of great value to my project. I like to thank Dr. Yi-cheng Wang for providing the necessary help with graphene oxide synthesis and SEM images. I like to thank Dr. Anu Prathap and Dr. Yuanjie Teng for working together with me to prepare ITO electrodes. I like to thank Jiehao Guna for helping with SEM images.

I am indebted to all the staff in the Department of Biological Systems Engineering at University of Wisconsin-Madison for making my PhD experience a pleasant one.

I am also grateful to the financial support from USDA Hatch (WIS01644) and the Andersons Research Grants Program.

Last but not least, to my parents, for their infinite love and endless support. They have always been by my side when I needed them and have given me strength. I also appreciate the suggestions and encouragement provided by my good friends Yue Wang, Qingqiu Zhao and Lisha Zhao during my PhD study. Once more, I am pleased to express my gratitude to all these great people.

TABLE OF CONTENTS

LIST OF FIGURES

LIST OF TABLES

CHAPTER 1 Introduction and Research Description

1.1 Background and Motivation

1.1.1 Mycotoxins in the food industry

Biotoxins are toxic substances produced by living organisms that may cause severe adverse effects to human and animal health if present in raw and processed food and feed. Based on their biological sources, biotoxins can be further classified into several groups: mycotoxin (produced by fungi), bacterial toxin (produced by bacteria), zootoxin (produced by animals) and phytotoxin (produced by plants) (Zhang et al., 2014).

Mycotoxins are toxic, low molecular weight (usually < 1 kDa) secondary metabolites that occur naturally and unavoidably. They can enter our food chain directly from the use of mycotoxins-contaminated foods or indirectly from the growth of toxigenic fungi on food (Bullerman, 1979). Intake of mycotoxins causes acute or chronic mycotoxicoses to human and animals. Although about 300-400 mycotoxins have been identified currently, only a small portion of them are of significant human and animal health concern. The most important mycotoxins in terms of natural occurrence and toxicity are aflatoxins (AF), ochratoxins(OT), fumonisins(FUM), deoxynivalenol (DON), and zearalenone (ZEA)(Marroquin-Cardona, Johnson, Phillips, & Hayes, 2014).

Aflatoxins are potent, natural toxins produced by *Aspergillus flavus*, *Aspergillus nomius*, or *Aspergillus parasiticus* (Li, Yu, Li, & Wu, 2015), which frequently contaminate foods and animal feedstuffs. In particular, feeds with high concentrations of plant materials, such as peanut, corn, soybean and rice, are more susceptible to mycotoxin contamination(Eivazzadeh-Keihan, Pashazadeh, Hejazi, de la Guardia, & Mokhtarzadeh, 2017). Aflatoxins have caused a significant

problem for the animal feed industry and been an ongoing risk to feed supply security. AFs are of great concern because of their detrimental effects on the health of human and animals such as carcinogenic, mutagenic, teratogenic, and immunosuppressive effects(Rhouati, Catanante, Nunes, Hayat, & Marty, 2016) Six out of 18 different types of aflatoxins that have been identified are considered important and are designated as B1, B2, G1, G2, M1, and M2, respectively. AFB1, one of the most common toxins in foods and feeds, has been classified as a group 1 carcinogen by the International Agency for Research on Cancer of World Health Organization(Pohanka, Malir, Roubal, & Kuca, 2008). Aflatoxins M1 and M2 are hydroxylated products of aflatoxins B1 and B2, respectively, and are associated with cow milk upon ingestion of B1 and B2 aflatoxins' contaminated feed. Moreover, once formed from B1 and B2 forms, aflatoxins M1 and M2 remain stable during milk processing (Dors, Caldas, 2011.).

FB1 and DON are the most prevalent among about 150 related mycotoxins known as trichothecenes that are formed by some species of *Fusarium* fungi. Since *Fusarium* fungi invade crops, their toxic compounds are often found in cereals. FB1 is highly toxic and commonly found in corn and corn-based foods Fumonisin B2 and fumonisin B3 are closely related metabolites of FB1, and may co-occur in lower concentrations in food samples. Some research reported that masked (conjugated) fumonisins bound to a food/feed matrix have been discovered in some food samples and these conjugates are non-extractable in the conjugated forms (Gelderblom et al., n.d.). Acute and chronic toxicity effects of FB1 include esophageal cancer and neural tube defects in humans, and cause carcinogenicity, hepatotoxicity, nephrotoxicity and embryotoxicity in laboratory animals (Foroud & Eudes, 2009).

DON is the most common trichothecene, although it is not a carcinogen to humans, it can cause poisonous health effects such as anorexia, weight loss, malnutrition, endocrine dysfunction and immune alterations (Ran et al., 2013).

ZEA is also produced by some Fusarium species and usually occurs in corn. Although it is not classifiable as carcinogen to humans, it is still a risky mycotoxin due to estrogenic activity along with anabolic effects. OTA is a mycotoxin from *Aspergillus ochraceus* and *Penicillium verrucosum*, and it is dangerous due to its carcinogenic and nephrotoxic activity (Fazekas, Tar, Kovács, & Kovacs, 2005).

Mycotoxins contamination of grains lowers the quality, value, and safety of foods and feeds, resulting in profound economic losses and health risks. Although economic losses caused by mycotoxins are impossible to accurately measure, the mean annual cost of crop losses in the United States due to three major mycotoxins (AF, FUM, and DON)) is estimated over $900 million (CAST, 2003).

Unlike bacterial, viral or other toxic foodborne contaminants, mycotoxins can easily withstand digestion or temperature treatments like cooking and freezing, and retain toxicity in foods (Anderson, Kowtha, & Taitt, 2010). Many mycotoxins are dangerous when present even in trace amounts. Aflatoxin is the one of the most toxic group of mycotoxins. The US Food and Drug Administration (FDA) has established the following action levels (regulation) for AF: 1) 20 parts per billion (ppb) in all products (except milk) for human consumption; 2) 0.5 ppb in dried milk and 0 ppb in liquid milk; 3) 20 ppb in corn for young animals and dairy cattle; and 4) 100 ~ 300 ppb in corn and peanut products in feeds depending on kind and purpose of the animals. The FDA has also recommended maximum FUM levels of 2 to 4 parts per million (ppm) for food intended for human consumption and 5 to 100 ppm for animals. The advisory levels of DON in finished

wheat products for human consumption is 1 ppm (FDA, 2011). Biotic factors, such as grain type and maturity, coupled with the prevailing abiotic factors, such as water content and temperature, and also preservative concentration will influence the safe storage life and the level of mycotoxin contamination.

Among the most important issues facing grain and livestock producers in Wisconsin and elsewhere are preventing mycotoxin contamination of food and feed and reducing the deleterious effects of mycotoxins on livestock. The number one grain crop in Wisconsin is corn. In addition to being a food crop, corn is now increasingly used for biofuel production. Thus, mycotoxins in grains become concentrated in the ethanol production byproduct known as the distillers grain (DG). This makes mycotoxin contamination become a major concern for biofuel producers who sell DG as animal feed to supplement their income. Therefore, the primary need, for everyone involved in the grain industry is to have a reliable method to rapidly assess the grain quality pertaining to mycotoxins.

Some fungi produce more than one toxins and more than one fungal species can infest plants with synergistic effects, variable patterns of contamination have been observed, and when contamination occurs, often multiple toxins are detectable (Miller, 1992). For example, AF and FUM are co-contaminants often found in corn (Castells, Marin, Sanchis, & Ramos, 2008; Sun et al., 2011; Theumer, Lopez, Aoki, Canepa, & Rubinstein, 2008; Theumer, Lopez, Masih, Chulze, & Rubinstein, 2003), milled corn fractions (Castells et al., 2008; Pietri, Bertuzzi, Agosti, & Donadini, 2010; Pietri, Zanetti, & Bertuzzi, 2009), rice and wheat flour (Sun et al., 2011), and malted barley (Pietri et al., 2010); DON, ZEA, and nivalenol in wheat (Muthomi, Ndung'u, Gathumbi, Mutitu, & Wagacha, 2008); patulin, cyclopiazonic acid, penicillic acid, diacetoxyscirpenol (WAREING, 1998) and AF (Eboku, 2010) in cassava; and AF, FUM, OTA,

and ZEA in sows/sow feeds (Carina Maricel Pereyra, 2010). DON and OTA are also common co-contaminants in wheat (Arino, Herrera, Juan, & Estopanan, 2009; Birzele, Prange, & Kramer, 2000; Conkova, Laciakova, Styriak, Czerwiecki, & Wilczynska, 2006; Hajjaji et al., 2006).

Due to these widespread co-occurrences of multiple toxins in food matrices and possible additive or synergistic adverse effects in humans (Carlson et al., 2001; Monbaliu et al., 2009; Theumer et al., 2003), a system to sensitively and simultaneously detect multiple toxins is highly desirable. However, such multi-toxin detection methods are not available on a rapid, easy-to-use and portable biosensor platform.

1.1.2 Analytical methods and commercially available kits for mycotoxins monitoring

Conventional technologies for the detection of mycotoxins include enzyme-linked immunosorbent assay (ELISA), thin layer chromatography (TLC), HPLC and mass spectrometry (MS), which are suitable for detecting even trace levels of toxins (~0.01 to 0.1 ppb) (Afsah-Hejri, Jinap, Arzandeh, & Mirhosseini, 2011; Akiyama, Chen, Miyahara, Toyoda, & Saito, 1996; Dugan, 2005; Monbaliu et al., 2009; Soares, Rodrigues, Freitas-Silva, Abrunhosa, & Venancio, 2010; Sun et al., 2011; Zheng, Humphrey, King, & Richard, 2005). Liquid chromatography-tandem mass spectrometry (LC-MS) method has been recently developed for multi-mycotoxin detection (Ediage, Mavungu, Monbaliu, Peteghem, & Saeger, 2011; Monbaliu et al., 2009). However, these wet chemistry methods are expensive, lab-based, and time-consuming and hence are not suitable for rapid and on-site testing (Lee, Wang, Allan, & Kennedy, 2004). These techniques also need relatively large sample volume, particularly those with LC, making the detection very difficult. Therefore, an easy-to-perform in-field surveillance strategy for sensitive and simultaneous detection of multiple mycotoxins in foods is urgently needed. Such an in-field monitoring system will make detecting toxin contaminations at the farm level a reality enabling implementation of

suitable preventive strategies at the source before the toxins enter our food chain and thereby averting potentially catastrophic health risks and economic losses.

Many USDA's Grain Inspection, Packers and Stockyards Administration (USDA/GIPSA) approved, commercially available test kits for mycotoxin monitoring are based on immunological techniques. These immunological techniques can be further divided into two categories: ELISA and immunoaffinity column-based (IAC) methods. These test kits provide both qualitative and quantitative measurements, and can be used either in the lab or on-site. The advantages of the immunological methods are their ease of use and the short assay time. Especially for those who only wish to know that the toxin concentration in a sample is above or below the toxic levels recommended in animal feed, the immunological test kits are able to provide a quick yes or no answer.

Neogen's AGRI-SCREEN and VERATOX, and AgraQuant from Romer Labs are based on competitive ELISA technology. The test kits are available for AF, DON, FUM, OT and T-2 toxin. Antibodies specific for the target mycotoxin are fixed to the wall of a microwell, and a solution of enzyme conjugated mycotoxins is provided with the kit. The corn extract is mixed with a known amount of the mycotoxin-enzyme solution and placed into the microwell. The mycotoxin from the extracted corn sample and mycotoxin-enzyme conjugate then compete with each other for binding to the antibodies in the microwell. The more mycotoxins in the corn extract, the less mycotoxin-enzyme conjugates bind to the microwell. By adding a colorless substrate to the microwell, the enzyme present in the microwell converts the substrate to a blue colored product; and the intensity of the blue color is proportional to the amount of mycotoxin-enzyme conjugates. Quantitative measurements can be obtained if a spectrophotometer is available.

Vicam's columns use IAC and chromatography technology. The columns are available for AF, DON, FUM, ZEA, OT and T-2 toxin. The columns contain antibody immobilized beads. While the sample extract runs through the affinity column, only target mycotoxins bind to the antibody beads, and other materials in the extract are washed off the column. The mycotoxin is then removed from the column using methanol. Then a fluorometer can be used to determine the concentration of mycotoxins.

Another example of commercial kits in the market is lateral flow based kits. The Agrastrip Aflatoxin test kit provided by Romer Labs is more amenable for field screening and uses lateral flow strips (Lee et al., 2004) but is only semi-quantitative and more susceptible to false positives compared to ELISA.

In summary, there are some commercially available rapid test kits for on-site mycotoxins detection, however, kits from different suppliers could demonstrate remarkable different quality, making the rapid test kits less competitive than traditional HPLC analytical method (Sun, Gu, Li, Yao, & Dong, 2015). In addition, taking ELISA kits as an example, the price of one ELISA kit is as high as $534 from Sigma-Aldrich, which is not quite affordable for large amount screening of mycotoxins.

1.1.3 Electrochemical biosensors

Electrochemical biosensors are an important category of biosensors that are based on electrochemical transduction processes. They offer significant advantages such as high sensitivity, short assay time, straightforward operation, adaptable to microfabrication and so on. These features make electrochemical biosensors highly compatible for a wide range of applications, including food analysis (Baldrich & Garcia-aljaro, 2010; Chen et al., 2013;

Conzuelo et al., 2013) environmental monitoring (Zhang et al., 2014), medical and clinical tests, etc. (Ammida, Micheli, & Palleschi, 2004; Grieshaber, MacKenzie, Vörös, & Reimhult, 2008; Seenivasan, Singh, Warrick, Ahmad, & Gunasekaran, 2017).

Essential criteria for a good electrochemical biosensor include low detection limit, wide working range, great specificity, long shelf life, simplicity, affordability, and rapidness, etc. To satisfy these criteria, electrochemical biosensors have been substantially studied in combination with other technologies for enhanced performance, such as nanotechnology for sensor fabrication and electrode modification, and immunosensing technology for selective target recognition ((Ammida et al., 2004; Chen et al., 2013; Conzuelo et al., 2013; Piermarini, Micheli, Ammida, Palleschi, & Moscone, 2007; Singh et al., 2013; Srivastava et al., 2013).

Immunosensors are known as analytical devices in which antibody serves as a receptor and the selective antibody-antigen binding event is detected and converted into an electric signal by a transducer (e.g., electrochemical transduction in case of an electrochemical sensor), and the signal is then amplified and displayed for further analysis (Luppa, Sokoll, & Chan, 2001). Nowadays, the recognition receptors are not only limited to antibodies, some examples of other receptors include DNA, aptamers, artificial antibody fragments and molecularly imprinted polymers (Campas, Garibo, & Prieto-Simon, 2012; Romanazzo et al., 2010). The flexible choice of receptors increases the opportunity of detecting a variety of targets. Therefore, an electrochemical immunosensor would take advantage of both immunosensors and electrochemical sensors, to achieve high sensitivity and good selectivity simultaneously.

Above discussion demonstrates the high potential of the electrochemical immunosensors for food safety and quality assurance in a variety of foods and agricultural products, in terms of

high sensitivity, specificity, ease of use, time saving and low cost. They are able to satisfy the strict regulatory limits of food contaminants and allow for on-site application due to the portable feature. Compared to traditional sensing system that requires complicated instruments such as HPLC, electrochemical immunosensor is a great alternative that has a promising future.

1.2 Research Description

Taking advantages of the multiple sensing techniques (e.g. electrochemical methods, immunoassay, microfluidic devices, etc.) and novel nanomaterials can drastically improve the performance of biosensors in terms of detection time, sensitivity, specificity, shelf life, etc. These enhancement offer new opportunities for creating ultra-sensitive smart sensing methods that are capable of automatic and remote detection of mycotoxins in grain.

While the opportunities stated above are exciting, the main problem with currently available technologies for mycotoxins detection is minimizing the food matrix interfering while still maintaining high sensitivity, good selectivity and low limit of detection in presence of multiple mycotoxins, which is one major ongoing research effort. Therefore, this research will address the above-mentioned challenges.

The significance of this work is multifold. First, the developed device may find applications in on-site and real-time measurements of multiple mycotoxins concentrations in food complex. Second, the incorporation of microfluidic devices into the electrochemical biosensor will bring the sensing systems toward ultra-sensitive and more reliable sensing. Third, the affordable electrode materials and small consumption of reagents could significantly bring down the cost of

each test. Finally the knowledge obtained from the immobilization of various nanomaterials onto electrodes provides some new insights into the nanomaterial/biomolecules interactions.

The ultimate goal of this project is to develop an affordable and portable biosensor for rapid, sensitive and accurate monitoring of mycotoxin levels in agriculture products, either individually or simultaneously. To be more specific, this dissertation work mainly focuses on electrochemical immuno-biosensors with various working electrode modification strategies to improve the sensing performance. Three different mycotoxins were used as analytes to investigate the effectiveness of the developed electrochemical immunosensors, including Afaltoxin B1 (AFB1), Fumonisin B1 (FB1) and Deoxynivalenol (DON). The developed biosensors in this study are as follows:

(1) PDDA, carbon nanotube (CNT) and AuNPs-modified screen printed electrode (SPE) for the detection of AFB1. (Chapter 3)

(2) Polypyrrole, graphene oxide (GO) and AuNPs-modified SPE for the detection of FB1 and DON. (Chapter 4)

(3) AuNPs-modified indium tin oxide (ITO) electrode incorporated with microfluidic system for simultaneous detection of FB1 and DON. (Chapter 5)

References

Afsah-Hejri, L., Jinap, S., Arzandeh, S., & Mirhosseini, H. (2011). Optimization of HPLC conditions for quantitative analysis of aflatoxins in contaminated peanut. Food Control, 22(3-4), 381-388. doi:DOI 10.1016/j.foodcont.2010.09.007

Akiyama, H., Chen, D. Y., Miyahara, M., Toyoda, M., & Saito, Y. (1996). Simple HPLC determination of aflatoxins B-1, B-2, G(1) and G(2) in nuts and corn. Journal of the Food Hygienic Society of Japan, 37(4), 195-201.

Ammida, N. H. S., Micheli, L., & Palleschi, G. (2004). Electrochemical immunosensor for determination of aflatoxin B1 in barley. Analytica Chimica Acta, 520(1-2), 159-164. doi:10.1016/j.aca.2004.04.024

Anderson, G. P., Kowtha, V. A., & Taitt, C. R. (2010). Detection of Fumonisin B1 and Ochratoxin A in Grain Products Using Microsphere-Based Fluid Array Immunoassays. Toxins, 2(2), 297-309.

Arino, A., Herrera, M., Juan, T., & Estopanan, G. (2009). Comparison of deoxynivalenol, ochratoxin A and aflatoxin B1 levels in conventional and organic durum semolina and the effect of milling. Journal of Food and Nutrition Research, 48(2), 92-99.

Baldrich, E., & Garcia-aljaro, C. (2010). Pathogen Detection Methods: Biosensor Development: Nova Science Pub Inc.

Birzele, B., Prange, A., & Kramer, J. (2000). Deoxynivalenol and ochratoxin A in German wheat and changes of level in relation to storage parameters. Food Additives and Contaminants, 17(12), 1027-1035.

Bullerman, L. B. (1979). Significance of Mycotoxins to Food Safety and Human Health. Journal of Food Protection, 42(1), 65-86.

Campas, M., Garibo, D., & Prieto-Simon, B. (2012). Novel nanobiotechnological concepts in electrochemical biosensors for the analysis of toxins. Analyst, 137(5), 1055-1067. doi:10.1039/C2AN15736E

Carina Maricel Pereyra, L. R. C., Stella Maris Chiacchiera, and Ana María Dalcero. (2010). Fungi and Mycotoxins in Feed Intended for Sows at Different Reproductive Stages in Argentina. Vet Med Int., 2010, 569108-569115. doi:10.4061/2010/569108

Carlson, D. B., Williams, D. E., Spitsbergen, J. M., Ross, P. F., Bacon, C. W., Meredith, F. I., & Riley, R. T. (2001). Fumonisin B-1 promotes aflatoxin B-1 and N-methyl-N '-nitro-nitrosoguanidine-initiated liver tumors in rainbow trout. Toxicology and Applied Pharmacology, 172(1), 29-36. doi:DOI 10.1006/taap.2001.9129

CAST. (2003). Mycotoxins: Risk in plant, animal, and human systems, Executive summary . Ames, IA.

Castells, M., Marin, S., Sanchis, V., & Ramos, A. J. (2008). Distribution of fumonisins and aflatoxins in corn fractions during industrial cornflake processing. International Journal of Food Microbiology, 123(1-2), 81-87. doi:DOI 10.1016/j.ijfoodmicro.2007.12.001

Chen, M., Zhao, C., Chen, W., Weng, S., Liu, A., Liu, Q., . . . Lin, X. (2013). Sensitive electrochemical immunoassay of metallothionein-3 based on K3[Fe(CN)6] as a redox-active signal and C-dots/Nafion film for antibody immobilization. Analyst, 138(24), 7341-7346. doi:10.1039/c3an01351k

Conkova, E., Laciakova, A., Styriak, I., Czerwiecki, L., & Wilczynska, G. (2006). Fungal contamination and the levels of mycotoxins (DON and OTA) in cereal samples from Poland and East Slovakia. Czech Journal of Food Sciences, 24(1), 33-40.

Conzuelo, F., Campuzano, S., Gamella, M., Pinacho, D. G., Reviejo, A. J., Marco, M. P., & Pingarrón, J. M. (2013). Integrated disposable electrochemical immunosensors for the simultaneous determination of sulfonamide and tetracycline antibiotics residues in milk. Biosensors and Bioelectronics, 50(0), 100-105. doi:http://dx.doi.org/10.1016/j.bios.2013.06.019

Dugan, E. A. (2005). The detection of aflatoxins by TLC. Lc Gc North America, 51-51.

Eboku, A. N. K. a. D. (2010). Mould and Aflatoxin Contamination of Dried Cassava Chips in Eastern Uganda: Association with Traditional Processing and Storage Practices. Journal of Biological Sciences, 10(8), 718-729.

Ediage, E. N., Mavungu, J. D. D., Monbaliu, S., Peteghem, C. V., & Saeger, S. d. (2011). A validated multi–analyte LC–MS/MS method for quantification 1 of 25 mycotoxins in cassava flour, peanut cake and maize Samples. J. Ag. and Food Chemistry, (in press).

Grieshaber, D., MacKenzie, R., Vörös, J., & Reimhult, E. (2008). Electrochemical Biosensors - Sensor Principles and Architectures. Sensors, 8(3). doi:10.3390/s80314000

Hajjaji, A., El Otmani, M., Bouya, D., Bouseta, A., Mathieu, F., Collin, S., & Lebrihi, A. (2006). Occurrence of mycotoxins (ochratoxin A, deoxynivalenol) and toxigenic fungi in Moroccan wheat grains: impact of ecological factors on the growth and ochratoxin A production. Molecular Nutrition & Food Research, 50(6), 494-499. doi:10.1002/mnfr.200500196

Lee, N. A., Wang, S., Allan, R. D., & Kennedy, I. R. (2004). A rapid aflatoxin B-1 ELISA: Development and validation with reduced matrix effects for peanuts, corn, pistachio, and soybeans. Journal of Agricultural and Food Chemistry, 52(10), 2746-2755. doi:10.1021/jf0354038

Luppa, P. B., Sokoll, L. J., & Chan, D. W. (2001). Immunosensors—principles and applications to clinical chemistry. Clinica Chimica Acta, 314(1), 1-26. doi:https://doi.org/10.1016/S0009-8981(01)00629-5

Miller, J. D. (1992). Fungi as Contaminants in Indoor Air. Atmospheric Environment Part a-General Topics, 26(12), 2163-2172.

Monbaliu, S., Van Poucke, C., Detavernier, C. l., Dumoulin, F. d. r., Van De Velde, M., Schoeters, E., . . . De Saeger, S. (2009). Occurrence of Mycotoxins in Feed as Analyzed by a Multi-Mycotoxin LC-MS/MS Method. Journal of Agricultural and Food Chemistry, 58(1), 66-71. doi:10.1021/jf903859z

Muthomi, J. W., Ndung'u, J. K., Gathumbi, J. K., Mutitu, E. W., & Wagacha, J. M. (2008). The occurrence of Fusarium species and mycotoxins in Kenyan wheat. Crop Protection, 27(8), 1215-1219. doi:10.1016/j.cropro.2008.03.001

Piermarini, S., Micheli, L., Ammida, N. H., Palleschi, G., & Moscone, D. (2007). Electrochemical immunosensor array using a 96-well screen-printed microplate for aflatoxin B1 detection. Biosens Bioelectron, 22(7), 1434-1440. doi:10.1016/j.bios.2006.06.029

Pietri, A., Bertuzzi, T., Agosti, B., & Donadini, G. (2010). Transfer of aflatoxin B1 and fumonisin B1 from naturally contaminated raw materials to beer during an industrial brewing process. Food Additives and Contaminants Part a-Chemistry Analysis Control Exposure & Risk Assessment, 27(10), 1431-1439. doi:Doi 10.1080/19440049.2010.489912

Pii 923380521

Pietri, A., Zanetti, M., & Bertuzzi, T. (2009). Distribution of aflatoxins and fumonisins in dry-milled maize fractions. Food Additives and Contaminants Part a-Chemistry Analysis Control Exposure & Risk Assessment, 26(3), 372-380. doi:Doi 10.1080/02652030802441513

Pii 908706643

Romanazzo, D., Ricci, F., Volpe, G., Elliott, C. T., Vesco, S., Kroeger, K., . . . Palleschi, G. (2010). Development of a recombinant Fab-fragment based electrochemical immunosensor for deoxynivalenol detection in food samples. Biosensors and Bioelectronics, 25(12), 2615-2621. doi:https://doi.org/10.1016/j.bios.2010.04.029

Seenivasan, R., Singh, C. K., Warrick, J. W., Ahmad, N., & Gunasekaran, S. (2017). Microfluidic-integrated patterned ITO immunosensor for rapid detection of prostate-specific membrane antigen biomarker in prostate cancer. Biosens Bioelectron, 95, 160-167. doi:10.1016/j.bios.2017.04.004

Singh, C., Srivastava, S., Ali, M. A., Gupta, T. K., Sumana, G., Srivastava, A., . . . Malhotra, B. D. (2013). Carboxylated multiwalled carbon nanotubes based biosensor for aflatoxin detection. Sensors and Actuators B: Chemical, 185, 258-264. doi:10.1016/j.snb.2013.04.040

Soares, C., Rodrigues, P., Freitas-Silva, O., Abrunhosa, L., & Venancio, A. (2010). HPLC method for simultaneous detection of aflatoxins and cyclopiazonic acid. World Mycotoxin Journal, 3(3), 225-231. doi:Doi 10.3920/Wmj2010.1216

Srivastava, S., Kumar, V., Ali, M. A., Solanki, P. R., Srivastava, A., Sumana, G., . . . Malhotra, B. D. (2013). Electrophoretically deposited reduced graphene oxide platform for food toxin detection. Nanoscale, 5(7), 3043-3051. doi:10.1039/c3nr32242d

Sun, G., Wang, S., Hu, X., Su, J., Zhang, Y., Xie, Y., . . . Wang, J. S. (2011). Co-contamination of aflatoxin B-1 and fumonisin B-1 in food and human dietary exposure in three areas of China. Food Additives and Contaminants Part a-Chemistry Analysis Control Exposure & Risk Assessment, 28(4), 461-470. doi:Doi 10.1080/19440049.2010.544678

Theumer, M. G., Lopez, A. G., Aoki, M. P., Canepa, M. C., & Rubinstein, H. R. (2008). Subehronic mycotoxicoses in rats. Histopathological changes and modulation of the sphinganine to sphingosine (Sa/So) ratio imbalance induced by Fusarium verticillioides culture material, due to the coexistence of aflatoxin B1 in the diet. Food and Chemical Toxicology, 46(3), 967-977. doi:DOI 10.1016/j.fct.2007.10.041

Theumer, M. G., Lopez, A. G., Masih, D. T., Chulze, S. N., & Rubinstein, H. R. (2003). Immunobiological effects of AFB1 and AFB1-FB1 mixture in experimental subchronic mycotoxicoses in rats. Toxicology, 186(1-2), 159-170. doi:Pii S0300-483x(02)00603-0

WAREING, P. W., WESTBY, A., GIBBS, J.A., ALLOTEY, L.T. and HALM, M. (1998). Fungal and mycotoxin contamination of kokonte, a dried cassava product in Ghana. International Journal of Food Science and Technology, 34, 5082.

Zhang, Z., Yu, L., Xu, L., Hu, X., Li, P., Zhang, Q., . . . Feng, X. (2014). Biotoxin sensing in food and environment via microchip. ELECTROPHORESIS, 35(11), 1547-1559. doi:10.1002/elps.201300570

Zheng, Z. M., Humphrey, C. W., King, R. S., & Richard, J. L. (2005). Validation of an ELISA test kit for the detection of total aflatoxins in grain and grain products by comparison with HPLC. Mycopathologia, 159(2), 255-263. doi:DOI 10.1007/s11046-004-8666-0

A Guide for Grain Elevators, Feed Manufacturers, Grain Processors and Exporters National Grain and Feed Association FDA Regulatory Guidance for Mycotoxins A Guide for Grain

Elevators, Feed Manufacturers, Grain Processors and Exporters by National Grain and Feed Association. (2011).

Anderson, G. P., Kowtha, V. A., & Taitt, C. R. (2010). Detection of fumonisin b1 and ochratoxin a in grain products using microsphere-based fluid array immunoassays. *Toxins (Basel)*, *2*(2), 297–309. https://doi.org/10.3390/toxins2020297

Dorokhin, D., Haasnoot, W., Franssen, M. C. R., Zuilhof, H., & Nielen, M. W. F. (2011). Imaging surface plasmon resonance for multiplex microassay sensing of mycotoxins. *Analytical and Bioanalytical Chemistry*, *400*(9), 3005–3011. https://doi.org/10.1007/s00216-011-4973-8

Dors, G., Caldas, S., … V. F.-A., & 2011, undefined. (n.d.). Aflatoxins: Contamination, analysis and control. *Intechopen.com*. Retrieved from https://www.intechopen.com/download/pdf/20401

Eivazzadeh-Keihan, R., Pashazadeh, P., Hejazi, M., de la Guardia, M., & Mokhtarzadeh, A. (2017). Recent advances in Nanomaterial-mediated Bio and immune sensors for detection of aflatoxin in food products. *TrAC Trends in Analytical Chemistry*, *87*, 112–128. https://doi.org/10.1016/j.trac.2016.12.003

Fazekas, B., Tar, A., Kovács, M., & Kovacs, M. (2005). Aflatoxin and ochratoxin A content of spices in Hungary. *Food Addit Contam*, *22*(9), 856–863. https://doi.org/10.1080/02652030500198027

Foroud, N. A., & Eudes, F. (2009). Trichothecenes in Cereal Grains. *International Journal of Molecular Sciences*, *10*(1), 147–173. https://doi.org/10.3390/ijms10010147

Gelderblom, W. C., Marasas Wf Fau - Lebepe-Mazur, S., Lebepe-Mazur S Fau - Swanevelder, S., Swanevelder S Fau - Vessey, C. J., Vessey Cj Fau - Hall, P. de la M., Hall Pde, L., & Toxicology. (n.d.). Interaction of fumonisin B(1) and aflatoxin B(1) in a short-term carcinogenesis model in rat liver, (0300–483X (Print)).

Kadir, M. K. A., & Tothill, I. E. (2010). Development of an electrochemical immunosensor for fumonisins detection in foods. *Toxins*. https://doi.org/10.3390/toxins2040382

Kadota, T., Takezawa, Y., Hirano, S., Tajima, O., Maragos, C. M., Nakajima, T., … Sugita-Konishi, Y. (2010). Rapid detection of nivalenol and deoxynivalenol in wheat using surface plasmon resonance immunoassay. *Analytica Chimica Acta*, *673*(2), 173–178. https://doi.org/10.1016/J.ACA.2010.05.028

Li, Z. Z., Yu, Y., Li, Z. Z., & Wu, T. (2015). A review of biosensing techniques for detection of trace carcinogen contamination in food products. *Anal Bioanal Chem*, *407*(10), 2711–2726. https://doi.org/10.1007/s00216-015-8530-8

Marroquin-Cardona, A. G., Johnson, N. M., Phillips, T. D., & Hayes, A. W. (2014). Mycotoxins in a changing global environment--a review. *Food Chem Toxicol*, *69*, 220–230. https://doi.org/10.1016/j.fct.2014.04.025

Pohanka, M., Malir, F., Roubal, T., & Kuca, K. (2008). Detection of Aflatoxins in Capsicum Spice Using an Electrochemical Immunosensor. *Analytical Letters*, *41*(13), 2344–2353. https://doi.org/10.1080/00032710802350518

Raj, M. A., & John, S. A. (2013). Fabrication of Electrochemically Reduced Graphene Oxide Films on Glassy Carbon Electrode by Self-Assembly Method and Their Electrocatalytic Application. *The Journal of Physical Chemistry C*, *117*(8), 4326–4335. https://doi.org/10.1021/jp400066z

Ran, R., Wang, C., Han, Z., Wu, A., Zhang, D., & Shi, J. (2013). Determination of deoxynivalenol (DON) and its derivatives: Current status of analytical methods. *Food*

Control, *34*(1), 138–148. https://doi.org/10.1016/j.foodcont.2013.04.026

Rhouati, A., Catanante, G., Nunes, G., Hayat, A., & Marty, J. L. (2016). Label-Free Aptasensors for the Detection of Mycotoxins. *Sensors (Basel)*, *16*(12). https://doi.org/10.3390/s16122178

Seenivasan, R., Singh, C. K., Warrick, J. W., Ahmad, N., & Gunasekaran, S. (2017). Microfluidic-integrated patterned ITO immunosensor for rapid detection of prostate-specific membrane antigen biomarker in prostate cancer. *Biosensors and Bioelectronics*. https://doi.org/10.1016/j.bios.2017.04.004

Sun, D.-D., Gu, X., Li, J.-G., Yao, T., & Dong, Y.-C. (2015). Quality evaluation of five commercial enzyme linked immunosorbent assay kits for detecting aflatoxin b1 in feedstuffs. *Asian-Australasian Journal of Animal Sciences*, *28*(5), 691–6. https://doi.org/10.5713/ajas.14.0868

Wang, C., Qian, J., An, K., Huang, X., Zhao, L., Liu, Q., … Wang, K. (2017). Magneto-controlled aptasensor for simultaneous electrochemical detection of dual mycotoxins in maize using metal sulfide quantum dots coated silica as labels. *Biosens Bioelectron*, *89*(Pt 2), 802–809. https://doi.org/10.1016/j.bios.2016.10.010

Yang, J., & Gunasekaran, S. (2013). Electrochemically reduced graphene oxide sheets for use in high performance supercapacitors. *Carbon*, *51*, 36–44. https://doi.org/10.1016/j.carbon.2012.08.003

Yi, C., Qi, S., Zhang, D., & Yang, M. (2010). Covalent conjugation of multi-walled carbon nanotubes with proteins. *Methods Mol Biol*, *625*, 9–17. https://doi.org/10.1007/978-1-60761-579-8_2

Yue, S., Jie, X., Wei, L., Bin, C., Dou Dou, W., Yi, Y., … Tiesong, Z. (2014). Simultaneous detection of ochratoxin a and fumonisin b1 in cereal samples using an aptamer-photonic crystal encoded suspension array. *Analytical Chemistry*, *86*(23), 11797–11802. https://doi.org/10.1021/ac503355n

CHAPTER 2 Literature Review

1.1 Introduction

This comprehensive literature review will give an overview of biosensors with a focus on electrochemical biosensors, including basic concepts and classification, as well as scientific applications in mycotoxin detection. In this review, some limitations of electrochemical biosensors will also be discussed, and improvement strategies based on nanomaterials and microfluidic systems will be discussed in detail.

2.1 Electrochemical Biosensors Basics

2.1.1 Biosensors definition and classification

Biosensors are analytical devices designed for rapid and sensitive detection of analytes, such as a microorganism, a biomolecule, a whole cell, a biostructure etc. (Alonso-Lomillo, Domínguez-Renedo, & Arcos-Martínez, 2010; Su, Jia, Hou, & Lei, 2011; Zourob, Elwary, & Turner, 2008). Fig. 2.1 shows that a typical biosensor usually consists of three important elements, a biorecognition element (bioreceptor), a transducer, and a signal display (electronic system). The bioreceptor is a component which uses biomolecules or biomarkers that specifically interact with the analyte of interest. The biological recognition event produces a signal that is picked up by a transducer, and then being converted into a measurable electric signal relative to the concentration of the analyte under study. Finally the electric signal is amplified and processed to be displayed for further analysis (Ivnitski, Abdel-Hamid, Atanasov, & Wilkins, 1999; Mello & Kubota, 2002; J. Wang et al., 1997).

Biosensors can be classified either based on the bioreceptor types or according to the transduction processes. As shown in Fig. 2.1, biorecognition components include nucleic acids,

enzymes, antibodies and cells. Based on different transducers, biosensors could also be classified as electrochemical biosensors, optical biosensors, mass-sensitive biosensors, thermal biosensors and electrical biosensors.

Development of a biosensor is highly interdisciplinary, and involves the collaborative efforts of physics, chemistry, biology, medical, and engineering, etc.

In food safety and quality assurance point of view, biosensors are capable of testing the presence and concentration of food contaminants, detecting gasses generated by spoiled food, and monitoring the growth of microorganisms in fresh food. In case of environmental safety (Campuzano, Yáez-Sedeño, & Pingarrón, 2017; Ivnitski et al., 1999; Z. Li, Yu, Li, & Wu, 2015; Mello & Kubota, 2002), biosensors could be used to detect pollution (e.g. pathogens, heavy metals, toxic chemicals, etc.) in air, water, and soil (J. Wang et al., 1997).

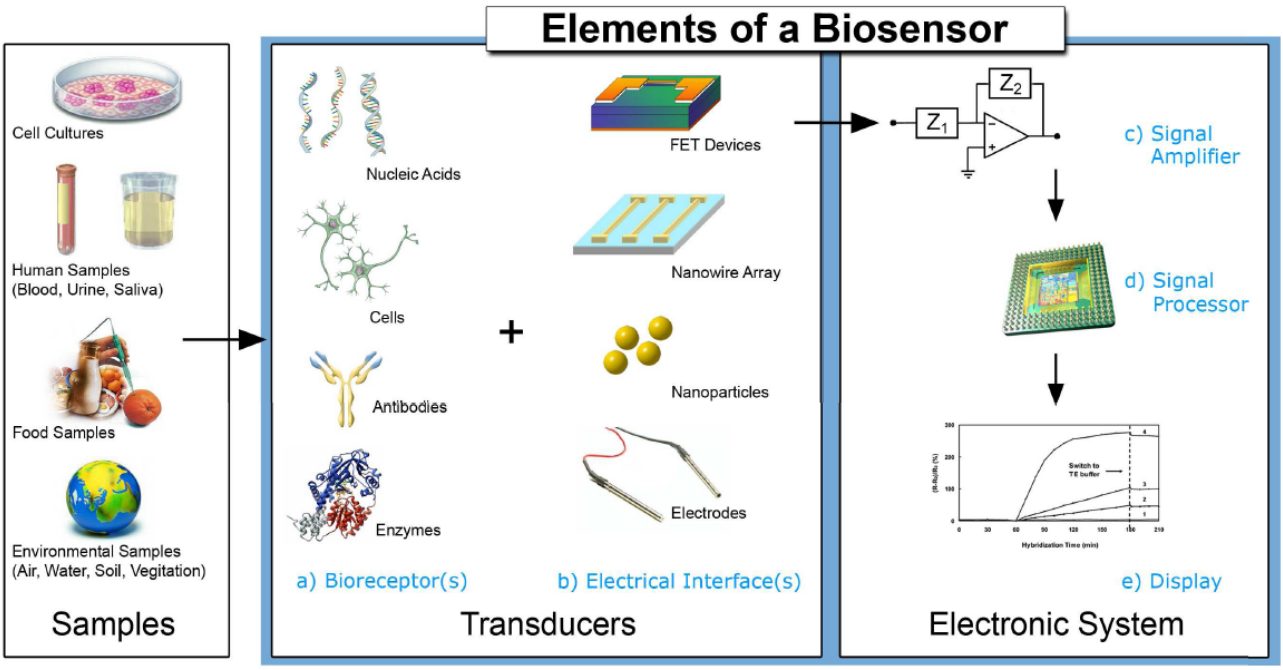

Figure 2.1 Essential elements of a typical biosensor (Grieshaber, MacKenzie, Vörös, & Reimhult, 2008)

2.1.2 Electrochemical techniques in biosensor

Electrochemical technique is one well-established transduction technique used in biosensors, which are normally based on enzymatic catalysis of a chemical reaction that involves electron transfer (Campuzano et al., 2017; "Chapter 10 Electrochemical Detection (Amperometry, Voltammetry and Coulometry),").

A widely used typical electrochemical cell consists of three electrodes: a working electrode, a counter electrode and a reference electrode. Among various electrochemical technologies, voltammetry and amperometry are definitely the most commonly utilized techniques that involve the application of a changing potential (voltammetry) or a fixed potential (amperometry) to a working electrode, followed by measurement of the current resulting from the reaction of analyzed species at the working electrode. Depending on the method how we apply the potential, the working electrode types, voltammetry techniques are further categorized as cyclic voltammetry, differential pulsed voltammetry, linear sweep voltammetry, etc.

2.2 Nanomaterials for Electrochemical Based Mycotoxin Biosensors

In recent years, nanomaterials such as carbon nanomaterials, metallic nanoparticles, magnetic nanoparticles, silica nanoparticles, quantum dots, and complex nanocomposite have been extensively employed with biosensor devices to enhance sensitivity, selectivity, reliability, etc. (Farré, Kantiani, Pérez, Barceló, & Barceló, 2009; Palchetti & Mascini, 2012). When it comes to electrochemical immunosensors, many superior features of nanomaterials, such as high conductivity, large surface area, great stability and biocompatibility, and easy to functionalize, etc. have facilitated dramatically improved sensor performance. For instance, CNTs have been used to improve the electrocatalytic properties, increase the surface area, and increase the

conductivity of working electrode. A ZEA microfluidic immunosensor and an enzymatic oxidase biosensor for aflatoxin based on MWCNTs have been reported (S. c. Li, Chen, Cao, Yao, & Liu, 2011; Panini, Bertolino, Salinas, Messina, & Raba, 2010). Herein we review recent advances of nanomaterial application in mycotoxins detection, with emphasis on carbon nanomaterials and metallic nanoparticles.

2.2.1 Carbon nanomaterials

Carbon nanomaterials mainly refer to graphene, graphene oxide (GO), reduced graphene oxide (RGO) and carbon nanotubes (CNTs).

Graphene is a two-dimensional carbon material that consists of a single layer of carbon atoms arranged in a hexagonal lattice. Excellent mechanical strength and electrical characteristics make graphene a good material for biosensor fabrication. However, graphene sheets tend to restack to form graphite and it is difficult to disperse in water due to the hydrophobic nature, which sometimes limits its application in laboratory (H. Guo, 2009; R.Saito, M.Fujita, G.Dresselhaus, & Dresselhaus, 1992). Graphene oxide (GO), a graphene derivative, has oxygen-containing functional groups on the surface (e.g., epoxides, carboxyl, carbonyl), which significantly improves the dispersion of GO sheets in polar solvents (Tan, Ambrosi, Khezri, Webster, & Pumera, 2014; Tiwari, Gupta, Pandey, & Mishra, 2015; Toh, Loh, Kamarudin, & Daud, 2014). But the electrical conductivity of GO is relatively low as the disturbance of its sp2 bonding network (Luo, Lu, Somers, & Johnson, 2009; Marcano et al., 2010). To recover the electrical conductivity, removal of those oxygen-containing surface functional groups through the reduction of GO sheets is necessary (Kuila et al., 2011; Pumera, 2011). The reduction could be carried out either electrochemically (Huang et al., 2013; Raj & John, 2013; X. Zhang, Zhang, Chen, Sun, & Ma,

2012) or chemically (Alazmi, Rasul, Patole, & Costa, 2016). Therefore, people can choose the appropriate graphene-related materials to conduct research based on their need. Fig. 2.2 shows one example of electrochemical biosensor using RGO as a electrode modification material (Srivastava et al., 2013). Due to the large surface area and excellent electrochemical properties, RGO was electrochemically deposited on an indium tin oxide (ITO) electrode to improve the electrode surface, and serves as the base for antibody immobilization as well.

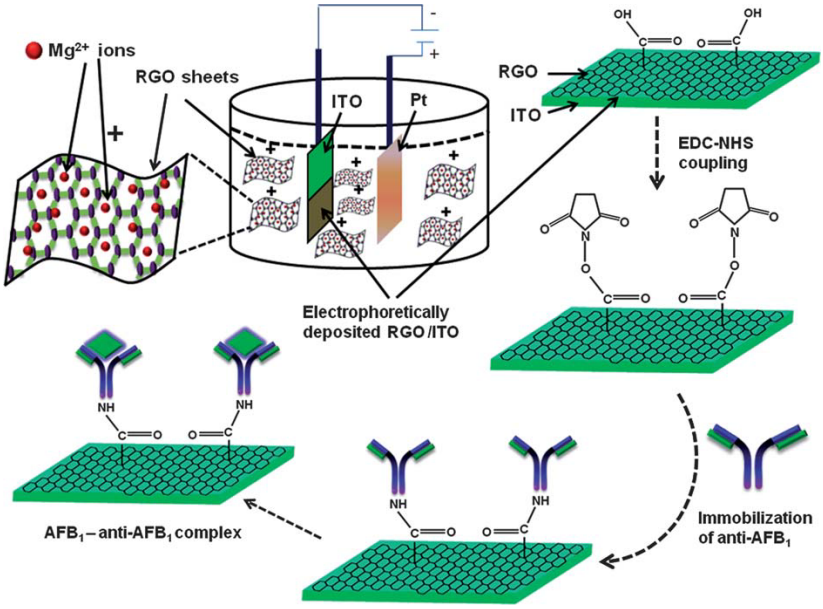

Figure 2.2 Schematic diagram of an BSA-anti-AFB1/RGO/ITO electrochemical immunosensor (Srivastava et al., 2013)

Since the discovery of CNTs in 1991 (S.Iijima, 1991), it has emerged as one of the most promising materials for the development of nanoscale biosensors. Carbon nanotubes are allotropes of carbon with diameters in the order of a few nanometers, while their length extends up to several millimeters. In addition to their large surface area, CNTs exhibit superior electrical conductivity, chemical inertness and mechanical strength (Ajayan, 1999). They are also one of

the strongest and stiffest materials, with tensile strength on the order of 63 GPa, and elastic modulus in the 1 TPa range (M.-F.Yu et al., 2000). Most of these unique properties are due to the bonding structures of the carbon atoms and the perfect alignment of the lattice along the length of the nanotubes. The electronic properties are believed to due to the diameter and helicity of the nanotubes. The structures of CNTs depend on how the graphite sheets are rolled up into hollow core tubes, which determines the helicity of CNTs. These structures are classified as armchair, zigzag and chiral (R.Saito et al., 1992). The armchair CNTs are conductive, while zigzag and chiral CNTs can be either conductive or semiconductive (N.Hamada, Sawada, & Oshiyama, 1992). Furthermore, depending on the number of rolled up graphite sheets, CNTs are defined as single-walled carbon nanotubes (SWCNTs) and multi-walled carbon nanotubes (MWCNTs). MWCNTs are made of nanotubes with many different diameters and helicity, with most of the nanotubes being conductive (Ajayan, 1999; T.W.Ebbesen, 1997). In addition, CNTs have high surface specificity and allow multiple modifications with functional groups for sensitive protein recognition. The superior electrical properties and biological compatibilities allow for the development of CNT-based sensors for diagnostics and biorecognition purposes. For instance, CNT-based Immunosensors have been widely studied in recent years.

For a potential immunosensing application, the surface of the CNTs needs to be functionalized with functional groups for the immobilization of antibodies through stable covalent bonding (R.J.Chen et al., 2003). Among various chemical modifications of CNTs, carboxylated MWCNT (COOH-MWCNT) have gained increasing attention of recent studies. The primary reason for the great popularity of this specifically modified type of CNTs is that COOH or carboxyl group attached to the MWCNTs can provide reactive sites for the covalent attachment of proteins through amidation process (T.Ramanathan, F.T.Fisher, R.S.Ruoff, & Brinson, 2005). Amidation

process between the amino group on the antibodies and the carboxyl groups on the CNTs is often facilitated by coupling agent (N.Shao, S.Lu, E.Wickstrom, & B.Panchapakesan, 2007). 1-(3-(dimethylamino)- propyl)-3-ethylcarbodiimide hydrochloride (EDC) is a widely used zero length cross-linker that reacts with carboxyl groups to form amine reactive intermediate. EDC then reacts with an amine group to produce a stable amide bond (Y.Gao & I.Kyratzis, 2008). However, EDC is not stable and suffers from low coupling efficiency due to hydrolysis of the intermediate in aqueous environment. Therefore, this process is complemented with N-hydroxysuccinimide (NHS) to suppress hydrolysis, and increase the efficiency of the cross-linking (D.Sehgal & I.K.Vijay, 1994). The EDC/NHS chemistry is usually used to facilitate the covalent bonding between the carboxyl groups on the surface of the CNTs and the primary amine groups ($–NH_2$) of antibodies through stable amidation process.

With antibodies successfully immobilized onto COOH-CNT surface, further actions could be taken to capture target that specifically recognized by the antibodies, which is the basic principle for an immunosensor to detect target toxins/bacteria/biomolecules.

2.3.2 Nanoparticles

Most nanoparticles exhibit unique mechanical, optical, magnetic or electrical properties compared to their bulk materials, effectively filling the gap between bulk materials and microstructures at atomic or molecular scales (Eivazzadeh-Keihan, Pashazadeh, Hejazi, de la Guardia, & Mokhtarzadeh, 2017). Especially those made from metal, semiconductors and oxides have been significantly utilized in biosensors, due to their special physical, chemical or biological properties. For instance, gold nanoparticles could be used as biomolecules immobilized via S-H bond on immunosensors. Silver and gold nanoparticles are used to fabricate

optical sensors due to their unique size-dependent color changing ability. Some nanoparticles could serve as catalysts in chemical reactions, and some metal nanoparticles could also be used for signal amplification (Z. Li et al., 2015; X. Wang, Niessner, Tang, & Knopp, 2016; Y.-C. Wang, Lu, & Gunasekaran, 2015). Table 2.1 summarizes selected representative literature of nanoparticles application in mycotoxin electrochemical biosensors.

Lin et al. (Lin et al., 2015) demonstrated an ultrasensitive amperometric immunoassay for AFB1 detection. The sensor was based on enzymatic hydrolysate-triggered displacement reaction with multifunctional silica particles doped with HRP-thionine conjugate. The LOD went as low as 2.7 pg/mL and the working range was from 3 pg/mL to 20 ng/mL. However, the nanocomposite preparation and the sensing procedure are quite time consuming.

Tang's group (Tang et al., 2014) reported a novel immunosensing platform using competitive displacement reaction between AFB1 and its pseudo-hapten polyethylenimine (PEI) for anti-AFB1 antibody (Fig. 2.3). Glucose molecules were encapsulated in the pores of PEI-coated mesoporous silica nanocontainers (PEI-MSN) by Antibody-AuNPs (molecular gates). Since AFB1 has higher affinity with antibody-AuNPs complex over PEI, the addition of target AFB1 molecules triggered the opening of molecular gates, thus the encapsulated glucose molecules were released and measured by a portable glucometer. The glucose concentration is proportional to AFB1 concentration in the sample, allowing for the determination of AFB1 in a wide range from 0.01 to 15 ng/mL.

Table 2.1 Application of nanoparticles in mycotoxin electrochemical biosensors

Mycotoxin	Nanoparticles	Working range (ng/mL)	LOD (ng/mL)	Reference
AFB1	AuNPs + SiO_2 NPs	0.003-20	0.0027	(Lin et al., 2015)
AFB1	AuNPs	0.006-5	0.0023	(Zhuang, Tang, Lai, Xu, & Tang, 2015)
AFB1	AuNPs	0.01-15	0.005	(Tang et al., 2014)
OTA	AuNPs	0.04-40	0.008	(Evtugyn et al., 2013)
OTA	AgNPs	0.028-4	0.02	(Karimi, Hayat, & Andreescu, 2017)
FB1	AuNPs	72-720000	1.44	(Chen et al., 2015)

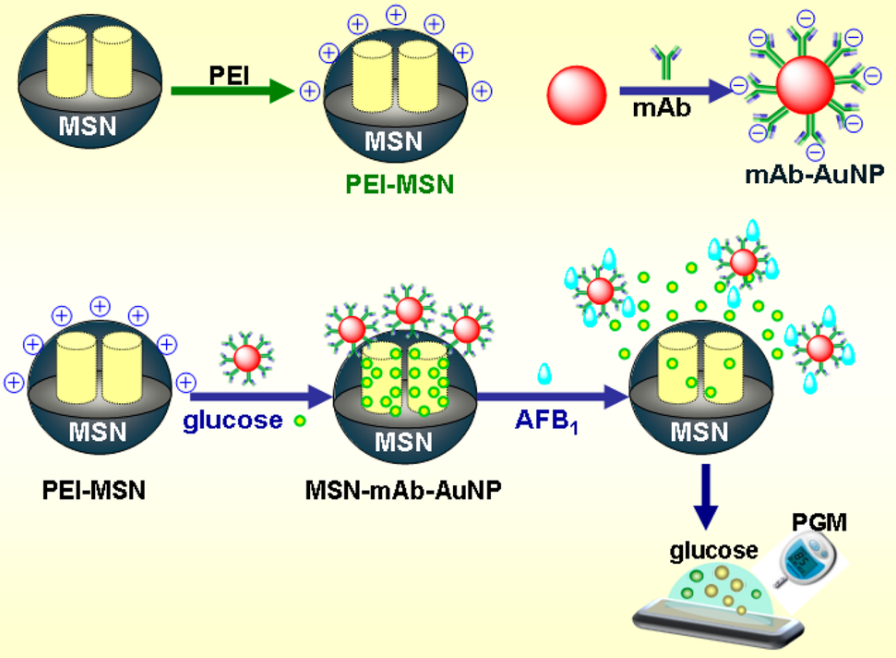

Figure 2.3 Detection principle of Tang's AFB1 immunosensing platform (Tang et al., 2014)

Evtugyn et al. (Evtugyn et al., 2013) developed an impedimetric aptasensor for OTA detection based on aptamer-coated AuNPs stabilized by a dendrimeric polymer Boltorn H30®. The interaction between OTA and the aptamer induced the conformational switch of the aptamer from linear to guanine quadruplex, resulting the consolidation of the surface layer and an increase of the charge transfer resistance.

Most recently, Karimi et al. (Karimi et al., 2017) reported an electrochemical biosensor for quantitative investigation of OTA with the aid of ssDNA-conjugated silver nanoparticles. The specific binding of ssDNA-AgNPs to targets would induce changes in collision frequency, attributed to the changes of electron transfer efficiency between the electrode and AgNPs. The obtained detection limit was 0.5 nM.

Chen et al. (Chen et al., 2015) presented an aptasensor coupled with electrochemical impedance spectroscopy for the detection of FB1 in maize. In this sensor, AuNPs were used as anchors of FB1 aptamers that would specifically recognize target FB1 toxins. Increasing resistance was observed upon binding of FB1 to aptamers, hence the FB1 concentration could be determined based on the magnitude of resistance changes.

2.3 Microfluidic devices for Electrochemical Based Mycotoxin Biosensors

Microfluidics refer to manipulation and control of a very small amount of fluids in fine channels that are typically in micrometer scale. This technique allows the reaction to happen with minimal amount of sample and reagent consumption, high-throughput, short assay time, and multiplexed tests to run simultaneously, which offers alternative and affordable tools for large scale on-site screening of analyses with reduced labor and resource input (Escarpa, 2014; Guo, Feng, Fang, Xu, & Lu, 2015; Soares et al., 2014; Z. Zhang et al., 2014). Nowadays, more and more scientists are aware of the superior capability of microfluidics and began to take advantage of it by combining microfluidics with existing sensing and analytical methods to boost the performance of biosensors. Another merit of microfluidic devices is that they have vast advantages in integrating all steps (sample pre-treatment, target separation and enrichment, target detection) of a biosening procedure, which arouses the opportunity for fabricating a highly compact portable sensor.

Although latest development of microfluidics in the biomedical field is thriving and has been reported by many researchers (de Souza, Alves, & Coltro, 2012; Sakai, Fujiwara, Arai, Yu, & Tatsuma, 2009; Seenivasan, Singh, Warrick, Ahmad, & Gunasekaran, 2017), application of microfluidic technique in food industry receives relative less attention. Only a very limited number of literature addressed the integration of microfluidics in existing biosensors for the

mycotoxin monitoring, among which only two studies used electrochemical techniques. Table 2.2 shows typical microfluidic based biosensors in determination of mycotoxins in last five years (2013 to 2017).

Novo's group (Novo et al., 2013) reported a biosensor device integrating microfluidics with ELISA and chemiluminescence for determining OTA in wine and beer. The biosensor is capable of simultaneously testing both the control and desired samples via a U-shaped microfluidic channel. The device requires 10 mL sample volume and a 45 min analysis time. The sensor could achieve the limit of detection at 0.1 and 2 ng/mL for beer and red wine extracts, respectively.

Olcer et al. (Olcer et al., 2014) reported a new sensing platform for the detection of DON in wheat called real-time electrochemical profiling (REP), which integrates microfluidics in an electrochemical immunosening platform. The applied potential to the sensing chip was 0.1 V followed by continuous current measurement. The microfluidic electrochemical profiling method was evaluated by assaying DON-spiked wheat samples and comparing the results with conventional ELISA method. A R^2 value of 0.97 was observed, indicating the reliability of the developed sensor.

Uludag et al. (Uludag et al., 2016) developed a completely automated lab-on-a-chip system for aflatoxin detection based on a competition immunoassay by combining microfluidic electrochemical chips and HPLC. The biochip contains 6 working electrodes with shared reference and counter electrodes. AFB1 spiked wheat and fig samples were tested and the outcome was compared with ELISA and HPLC results for confirmation. A R^2 value of 0.96 confirms the success of the biochip sensor.

Table 2.2 Application of microfluidics in mycotoxin biosensors

Mycotoxin	Sensing method	Working range (ng/mL)	LOD	Reference
OTA	ELISA + chemilluminescence	-	0.1 ng/mL (beer) 2 ng/mL (red wine)	(Novo, Moulas, França Prazeres, Chu, & Conde, 2013)
AF	Distance-readout microfluidic chip using target responsive hydrogel	0.25-40 μM	1.77 nM	(Ma et al., 2016)
DON	Microfluidic based real-time electrochemical immunoassay	6.25-250 ng/mL	6.25 ng/mL	(Olcer et al., 2014)
AF	Nano liquid chromatography on a chip	0.048-16 ng/g	0.004-0.008 ng/g	(Liu, Lin, Chan, Lin, & Fuh, 2013)
OTA	Aptamer + surface enhanced Raman spectroscopy	-	2.5 μM	(Galarreta, Tabatabaei, Guieu, Peyrin, & Lagugné-Labarthet, 2013)
AF	Microfluidic with automated MiSens electrochemical immunosensor	5.7-8.1 g/g	0.08-0.65 ppb	(Uludag et al., 2016)
OTA, DON, AFB1	microfluidic + photoconductors coupled with fluorescence microscopy	-	100 ng/mL (OTA & DON), 3 ng/mL (AFB1)	(Soares et al., 2017)

Most recently, Soares et al. reported a negative pressure-driven microfluidic multiplexed array using photoconductors coupled with fluorescence microscopy for simultaneous detection of three different mycotoxins, OTA, DON and AFB1. The assay was completed in 20 min with LOD of 100 ng/ml for OTA and DON and 3 ng/ml for AFB1(Soares et al., 2017).

References

Ajayan, P. M. (1999). Nanotubes from carbon. *Chem Rev, 99*, 1787-1800.

Alazmi, A., Rasul, S., Patole, S. P., & Costa, P. M. F. J. (2016). Comparative study of synthesis and reduction methods for graphene oxide. *Polyhedron, 116*(Supplement C), 153-161. doi:https://doi.org/10.1016/j.poly.2016.04.044

Alonso-Lomillo, M. A., Domínguez-Renedo, O., & Arcos-Martínez, M. J. (2010). Screen-printed biosensors in microbiology; a review. *Talanta, 82*(5), 1629-1636. doi:10.1016/j.talanta.2010.08.033

Campuzano, S., Yáez-Sedeño, P., & Pingarrón, J. (2017). Electrochemical Affinity Biosensors in Food Safety. *Chemosensors, 5*(1), 8. doi:10.3390/chemosensors5010008

. Chapter 10 Electrochemical Detection (Amperometry, Voltammetry and Coulometry). (1990). In P. R. Haddad & P. R. Haddad (Eds.), *Journal of Chromatography Library* (Vol. 46, pp. 291-321): Elsevier.

Chen, X., Huang, Y., Ma, X., Jia, F., Guo, X., & Wang, Z. (2015). Impedimetric aptamer-based determination of the mold toxin fumonisin B1. *Microchimica Acta, 182*(9), 1709-1714. doi:10.1007/s00604-015-1492-x

D.Sehgal, & I.K.Vijay. (1994). A method for the high efficiency of water-soluble carbodiimide-mediated amidation. *Analytical Biochemistry, 218*(87-91).

de Souza, F. R., Alves, G. L., & Coltro, W. K. (2012). Capillary-driven toner-based microfluidic devices for clinical diagnostics with colorimetric detection. *Anal Chem, 84*(21), 9002-9007. doi:10.1021/ac302506k

Eivazzadeh-Keihan, R., Pashazadeh, P., Hejazi, M., de la Guardia, M., & Mokhtarzadeh, A. (2017). Recent advances in Nanomaterial-mediated Bio and immune sensors for detection of aflatoxin in food products. *TrAC Trends in Analytical Chemistry, 87*, 112-128. doi:10.1016/j.trac.2016.12.003

Escarpa, A. (2014). Lights and shadows on food microfluidics. *Lab Chip, 14*(17), 3213-3224. doi:10.1039/c4lc00172a

Evtugyn, G., Porfireva, A., Stepanova, V., Kutyreva, M., Gataulina, A., Ulakhovich, N., . . . Hianik, T. (2013). Impedimetric Aptasensor for Ochratoxin A Determination Based on Au Nanoparticles Stabilized with Hyper-Branched Polymer. *Sensors, 13*(12). doi:10.3390/s131216129

Farré, M., Kantiani, L., Pérez, S., Barceló, D., & Barceló, D. (2009). Sensors and biosensors in support of EU Directives. *TrAC Trends in Analytical Chemistry, 28*(2), 170-185. doi:http://dx.doi.org/10.1016/j.trac.2008.09.018

Galarreta, B. C., Tabatabaei, M., Guieu, V., Peyrin, E., & Lagugné-Labarthet, F. (2013). Microfluidic channel with embedded SERS 2D platform for the aptamer detection of ochratoxin A. *Analytical and Bioanalytical Chemistry, 405*(5), 1613-1621. doi:10.1007/s00216-012-6557-7

Guo, L., Feng, J., Fang, Z., Xu, J., & Lu, X. (2015). Application of microfluidic “lab-on-a-chip” for the detection of mycotoxins in foods. *Trends in Food Science & Technology, 46*(2), 252-263. doi:10.1016/j.tifs.2015.09.005

H. Guo, X. W., Q. Qian, et.al. (2009). A Green Approach to the Synthesis of Graphene Nanosheets. *ACS Nano, 3*(9), 2653-2659.

Huang, D., Zhang, B., Zhang, Y., Zhan, F., Xu, X., Shen, Y., & Wang, M. (2013). Electrochemically reduced graphene oxide multilayer films as metal-free electrocatalysts

for oxygen reduction. *Journal of Materials Chemistry A, 1*(4), 1415. doi:10.1039/c2ta00552b

Ivnitski, D., Abdel-Hamid, I., Atanasov, P., & Wilkins, E. (1999). Biosensors for detection of pathogenic bacteria. *Biosensors and Bioelectronics, 14*(7), 599-624. doi:10.1016/s0956-5663(99)00039-1

Karimi, A., Hayat, A., & Andreescu, S. (2017). Biomolecular detection at ssDNA-conjugated nanoparticles by nano-impact electrochemistry. *Biosensors and Bioelectronics, 87*, 501-507. doi:https://doi.org/10.1016/j.bios.2016.08.108

Kuila, T., Bose, S., Khanra, P., Mishra, A. K., Kim, N. H., & Lee, J. H. (2011). Recent advances in graphene-based biosensors. *Biosens Bioelectron, 26*(12), 4637-4648. doi:10.1016/j.bios.2011.05.039

Li, S. c., Chen, J. h., Cao, H., Yao, D. s., & Liu, D. l. (2011). Amperometric biosensor for aflatoxin B1 based on aflatoxin-oxidase immobilized on multiwalled carbon nanotubes. *Food Control, 22*(1), 43-49. doi:http://dx.doi.org/10.1016/j.foodcont.2010.05.005

Li, Z., Yu, Y., Li, Z., & Wu, T. (2015). A review of biosensing techniques for detection of trace carcinogen contamination in food products. *Anal Bioanal Chem, 407*(10), 2711-2726. doi:10.1007/s00216-015-8530-8

Lin, Y., Zhou, Q., Lin, Y., Tang, D., Niessner, R., & Knopp, D. (2015). Enzymatic Hydrolysate-Induced Displacement Reaction with Multifunctional Silica Beads Doped with Horseradish Peroxidase–Thionine Conjugate for Ultrasensitive Electrochemical Immunoassay. *Analytical Chemistry, 87*(16), 8531-8540. doi:10.1021/acs.analchem.5b02253

Liu, H.-Y., Lin, S.-L., Chan, S.-A., Lin, T.-Y., & Fuh, M.-R. (2013). Microfluidic chip-based nano-liquid chromatography tandem mass spectrometry for quantification of aflatoxins in peanut products. *Talanta, 113*(Supplement C), 76-81. doi:https://doi.org/10.1016/j.talanta.2013.03.053

Luo, Z., Lu, Y., Somers, L. A., & Johnson, A. T. (2009). High yield preparation of macroscopic graphene oxide membranes. *J Am Chem Soc, 131*(3), 898-899. doi:10.1021/ja807934n

M.-F.Yu, O.Lourie, M.J.Dyer, K.Moloni, Kelly, T. F., & Ruoff, R. S. (2000). Strength and breaking mechanism of multiwalled carbon nanotubes under tensile load. *Science, 287*, 637-640.

Ma, Y., Mao, Y., Huang, D., He, Z., Yan, J., Tian, T., . . . Yang, C. J. (2016). Portable visual quantitative detection of aflatoxin B1 using a target-responsive hydrogel and a distance-readout microfluidic chip. *Lab on a Chip, 16*(16), 3097-3104. doi:10.1039/C6LC00474A

Marcano, D. C., Kosynkin, D. V., Berlin, J. M., Sinitskii, A., Sun, Z., Slesarev, A., . . . Tour, J. M. (2010). Improved Synthesis of Graphene Oxide. *ACS Nano, 4*(8), 4806-4814. doi:10.1021/nn1006368

Mello, L. D., & Kubota, L. T. (2002). Review of the use of biosensors as analytical tools in the food and drink industries. *Food Chemistry, 77*(2), 237-256. doi:10.1016/s0308-8146(02)00104-8

N.Hamada, Sawada, S.-I., & Oshiyama, A. (1992). New one-dimensional conductors:graphitic microtubules. *Physical Review Letters, 68*, 1579-1581.

N.Shao, S.Lu, E.Wickstrom, & B.Panchapakesan. (2007). Integrated molecular targeting of IGF1R and HER2 surface receptors and destruction of breast cancer cells using single wall carbon nanotubes. *Nanotechnology, 18*, 1-9.

Novo, P., Moulas, G., França Prazeres, D. M., Chu, V., & Conde, J. P. (2013). Detection of ochratoxin A in wine and beer by chemiluminescence-based ELISA in microfluidics with integrated photodiodes. *Sensors and Actuators B: Chemical, 176*(Supplement C), 232-240. doi:https://doi.org/10.1016/j.snb.2012.10.038

Olcer, Z., Esen, E., Muhammad, T., Ersoy, A., Budak, S., & Uludag, Y. (2014). Fast and sensitive detection of mycotoxins in wheat using microfluidics based Real-time Electrochemical Profiling. *Biosensors and Bioelectronics, 62*(Supplement C), 163-169. doi:https://doi.org/10.1016/j.bios.2014.06.025

Palchetti, I., & Mascini, M. (2012). Electrochemical nanomaterial-based nucleic acid aptasensors. *Analytical and Bioanalytical Chemistry, 402*(10), 3103-3114. doi:10.1007/s00216-012-5769-1

Panini, N. V., Bertolino, F. A., Salinas, E., Messina, G. A., & Raba, J. (2010). Zearalenone determination in corn silage samples using an immunosensor in a continuous-flow/stopped-flow systems. *Biochemical Engineering Journal, 51*(1–2), 7-13. doi:http://dx.doi.org/10.1016/j.bej.2010.04.005

Pumera, M. (2011). Graphene in biosensing. *Materials Today, 14*(7-8), 308-315. doi:10.1016/s1369-7021(11)70160-2

R.J.Chen, S.Bangsaruntip, K.A.Drouvalakis, N.W.Kam, M.Shim, Y.Li, . . . H.Dai. (2003). Noncovalent functionalization of carbon nanotubes for highly specific electronic biosensors. *Proc Natl Acad Sci USA, 100*, 4984-4989.

R.Saito, M.Fujita, G.Dresselhaus, & Dresselhaus, M. S. (1992). Electronic structure of graphene tubules based on C60. *Physical Review B, 46*, 1804-1811.

Raj, M. A., & John, S. A. (2013). Fabrication of Electrochemically Reduced Graphene Oxide Films on Glassy Carbon Electrode by Self-Assembly Method and Their Electrocatalytic Application. *The Journal of Physical Chemistry C, 117*(8), 4326-4335. doi:10.1021/jp400066z

S.Iijima. (1991). Helical microtubules of graphitic carbon. *Nature, 354*, 56-58.

Sakai, N., Fujiwara, Y., Arai, M., Yu, K., & Tatsuma, T. (2009). Electrodeposition of gold nanoparticles on ITO: Control of morphology and plasmon resonance-based absorption and scattering. *Journal of Electroanalytical Chemistry, 628*(1), 7-15. doi:http://dx.doi.org/10.1016/j.jelechem.2008.12.008

Seenivasan, R., Singh, C. K., Warrick, J. W., Ahmad, N., & Gunasekaran, S. (2017). Microfluidic-integrated patterned ITO immunosensor for rapid detection of prostate-specific membrane antigen biomarker in prostate cancer. *Biosens Bioelectron, 95*, 160-167. doi:10.1016/j.bios.2017.04.004

Soares, R. R., Novo, P., Azevedo, A. M., Fernandes, P., Aires-Barros, M. R., Chu, V., & Conde, J. P. (2014). On-chip sample preparation and analyte quantification using a microfluidic aqueous two-phase extraction coupled with an immunoassay. *Lab Chip, 14*(21), 4284-4294. doi:10.1039/c4lc00695j

Soares, R. R., Santos, D. R., Chu, V., Azevedo, A. M., Aires-Barros, M. R., & Conde, J. P. (2017). A point-of-use microfluidic device with integrated photodetector array for immunoassay multiplexing: Detection of a panel of mycotoxins in multiple samples. *Biosens Bioelectron, 87*, 823-831. doi:10.1016/j.bios.2016.09.041

Srivastava, S., Kumar, V., Ali, M. A., Solanki, P. R., Srivastava, A., Sumana, G., . . . Malhotra, B. D. (2013). Electrophoretically deposited reduced graphene oxide platform for food toxin detection. *Nanoscale, 5*(7), 3043-3051. doi:10.1039/c3nr32242d

Su, L., Jia, W., Hou, C., & Lei, Y. (2011). Microbial biosensors: A review. *Biosensors and Bioelectronics, 26*(5), 1788-1799. doi:10.1016/j.bios.2010.09.005

T.Ramanathan, F.T.Fisher, R.S.Ruoff, & Brinson, L. C. (2005). Amino-functionalized carbon nanotubes for binding to polymers and biological systems. *Chemistry of Materials, 17*, 1290-1295.

T.W.Ebbesen. (1997). Nanotubes,nanoparticles and aspects of fullerene related carbons. *Journal of Physics and Chemistry of Solids, 58*, 1979-1982.

Tan, S. M., Ambrosi, A., Khezri, B., Webster, R. D., & Pumera, M. (2014). Towards electrochemical purification of chemically reduced graphene oxide from redox accessible impurities. *Phys Chem Chem Phys, 16*(15), 7058-7065. doi:10.1039/c4cp00371c

Tang, D., Lin, Y., Zhou, Q., Lin, Y., Li, P., Niessner, R., & Knopp, D. (2014). Low-Cost and Highly Sensitive Immunosensing Platform for Aflatoxins Using One-Step Competitive Displacement Reaction Mode and Portable Glucometer-Based Detection. *Analytical Chemistry, 86*(22), 11451-11458. doi:10.1021/ac503616d

Tiwari, I., Gupta, M., Pandey, C. M., & Mishra, V. (2015). Gold nanoparticle decorated graphene sheet-polypyrrole based nanocomposite: its synthesis, characterization and genosensing application. *Dalton Trans, 44*(35), 15557-15566. doi:10.1039/c5dt01193k

Toh, S. Y., Loh, K. S., Kamarudin, S. K., & Daud, W. R. W. (2014). Graphene production via electrochemical reduction of graphene oxide: Synthesis and characterisation. *Chemical Engineering Journal, 251*, 422-434. doi:10.1016/j.cej.2014.04.004

Uludag, Y., Esen, E., Kokturk, G., Ozer, H., Muhammad, T., Olcer, Z., . . . Altintas, Z. (2016). Lab-on-a-chip based biosensor for the real-time detection of aflatoxin. *Talanta, 160*(Supplement C), 381-388. doi:https://doi.org/10.1016/j.talanta.2016.07.060

Wang, J., Rivas, G., Cai, X., Palecek, E., Nielsen, P., Shiraishi, H., . . . Flair, M. N. (1997). DNA electrochemical biosensors for environmental monitoring. A review. *Analytica Chimica Acta, 347*(1-2), 1-8. doi:10.1016/s0003-2670(96)00598-3

Wang, X., Niessner, R., Tang, D., & Knopp, D. (2016). Nanoparticle-based immunosensors and immunoassays for aflatoxins. *Anal Chim Acta, 912*, 10-23. doi:10.1016/j.aca.2016.01.048

Wang, Y.-C., Lu, L., & Gunasekaran, S. (2015). Gold nanoparticle-based thermal history indicator for monitoring low-temperature storage. *Microchimica Acta, 182*(7-8), 1305-1311. doi:10.1007/s00604-015-1451-6

Y.Gao, & I.Kyratzis. (2008). Covalent immobilization of proteins on carbon nanotubes using the cross-linker 1-ethyl-3-(3-dimethylaminopropyl)carbodiimide-a critical assessment. *Bioconjugate Chemistry, 19*, 1945-1950.

Zhang, X., Zhang, D., Chen, Y., Sun, X., & Ma, Y. (2012). Electrochemical reduction of graphene oxide films: Preparation, characterization and their electrochemical properties. *Chinese Science Bulletin, 57*(23), 3045-3050. doi:10.1007/s11434-012-5256-2

Zhang, Z., Yu, L., Xu, L., Hu, X., Li, P., Zhang, Q., . . . Feng, X. (2014). Biotoxin sensing in food and environment via microchip. *ELECTROPHORESIS, 35*(11), 1547-1559. doi:10.1002/elps.201300570

Zhuang, J., Tang, D., Lai, W., Xu, M., & Tang, D. (2015). Target-Induced Nano-Enzyme Reactor Mediated Hole-Trapping for High-Throughput Immunoassay Based on a Split-Type Photoelectrochemical Detection Strategy. *Analytical Chemistry, 87*(18), 9473-9480. doi:10.1021/acs.analchem.5b02676

Zourob, M., Elwary, S., & Turner, A. P. F. (2008). *Principles of bacterial detection : biosensors, recognition receptors, and microsystems*. New York: Springer.

CHAPTER 3 [1]Electrochemical Immunosensor for Rapid and Sensitive Detection of Aflatoxin B1

Abstract

Mycotoxin contamination of food and feed grains such as corn and wheat could pose serious health risks and cause economic losses. In addition, often several mycotoxins are present in the same sample. Therefore, an ideal mycotoxin detection system should not only be simple, rapid, and sensitive but also capable of simultaneously detecting multiple mycotoxins in a single test. We developed an electrochemical immunoarray biosensor to meet these requirements. The key elements of our sensor were incorporating novel nanomaterials for improved performance and fabricating disposable screen-printed electrodes (SPE) for in inexpensive portable use. The detection of toxins was based on specific immunoreactions between target toxins and their respective antibodies. Thus, the more target toxins are present in the sample, the more toxins are bound to antibodies, generating smaller current signals, which are measured to quantify the toxin concentrations. The sensor was rigorously tested, calibrated and optimized. The sensor system and test protocols were developed for on-site toxin detection even by unskilled users. This system was designed to lend itself for simultaneously detecting additional mycotoxins and/or testing multiple samples. Such an in-field monitoring system will enable implementation of preventive strategies at the source before the toxins enter our food chain.

[1] The contents of chapter have been presented at the 2014 Institute of Food Technology Annual Conference.

3.1 Introduction

Electrochemical sensors coupled with competitive and non-competitive immunoassays for AFB1 determination have been reported by researchers. For example, Piermarini et al. (Piermarini, Micheli, Ammida, Palleschi, & Moscone, 2007) have developed an immunosensor array of 96 SPE coupled with a multichannel electrochemical detection (MED) system using the intermittent pulse amperometry (IPA) technique has been also used for the detection of AFB_1. The immunoassay was then applied for analysis of corn samples spiked with AFB_1 before and after the extraction treatment, and the results showed that using this system, AFB_1 can be detected at a level of 30 pg/mL and with a working range between 0.05 and 2 ng/mL. The cross-reactivity test indicated that the antibody used for this assay could distinguish AFB_1 from other aflatoxins except AFG_1. Table 3.1 summarizes literatures related to AFB_1 detection using electrochemical immunosensors.

The detection limit of some study has reached 0.03 ng/mL (Piermarini et al., 2007), which is very sensitive. However, ELISA-based assay usually requires extra enzyme marker or secondary antibody to complete the detection process, which is costly and time consuming. Therefore the selectivity, sensitivity as well as the operation simplicity are still major technical challenges of the above analytical methods.

Table 3.1 Summary of electrochemical immunosensors for AFB1 detection.

Mycotoxin	Method	Effective range (ng/mL)	LOD (ng/mL)	Reference
AFB_1	IC/IPA on 96-well SPEs	0.05–2	0.03	(Piermarini et al., 2007)
AFB_1	IC/DPV on an 8x ELIME-array	0.8-9	0.6	(Ammida, Micheli, Piermarini, Moscone, & Palleschi, 2006)
AFB_1	IC/AMP on SPEs	0.1–10	0.09	(Ammida et al., 2006)
AFB_1	DC/AMP on SPEs	0.15–0.25	0.15	(Pemberton, Pittson, Biddle, Drago, & Hart, 2006)
AFB_1	IC/DPV in GCE doped with AuNPs	0.6–2.4	0.07	(Owino et al., 2007)
AFB_1	NC/AMP	0.1–12	0.05	(Sun, Qi, Dong, & Liang, 2008)
AFB_1	AChE inhibition/AMP on SPEs modified with PB	10 to 60	2	(Ben Rejeb et al., 2009)
AFB_1	Enzyme Biosensor (AFOx)/AMP using CNTs	1-225	0.5	(Li, Chen, Cao, Yao, & Liu, 2011)
AFB_1	DC/EIS on electropolymerized PANi-PSSA films	0.1-6	0.1	(Owino et al., 2007)

Abbreviations: IC: indirect competitive assay, AMP: amperometry, DC: direct competitive assay, AuNPs: gold nanoparticles, NC: no competitive, PB: Prussian blue, DPV: differential pulse voltammetry, EIS: electrochemical impedance spectroscopy, ELIME-assay: enzyme-linked immune-magnetic electrochemical assay, GCE: glassy carbon electrode, AChE: achetylcholinesterase enzyme, PANi-PSSA: polyaniline- polystyrenesulfonicacid.

In this chapter, we initially designed and fabricated an electrochemical immunosensor coupled with AuNPs and MWCNTs for the detection of AFB1. To be specific, we utilized an inexpensive and disposable SPE as the sensor platform, and functionalized the working electrode part of the SPE with CNT-COOH to 1) improve electrochemical response and 2) create a surface suitable for easy and stable antibody immobilization. Cyclic voltammetry (CV), DPV and Scanning Electron Microscopy (SEM) experiments were performed to characterize the modified electrode.

With the target toxin-specific antibody attached to the electrode, a control sample contains only PBS buffer (without target toxin in it) was tested by DPV technique and an initial peak current was recorded as the baseline. Therefore, when tested with samples contain target toxins, the desired toxins could be recognized and captured onto the immunoelectrode surface, resulting in reduced electrochemical current due to the insulating property of antibody-toxin complex. It is expected that the more toxins attached to the electrode, the greater the current decreases. Hence, the amount of target toxins present in the sample could be quantified based on the magnitude of the electrochemical signals obtained.

3.2 Experimental Section

3.2.1 Materials and reagents

AFB_1, polyclonal anti-Aflatoxin B1 antibody produced in rabbit ($aAFB_1$), poly(diallyldimethylammonium chloride) (PDDA) were purchased from Sigma-Aldrich. 4-aminobenzoic acid (4-ABA, 99%), 98% sulfuric acid, 62% nitric acid, dimethyl sulfoxide (DMSO) and 98+% NHS were purchased from ACROS Organics. BSA (>98%) and EDC (>98%) were purchased from Bioworld. All other chemicals were of analytical grade and were

used without further purification. De-ionized (DI) water (18 MΩ cm) was used for the preparation of buffer solutions.

3.2.2 Preparation of solutions

AFB_1 powder was dissolved in DMSO to prepare 1 mg/mL stock solution, then the stock solution was diluted to desired concentration using 10 mM, pH 7.4 phosphate buffered saline (PBS). 1% (w/w) BSA was prepared in PBS for the blocking of non-specific binding sites. 0.1% (w/w) PDDA solution was prepared in DI water and $aAFB_1$ solution with various concentrations was prepared in PBS. 3 mM of 4-ABA was made using ethanol and DI water. EDC/NHS (2 mM/5mM) mixture was prepared in PBS solution (pH 6). All PBS buffer used in this study are prepared as pH 7.4, 10 mM unless otherwise stated.

3.2.3 Carboxylation of MWCNTs.

There are many sophisticated methods for CNTs oxidation. We decided to use a mixture of nitric acid/sulfuric acid to modify MWCNTs with carboxyl groups. 10 mg MWCNTs was added into 5 mL of a 1:3 (v/v) concentrated solution of HNO_3/H_2SO_4. The mixture was subject to sonication for 15 min and then was heated to 70 °C for 8 h without stirring (Wepasnick et al., 2011). After 8 h acid 5treatment, wait for the mixture to cool down to room temperature and wash with DI water and centrifuge at 10,000 rpm for several times until the supernatant was clear. The treated MWCNTs sediment was then dried in an oven at 65 °C for 3 h and the dried product was dissolved in water to prepare 0.1 mg/mL CNT-COOH solution.

Infrared and ultraviolet spectra analysis of treated MWCNTs have been carried out using the following equipment: Fourier Transform Infrared Spectrometer (FT-IR Spectrum 100, Perkin Elmer) and UV/Vis spectrophotometer (Lambda 25, Perkin Elmer).

3.2.4 Preparation of aAFB$_1$-(PDDA/CNT-COOH)n immunoelectrode

Fig. 3.1(a) shows the scheme of the immunoelectrode fabrication. First of all, 5 µL of 3 mM 4-ABA was deposited on the SPE surface to make the surface negatively charged (Huang et al., 2013). 5 µL of 0.1%(w/w) PDDA solution was then uniformly spread on the electrode surface and was incubated for 15 min at room temperature (25 ◦C). Then 5 µL of 0.1 mg/mL carboxyl group functionalized CNT solution was deposited and incubated in the same manner. PD DA/CNT-COOH step was repeated to deposit multiple layers of (PDDA/CNT-COOH) on the electrode surface. A mixture solution of 0.4 M EDC and 0.10 M NHS was added and incubated for 1 h to initiate cross-linking reactions between carboxyl groups on MWCNTs and amine groups in aAFB$_1$ (Yi, Qi, Zhang, & Yang, 2010). Finally, 5 µL aAFB$_1$ antibody was immobilized on the electrode surface and incubated at room temperature for one hour. Then BSA (1% w/w) solution was applied as blocking agent for 15 min. After each immobilization step, PBS solution was applied to wash off unbound molecules.

3.2.5 Electrode characterization and AFB$_1$ detection

Electrochemical analysis was conducted using an Autolab Potentiostat/ Galvanostat (Metrohm USA) to characterize the electrode before and after each step of modification. The freshly prepared immunoelectrode was dipped into sample solution containing AFB$_1$ and incubated for 20 min to allow antibody-antigen interaction, then DPV measurement was

conducted with 1mM $K_3Fe(CN)_6$ in PBS, and peak current was recorded and compared (Fig. 3.1(b)).

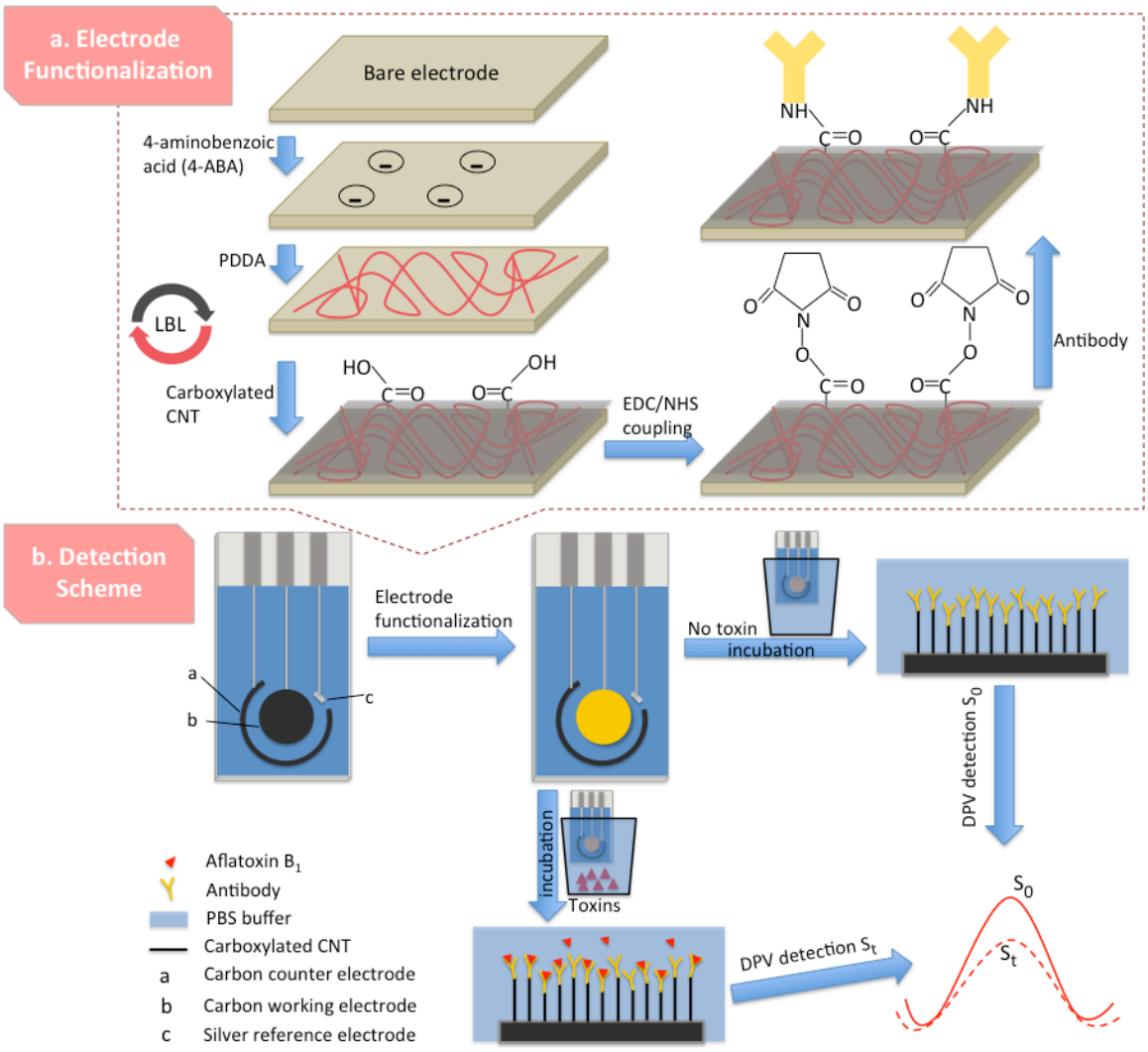

Figure 3.1 (a) Fabrication of (PDDA/CNT-COOH)n-aAFB1 immunoelectrode and (b) scheme of AFB1 detection.

3.3 Results and discussion

3.3.1 Carboxylation of MWCNTs

Fig. 3.2 (a) shows the UV-vis spectrum of acid-treated MWCNTs. There is an absorption peak observed at 265 nm, which is a typical absorption spectrum of carboxylated CNTs. Fig. 3.2 (b) shows the FT-IR spectra of as-received MWCNTs and functionalized MWNTs. The spectrum of the as-received MWNTs shows a C=C stretching peak at 1678 cm^{-1}. Decreased absorbance of C=C in treated MWCNTs indicates oxidation of carbon by mixed acid. As a result, the discernable C=O stretching peak observed at 1715 cm^{-1} suggests the formation of carboxylic acid after acid treatment (Yudianti et al., 2011). According to above results, we have concluded that 8 h of mixed acid treatment at 70 °C is sufficient to functionalize the CNTs by introducing COOH group at the CNT sidewalls.

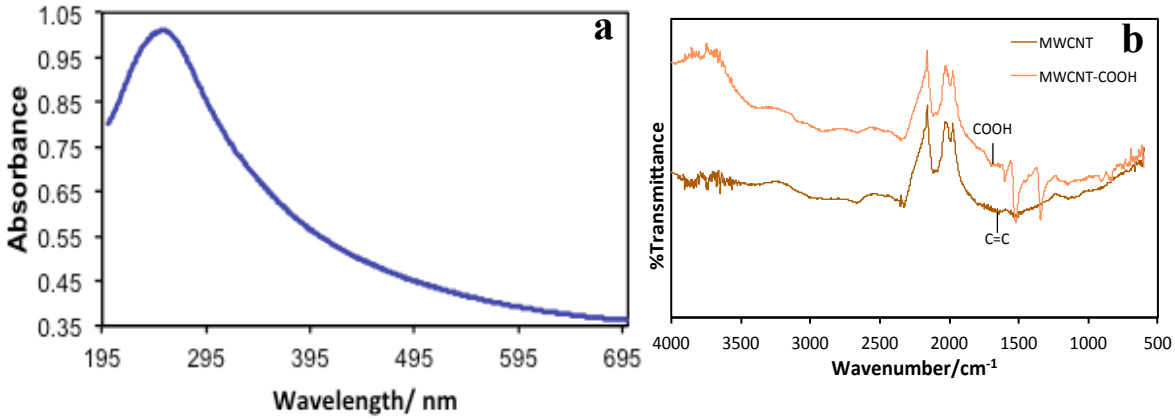

Figure 3.2 (a) UV-vis spectrum of acid treated MWCNTs, (b) FT-IR spectra of as-received MWCNTs and acid treated MWCNTs.

3.3.2 Optimize Number of (PDDA/CNT-COOH) Layers

DPV signals in Fig. 3.3 (right) clearly demonstrates that the current response significantly increases ($I_{(iii)}$-$I_{(ii)}$=7.45 μA) after three layers of (PDDA/CNT-COOH) deposition, which suggests a great improvement of electrode conductivity. Adding a fourth layer did not further improve the electrochemical response of the electrode. After immobilization of fifth layer, even a slight drop of peak current was observed. A possible reason for the changes in DPV signals could be for the first three layers, the SPE surface covered by (PDDA/CNT-COOH) was proportional to the number of layers, giving the electrode surface increased conductivity; then the surface coverage nearly saturated after three layers deposition, thus no apparent changes was observed after adding the fourth layer. When there was more than three layers, they overlapped on the electrode (after the fifth layer) and even hindered the electron transfer between the electrode and surroundings, causing a drop in peak current. SEM (LEO-440) images (Fig. 3.4) strongly support this explanation. The enlarged view of a randomly selected area on the electrode shows relatively uniform and high coverage of (PDDA/CNT-COOH) after three layers immobilization. CV results also agreed with the DPV data. Considering both time and efficient factors, the number of (PDDA/CNT-COOH) to be immobilized on the SPE was determined as three.

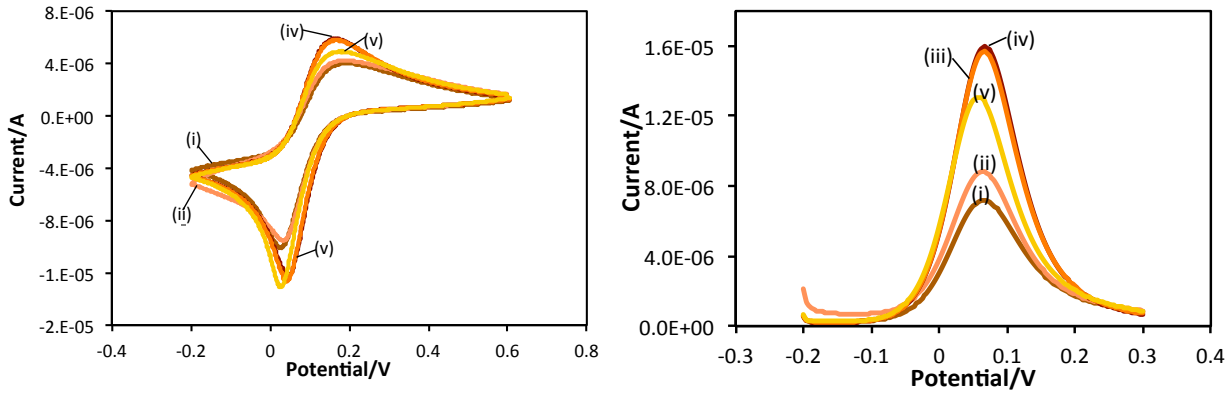

Figure 3.3 CV (left) and DPV (right) after one to five (i to v) (PDDA/CNT-COOH) layers deposited on electrode in PBS (10 mM, pH 7.4) solution containing 1mM [Fe(CN)6]3-/4-. CV scan rate 50 mV/s, applied potential range: -0.2 to 0.6 V. DPV applied potential range:

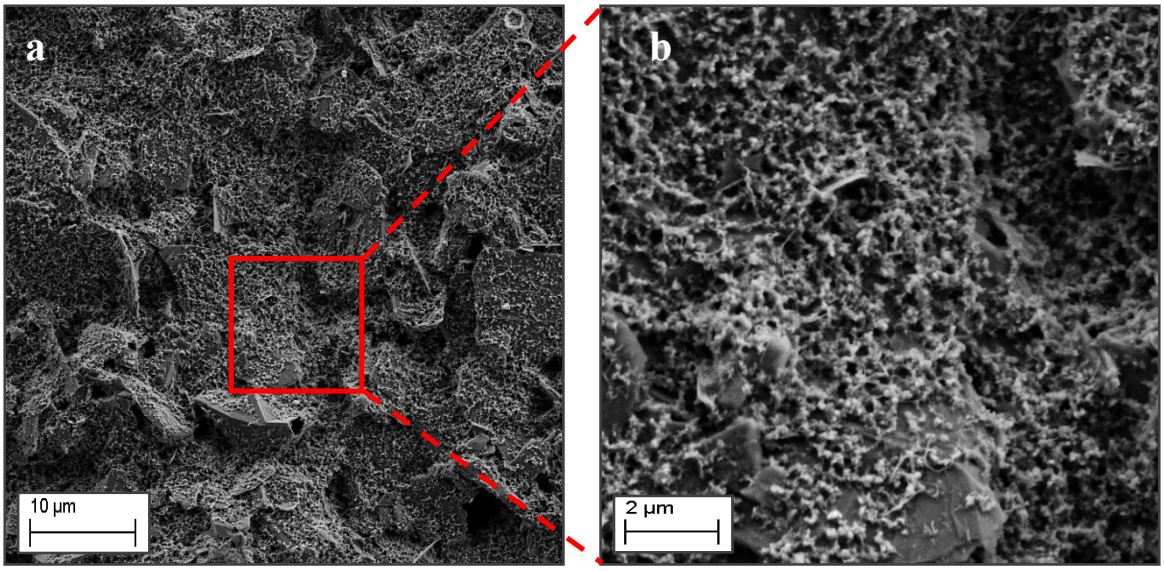

Figure 3.4 SEM images of (a) SPE covered by three layers of (PDDA/CNT-COOH) and (b) enlarged view of the selected area.

3.3.3 Characterization of Modified Electrode

DPV and CV investigations of the critical immobilization steps were performed to characterize the detection mechanisms of the immumoelectrode. There are no sharp peaks of bare SPE in either CV or DPV curve, indicating relatively poor conductivity of the electrode. However, CV curve (Fig. 3.5 left (ii)) of $(PDDA/CNT\text{-}COOH)_3$ modified electrode shows the highest peak currents at both anode and cathode, and a smallest peak separation of approximate 0.234 V among the three. Coupled with the DPV curves (Fig. 3.5 right) they demonstrates the excellent charge transfer property of the $(PDDA/CNT\text{-}COOH)_3$ modified electrode. After antibodies were immobilized onto the electrode, the current response significantly decreased because of the non-conducting property of the antibodies.

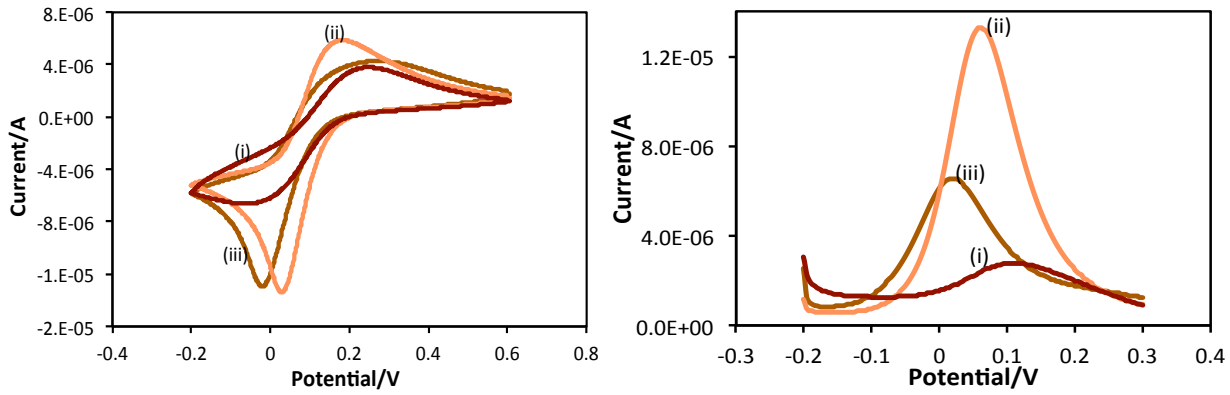

Figure 3.5 CV (left) and DPV (right) of (i) bare SPE, (ii) 3 layers of (PDDA/CNT-COOH) deposited on electrode, (iii) (PDDA/CNT-COOH)3-aAFB1 immunoelectrode in PBS (10 mM, pH 7.4) solution containing 1mM [Fe(CN)6]3-/4- . CV scan rate 50 mV/s, applied potential range -0.2 to 0.6 V. DPV applied potential range -0.2 to 0.3 V.

3.3.4 AFB_1 Detection

As shown in Fig. 3.6 (left column) the DPV peak current decreased when AFB_1 was captured onto the immunoelectrode via immunoreaction, which indicates that the formed insulated antibody-antigen complex significantly hindered the charge transfer on the electrode.

In addition, peak current further reduced with increasing AFB_1 concentration. The right column of Fig. 3.6 shows calibration curves for different AFB_1 concentration ranges with optimized antibody loading (Table 3.2) for each range. From all the results shown above, with appropriate antibody loading, the detection limit of the developed sensor could go down to 0.01 ppb, and we are confident to detect AFB_1 up to 90 ppb in samples. The detection sensitivity for each specific working range are 58.18, 5.03, 0.55 and 0.035 μA/ppb, respectively. According to the action levels of AFB_1 established by US Food and Drug Administration (FDA), our sensing method is able to detect AFB_1 from most of the foods for human and animal consumption.

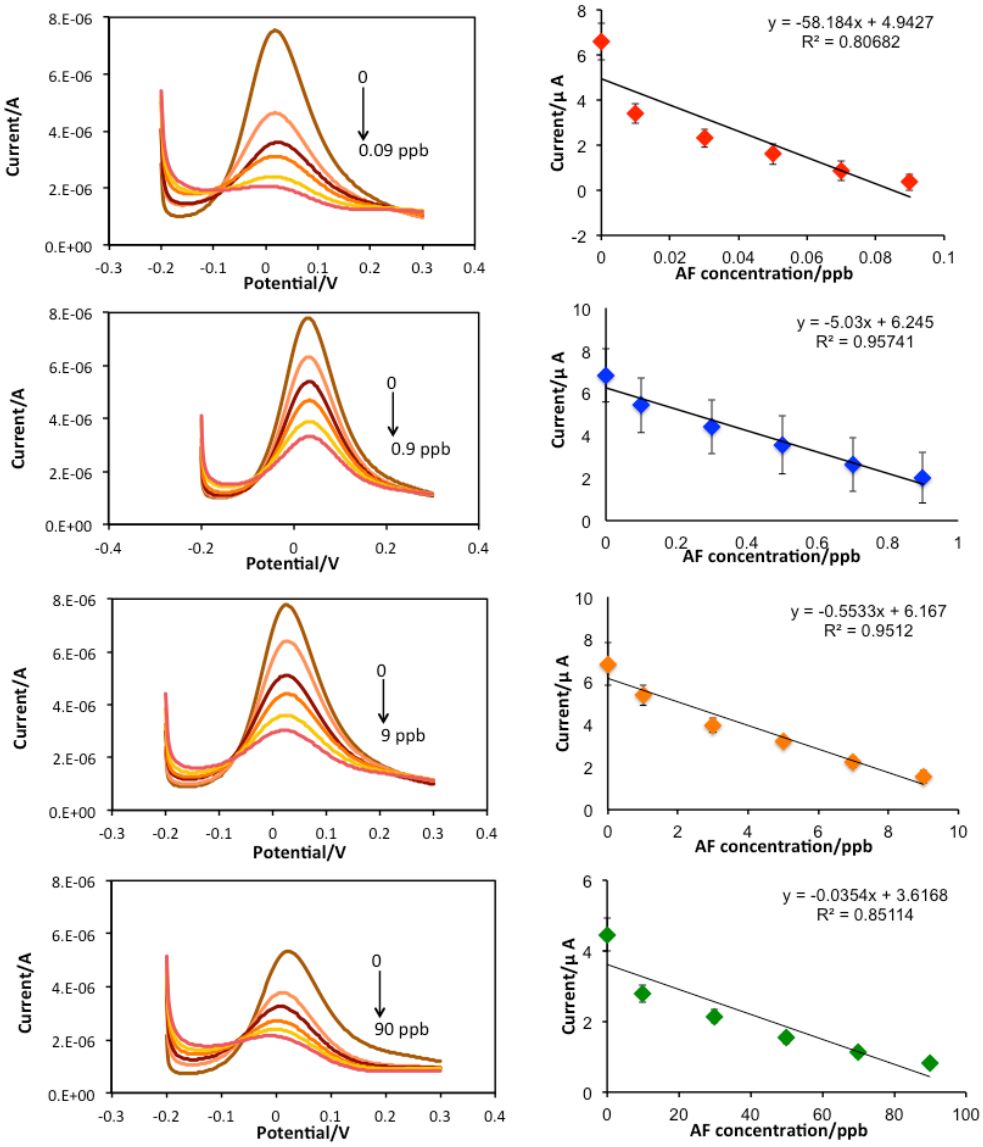

Figure 3.6 DPV signals (left) and calibration curves (right) for four different AFB1 concentration ranges with optimal antibody loading for each range. DPV applied potential range: -0.2 to 0.3 V.

Table 3.2 AFB1 concentration ranges and their corresponding optimized antibody loading

	AFB_1 concentration/ppb	Antibody concentration/ng.mL^{-1}
a	0-0.09	10
b	0-0.9	50
c	0-9	500
d	0-90	1000

3.4 Conclusions

An electrochemical immunosensor based on carbon nanotubes modified electrode has been fabricated for the detection of AFB_1. SEM images show high surface coverage of the PDDA/CNT-COOH layers onto the electrode, and these PDDA/CNT-COOH layers have significantly improved the conductivity of the SPE, resulting a higher current signal in electrochemical measurements. CV and DPV techniques were used to characterize the functionalized electrode and detect AFB_1 in PBS buffer. The immumoelectrode was capable of detecting AFB_1 in four different concentration ranges (0 to 90 ppb) with optimized antibody loading for each range, respectively. The limit of detection was 0.01 ppb. These results have proved that the proposed sensor works efficiently, and have established the foundation of fabricating a multi-channel immunosensor in the future.

Using our detection method, it is possible to achieve picogram level detections with small sample volume of ~5 μL, while most optimized ELISA can only achieve detection limits of 10 to100 pg/mL requiring 50 to 150 μL samples. Furthermore, our approach affords a stronger antibdoy immobilization than physical adsorption in ELISA. Therefore, a large number of our immunoarrays can be made and stored ready for in-field use with little loss of antibodies. Also, our system will only require minimal sample preparation. With initial peak current levels and calibration curves pre-determined, which can be used throughout, only one run is needed for

simultaneous determination of all target contaminants, which can be completed very quickly (within minutes). Another major advantage with regards to the ease of functionalization of the electrode and the screen-printing technology is their potential for mass production for widespread in-field use. The successful completion of this project will result in a rapid, sensitive, and inexpensive (disposable), system for detecting multiple mycotoxins (up to four in our for WEs configuration and more if redesigned and matched with number of measurement channels available in the portable electrochemical analyzer) simultaneously in an easy-to-perform in-field test. We expect county agents, other extension personnel, and farmers can perform this test for routine monitoring and tracking of contamination of their produce with dangerous toxins.

Further more, the sensor platform we develop will be broad-based such that mycotoxins other than aflatoxins can be detected rapidly, selectively, and sensitively. Thus our system will enhance the capabilities of biosensor research and applications for multiple targets.

References

Ammida, N. H. S., Micheli, L., Piermarini, S., Moscone, D., & Palleschi, G. (2006). Detection of Aflatoxin B1 in Barley: Comparative Study of Immunosensor and HPLC. *Analytical Letters, 39*(8), 1559-1572. doi:10.1080/00032710600713248

Ben Rejeb, I., Arduini, F., Arvinte, A., Amine, A., Gargouri, M., Micheli, L., . . . Palleschi, G. (2009). Development of a bio-electrochemical assay for AFB1 detection in olive oil. *Biosensors and Bioelectronics, 24*(7), 1962-1968. doi:http://dx.doi.org/10.1016/j.bios.2008.10.002

Huang, D., Zhang, B., Zhang, Y., Zhan, F., Xu, X., Shen, Y., & Wang, M. (2013). Electrochemically reduced graphene oxide multilayer films as metal-free electrocatalysts for oxygen reduction. *Journal of Materials Chemistry A, 1*(4), 1415. doi:10.1039/c2ta00552b

Li, S. c., Chen, J. h., Cao, H., Yao, D. s., & Liu, D. l. (2011). Amperometric biosensor for aflatoxin B1 based on aflatoxin-oxidase immobilized on multiwalled carbon nanotubes. *Food Control, 22*(1), 43-49. doi:http://dx.doi.org/10.1016/j.foodcont.2010.05.005

Owino, J. O., Ignaszak, A., Al-Ahmed, A., Baker, P. L., Alemu, H., Ngila, J., & Iwuoha, E. (2007). Modelling of the impedimetric responses of an aflatoxin B1 immunosensor prepared on an electrosynthetic polyaniline platform. *Analytical and Bioanalytical Chemistry, 388*(5-6), 1069-1074. doi:10.1007/s00216-007-1333-9

Pemberton, R. M., Pittson, R., Biddle, N., Drago, G. A., & Hart, J. P. (2006). Studies Towards the Development of a Screen‐Printed Carbon Electrochemical Immunosensor Array for Mycotoxins: A Sensor for Aflatoxin B1. *Analytical Letters, 39*(8), 1573-1586. doi:10.1080/00032710600713289

Piermarini, S., Micheli, L., Ammida, N. H., Palleschi, G., & Moscone, D. (2007). Electrochemical immunosensor array using a 96-well screen-printed microplate for aflatoxin B1 detection. *Biosens Bioelectron, 22*(7), 1434-1440. doi:10.1016/j.bios.2006.06.029

Sun, A.-L., Qi, Q.-A., Dong, Z.-L., & Liang, K. (2008). An electrochemical enzyme immunoassay for aflatoxin B1 based on bio-electrocatalytic reaction with room-temperature ionic liquid and nanoparticle-modified electrodes. *Sensing and Instrumentation for Food Quality and Safety, 2*(1), 43-50. doi:10.1007/s11694-008-9040-6

Wepasnick, K. A., Smith, B. A., Schrote, K. E., Wilson, H. K., Diegelmann, S. R., & Fairbrother, D. H. (2011). Surface and structural characterization of multi-walled carbon nanotubes following different oxidative treatments. *Carbon, 49*(1), 24-36. doi:10.1016/j.carbon.2010.08.034

Yi, C., Qi, S., Zhang, D., & Yang, M. (2010). Covalent conjugation of multi-walled carbon nanotubes with proteins. *Methods Mol Biol, 625*, 9-17. doi:10.1007/978-1-60761-579-8_2

Yudianti, R., H.Onggo, Sudirman, Y.Saito, T.Iwata, & J.Azuma. (2011). Analysis of Functional Group Sited on Multi-Wall Carbon Nanotube Surface. *The Open Materials Science Journal, 5*, 242-247.

CHAPTER 4 [2]An Electrochemical Immunosensor for Rapid and Sensitive Detection of Mycotoxins Fumonisin B1 and Deoxynivalenol

Abstract

We report an electrochemical immunosensing method for rapid and sensitive detection of two mycotoxins, fumonisin B1 (FB1) and deoxynivalenol (DON). A disposable screen-printed carbon electrode (SPE) was used as sensing platform. The working electrode part of SPE was modified by gold nanoparticles (AuNPs) and polypyrrole (PPy)-electrochemically reduced graphene oxide (ErGO) nanocomposite film for effective anti-toxin antibody immobilization, enhanced electrical conductivity, and biocompatibility. Under optimized test conditions, the limit of detection and linear range achieved for FB1 were 4.2 ppb and 0.2 to 4.5 ppm (%RSD=4.9%); and the corresponding values for DON were 8.6 ppb and 0.05 to 1 ppm (%RSD=5.7%). The immunosensor can specifically detect the target toxin in co-existing toxins environment. The sensor exhibited high sensitivity and low matrix interference when tested using extracts obtained from spiked corn samples. Hence, our electrochemical immunosensing scheme can be adopted for highly sensitive and rapid detection of multiple co-contaminant mycotoxins in food and feed products.

[2] This chapter has been published: Lu, L., Seenivasan, R., Wang, Y. C., & Gunasekaran, S. (2016). An Electrochemical Immunosensor for Rapid and Sensitive Detection of Mycotoxins Fumonisin B1 and Deoxynivalenol. *Electrochimica Acta, 213,* 89-97.

4.1 Introduction

Mycotoxins such as aflatoxin (AF), deoxynivalenol (DON), fumonisin B1 (FB1), ochratoxin A (OTA) and zearalenone are a group of toxic secondary metabolites produced by certain fungi. They naturally contaminate foods and feeds (Frisvad & Thrane, 1987), which lower the product quality, pose severe health risk to humans and animals, and cause profound economic losses worldwide (CAST, 2003). FB1 is the most common and economically important form of fumonisin (FUM), given its hepatotoxic and nephrotoxic effects in all animal species tested (Anderson, Kowtha, & Taitt, 2010; CAST, 2003). DON occurs predominantly in grains such as wheat and barley infected by *Fusarium* head blight (FHB) or scab (Arino, Herrera, Juan, & Estopanan, 2009; Pietri, Zanetti, & Bertuzzi, 2009). The US Food and Drug Administration has suggested the action levels of 2 to 4 parts per million (ppm) for FUM and 1 ppm for DON in foods intended for human consumption (NGFA, 2011). In addition, the co-occurrence of mycotoxins in nature has increased their likelihood of consumption and may cause additive and/or synergistic effects (Carlson et al., 2001; Chu & Li, 1994). For example, AF and FUM are co-contaminants often found in corn (Castells, Marin, Sanchis, & Ramos, 2008; Sun et al., 2011; Theumer, Lopez, Aoki, Canepa, & Rubinstein, 2008) and milled corn fractions (Castells et al., 2008; Pietri et al., 2009); DON and OTA are common co-contaminants in wheat (Arino et al., 2009; Birzele, Prange, & Kramer, 2000; Hajjaji et al., 2006).

Due to the widespread prevalence of multiple mycotoxins in foods and feeds, research has focused on developing effective methods for highly sensitive and selective detection of mycotoxins to screen foods and feeds. Traditional analytical methods include liquid chromatography–mass spectrometry (LC-MS), high performance liquid chromatography (HPLC), and thin-layer chromatography (TLC), which can detect toxins in the range of ~0.01 to

0.1 parts per billion (ppb) (Dugan, 2005; Liu, Xu, He, He, & Xiong, 2013; Monbaliu et al., 2009; Ran et al., 2013; Soares, Rodrigues, Freitas-Silva, Abrunhosa, & Venancio, 2010). However, these laboratory methods are not suitable for rapid, on-site testing because they are labor- and time-intensive as well as expensive (Lee, Wang, Allan, & Kennedy, 2004). Other screening methods used for mycotoxins detection are enzyme-linked immunosorbent assay (ELISA), surface plasmon resonance (SPR), lateral flow immunoarray (LFI), immunochip, electronic nose, etc. (Ran et al., 2013). Though ELISA is widely used, its shortcomings include cross-reactivity and possible false-positive or false-negative results (Ran et al., 2013); also, additional reagents are necessary to ensure the stability of stored antibody coating on the microwell plates (Kolosova, Shim, Yang, Eremin, & Chung, 2005). SPR sensor is sensitive to temperature, and LFI and electronic nose have low sensitivity, while immunochip involves complex labeling process and requires professional technicians to run the test (Ran et al., 2013).

Electrochemical biosensors are attractive due to their advantages of operational simplicity, high sensitivity, low cost, and portable on-field use. Kadir and Tothill developed the ELISA-based chronoamperometric immunosensor using screen-printed gold electrode for detection of FUM with a limit of detection (LOD) of 5 µg/L (5 ppb) (Kadir & Tothill, 2010). However, the use of secondary antibody in this work increases the cost and complexity. Ezquerra et al. reported an electrochemical immunoassay with the help of dispersed paramagnetic particles for FB1 detection with LOD of 0.58 ± 0.05 µg/L (Ezquerra, Vidal, Bonel, & Castillo, 2015). But this method requires additional tracer as well as an external magnetic field, also involves a step to transfer the modified magnetic beads to the electrode surface, which is somewhat complicated.

Novel nanomaterials are widely used for effective antibody immobilization and highly sensitive biosensor development. Srivastava et al. synthesized and deposited chemically active

reduced graphene oxide onto an indium tin oxide-coated glass substrate and this platform has been utilized for covalent attachment of the AFB1 antibodies for AFB1 detection (LOD=0.12 ng/mL) (Srivastava et al., 2013). Romanazzo et al. developed a recombinant fragment antigen-binding fragment based electrochemical immunosensor for DON detection (Romanazzo et al., 2010). Zhilei et al. reported a sensor for using fullerene C-60, an ionic liquid and ferrocene on a chitosan film at a glassy carbon electrode to detect DON (Zhilei et al., 2011). Some literature reports that incorporating nanomaterials and conducting polymers together in sensor platform affords large surface area, biocompatibility, ease of functionalization, and significantly enhances the sensitivity, reproducibility, and stability (German, Voronovic, Ramanavicius, & Ramanaviciene, 2012; Seenivasan, Chang, & Gunasekaran, 2015). Among nanomaterials, graphene oxide (GO)/polypyrrole (PPy) nanocomposite, electrochemically reduced graphene oxide (ErGO) and gold nanoparticles (AuNPs) are particularly suitable for biosensor applications due to their high electrical conductivity, good biocompatibility and chemical stability (Bagci, Wang, & Gunasekaran, 2015; Guan, Wang, & Gunasekaran, 2015; Kuila et al., 2011; Pumera, 2011; Y. C. Wang & Gunasekaran, 2012; Zhong, Gao, Xue, & Wang, 2015). PPy has been one of the most studied conducting polymers due to its great electrical conductivity, ease of preparation and low cost. However, it has some drawbacks such as mechanically weak and instability in conductivity (Zhong et al., 2015). Researchers have discovered that GO demonstrates a synergistic effect in PPy/GO composites that could improve both mechanical properties and electrical conductivity compared to PPy itself (Zhong et al., 2015). Therefore, combining such advantages of conducting polymers and nanomaterials (German et al., 2012; Xu et al., 2013), we developed a label-free electrochemical immunosensing method using disposable screen-printed carbon electrode (SPE)

modified by AuNPs and PPy/ErGO film for effective antibody immobilization and improved electrical conductivity to enable highly sensitive and selective detection of FB1 and DON.

4.2 Experimental

1.1.1 Materials and chemicals

SPEs (TE100) were purchased from CH Instruments, Inc. (Bee Cave, TX, USA). Graphite flakes (~150 μm), FB1, DON and bovine serum albumin (BSA) were purchased from Sigma-Aldrich (St. Louis, MO, USA). Hydrogen tetrachloroaurate(III) trihydrate ($HAuCl_4 \cdot 3H_2O$), nitric acid (63 %), pyrrole (99% extra pure) and 3-mercaptopropionic acid (MPA, 99+%) were supplied by ACROS Organics (Morris Plains, NJ, USA). Monoclonal anti-DON mouse antibody (1 mg/mL) and monoclonal anti-FB1 mouse antibody (1 mg/mL) were purchased from Antibodies-online.com (Atlanta, GA, USA). Immobilization of antibodies onto the electrode surface was performed using 1-ethyl-3-(3-dimethylaminopropyl) carbodiimide (EDC) and N-hydroxysuccinimide (NHS) chemistry with a minimum purity of 98% or higher (Bioworld, Dublin, OH, USA and Acros Organics). Phosphate buffered saline (PBS) 10X, methanol (99.8%), sulfuric acid (96 %), hydrogen peroxide (50 %), and hydrochloric acid (36.5–38 %) were from Fisher Scientific (Rockford, IL, USA). Potassium ferrocyanide trihydrate (reagent grade) and potassium chloride were acquired from Fisher Science Education (Hanover Park, IL, USA). Potassium ferricyanide, sodium phosphate monobasic (NaH_2PO_4) and sodium phosphate dibasic (Na_2HPO_4) were certified A.C.S. reagents from Thermo Fisher Scientific (Fair Lawn, NJ, USA). All chemicals were used as received without any purification, and deionized (DI) water of resistivity ≥18.2 MΩ·cm (Ultrapure water system, Millipore, Billerica, MA, USA) used for solution preparation and all experiments.

A detailed description of all solution preparation, synthesis of GO and AuNPs, and extraction of spiked toxins in corn samples were presented in the supplementary material.

4.2.1 Immunosensor fabrication

The immunosensor fabrication steps in preparing the working electrode surface of SPE for mycotoxin detection is illustrated in **Scheme 4.1A**. SPE was first rinsed with DI water to remove any existing impurities. PPy/GO nanocomposite film was grown using our modified procedure (Seenivasan, Chang, et al., 2015) by electrochemical deposition over the bare SPE placed in nitrogen-purged solution containing 0.025 M pyrrole, 0.33 mg/mL GO and 0.1 M KCl under gentle stirring. Cyclic voltammetry (CV) scans were then applied between –0.2 V and +0.9 V for 15 complete cycles at 50 mV/s scan rate. In this process, pyrrole was electro-polymerized into PPy and PPy/GO nanocomposite film was deposited on the working electrode surface of SPE effectively with GO being partially reduced. Then, fully reduced PPy/ErGO film was obtained by applied the CV scanning from 0.0 to –1.4 V at 50 mV/s scan rate in N_2 purged 0.05 M phosphate buffer (Na_2HPO_4/NaH_2PO_4) solution (pH 7.0) for 25 complete cycles (Guo, Wang, Qian, Wang, & Xia, 2009); the film was then rinsed with DI water and dried at room temperature. The ErGO/PPy film surface was drop-coated with 20 µL AuNPs solution and allowed to dry under ambient condition. The AuNPs-PPy/ErGO-modified SPE was immersed in 2 mL of 10 mM MPA solution and incubated for 6 h at room temperature to form Au-S bond (F. Wang, Wang, Chen, & Dong, 2007). After rinsing with DI water, the MPA-functionalized electrode was transferred to a mixture solution of EDC/NHS as crosslinker and incubated for one hour at room temperature to activate the carboxyl groups for effective immobilization of antibodies on the electrode surface (Yi, Qi, Zhang, & Yang, 2010). The electrode was washed

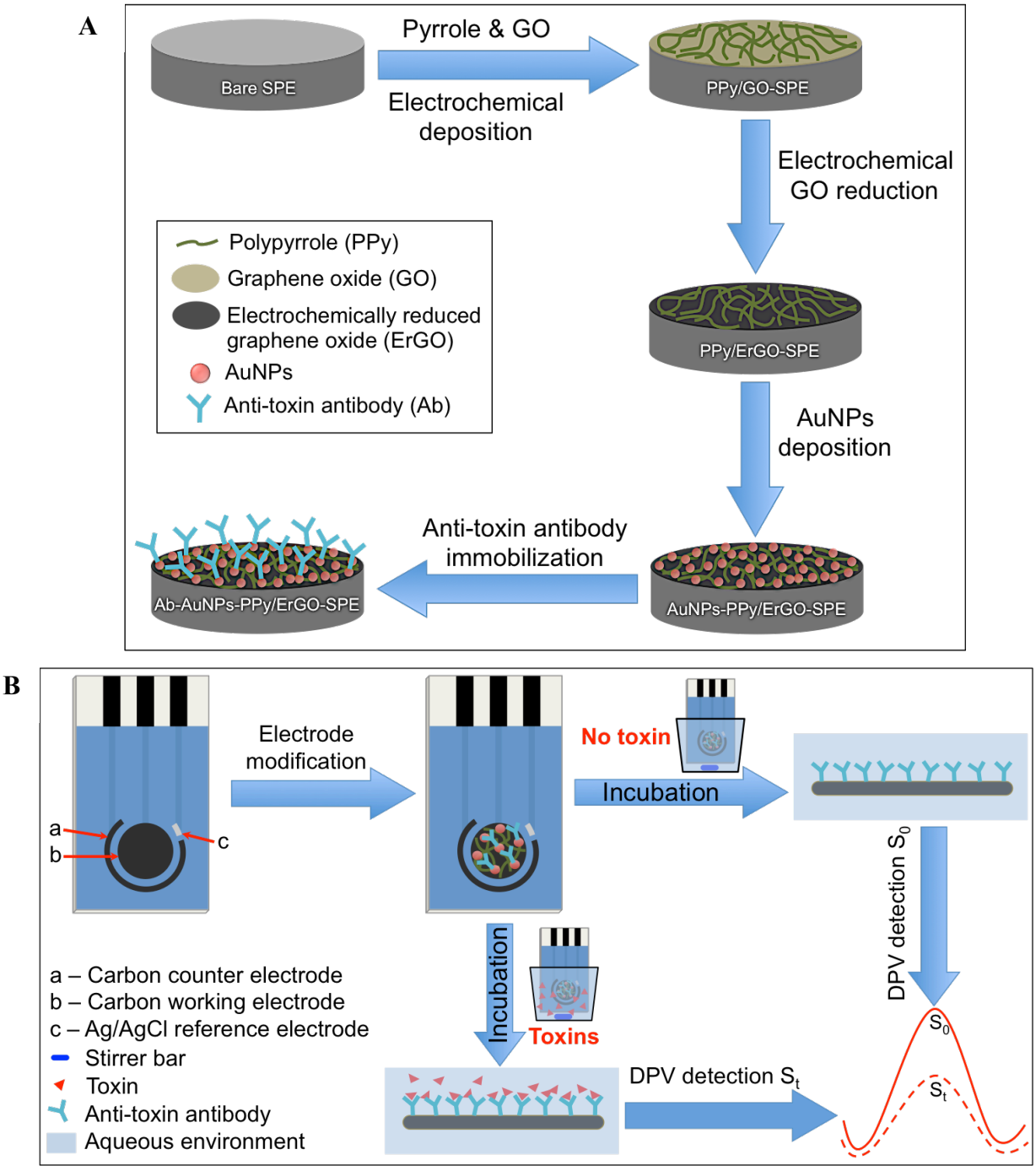

Scheme 4.1 (A) Illustration of step-by-step immunosensor fabrication and (B) Electrochemical immunosensing employed for detection of mycotoxins.

three times with DI water to remove any excess EDC/NHS and by-products followed by incubated with 40 µL of anti-FB1 or anti-DON antibody (Ab) solution (pH 9.0) at 4 °C for 12 h to allow sufficient antibody immobilization. Finally, the electrode was incubated with 1% BSA for 30 min to block unoccupied sites and washed with 1X PBS (Seenivasan, Maddodi, Setaluri, & Gunasekaran, 2015). The fabricated Ab-AuNPs-PPy/ErGO-SPE was stored in 1X PBS (pH 7.4) at 4 °C when not in use.

4.2.2 Instruments and measurements

Fourier transform infrared spectrometer (FT-IR, Spectrum-100, PerkinElmer) was used for characterization of synthesized GO. UV/Vis spectrophotometer (Lambda-25, PerkinElmer) was also used to characterize the synthesized GO and AuNPs. All electrochemical experiments were performed in CHI-660D electrochemical workstation (CH Instruments, Inc. USA) with a conventional three-electrode system. CV and differential pulse voltammetry (DPV) of redox couple 5 mM $[Fe(CN)_6]^{3-}/[Fe(CN)_6]^{4-}$ containing 1 M KCl as supporting electrolyte was employed to investigate the electron transfer behavior of SPE after each modification step and for target toxins (FB1/DON) detection. Scanning electron microscopy (SEM) images were obtained using a LEO 1530 scanning electron microscope.

4.2.3 Solution preparation

1X PBS (pH 7.4) solution was prepared from 10X PBS and pH was adjusted using 0.1 M HCl / 0.1 M NaOH unless otherwise stated. MPA solution at 0.1 M concentration was prepared in pure ethanol and then diluted by DI water to a concentration of 10 mM. EDC/NHS (2 mM/5mM) mixture was prepared in 1X PBS (pH 6.0). Antibody stock solutions (1 mg/mL) were diluted to

desired concentrations using 1X PBS (pH 9.0). DON and FB1 stock solutions at 1 mg/mL were prepared by ethanol and then diluted to required concentrations using DI water; they were stored at 4 °C in the dark.

4.2.4 Synthesis of graphene oxide

Graphene oxide (GO) was prepared according to the modified Hummers' method (Marcano et al., 2010; Y.-C. Wang, Cokeliler, & Gunasekaran, 2015). Briefly, graphite flakes (3.0 g) and $KMnO_4$ (18.0 g) were mixed with 1:9 concentrated H_3PO_4/H_2SO_4 solution and stirred and heated at 50 °C. After 12 h the above mixture was cooled to room temperature and then poured slowly onto ice (~400 mL) with hydrogen peroxide. 200 mL of HCl aqueous solution was then added in to the mixture. Finally, the material was purified by dialysis for one week to remove acids and metal species. The resulting product was filtered and the retentate was dried overnight at room temperature; further, it was dispersed in DI water and the dispersion was sonicated under ambient conditions for one hour to obtain a homogeneous GO suspension (1 mg/mL), which was stable for several months.

4.2.5 Synthesis of gold nanoparticles

AuNPs were synthesized per published method (Turkevich, Stevenson, & Hillier, 1951) with slight modification. Briefly, 2 mL of 10 mM $HAuCl_4$ solution was added into 18 mL DI water and brought to boiling under vigorous stirring. Then 2 mL of 1% trisodium citrate dehydrate solution was added quickly into the boiling solution. After the solution color changed to wine-red in 2-3 min, the mixture was kept boiling for another 10 min, and then cooled down to room temperature.

4.2.6 Sample extraction from spiked corn

The presence of any organic solvent may pose problems to toxin-antibody interaction as well as electrochemical measurements. Extraction methods using pure water as the extraction solvent have been proved to be very efficient for DON extraction with negligible matrix effect (Cahill et al., 1999; Romanazzo et al., 2010). So, DI water was selected as the extraction solvent for DON analysis in this study. However, FB1 is not water-soluble, thus methanol/water (20:80 v/v) solution was employed for FB1 extraction (Kolosova et al., 2005). Ground corn samples were spiked with toxins at various concentrations (FB1: 100, 500, 2000, 4000 µg/kg; DON: 100, 500, 1000 µg/kg) and 5 g of the spiked sample was extracted in 25 mL extraction solution (DON: DI water, FB1: methanol/water) at room temperature with stirring for 15 min. The extraction was then centrifuged at 10,000 rpm for 5 min. The supernatant was carefully collected and 0.2 mL of the supernatant was taken and diluted for 10-fold using 1X PBS buffer for antibody-toxin recognition. Both extraction methods for DON and FB1 were employed without any further purification step.

4.3 Results and Discussion

The sensing scheme employed the target mycotoxins detection system is illustrated in **Scheme 4.1B.** With the target mycotoxin-specific antibody attached on the working surface of SPE, a blank sample is tested and the DPV peak current is recorded as the signal baseline. When samples containing mycotoxins are tested, after 40 min of incubation, the antibody-toxin interaction at the electrode surface results in reduced electrochemical current due to the insulating property of the antibody-toxin complex (Sunday et al., 2015). The decrease in DPV current is proportional to the antibody vs. target toxin concentration of the tested sample. Hence,

the amount of target toxins present in the sample could be quantified based on the magnitude of the electrical signal obtained.

4.3.1 FT-IR and UV-Vis characterization of synthesized GO

FTIR spectrum of GO in **Fig. 4.1**a reveals the characteristic –OH (at 3347 cm^{-1}), C=O (at 1729 cm^{-1}), C=C (at 1624 cm^{-1}), and C-O (at 1071 cm^{-1}) bonds were observed, which indicates the presence of oxygenated groups on GO (Seenivasan, Chang, et al., 2015; X. Wang et al., 2013). The characteristic UV-vis spectrum of the as-synthesized GO suspension is presented in **Fig. 4.1b** The peak of the spectrum at 226 nm corresponds to the π→π* transitions of the aromatic C=C bond. A shoulder at ~300 nm is attributed to n→π* transition of the carbonyl groups (C=O bond) (Luo, Lu, Somers, & Johnson, 2009; Seenivasan, Chang, et al., 2015).

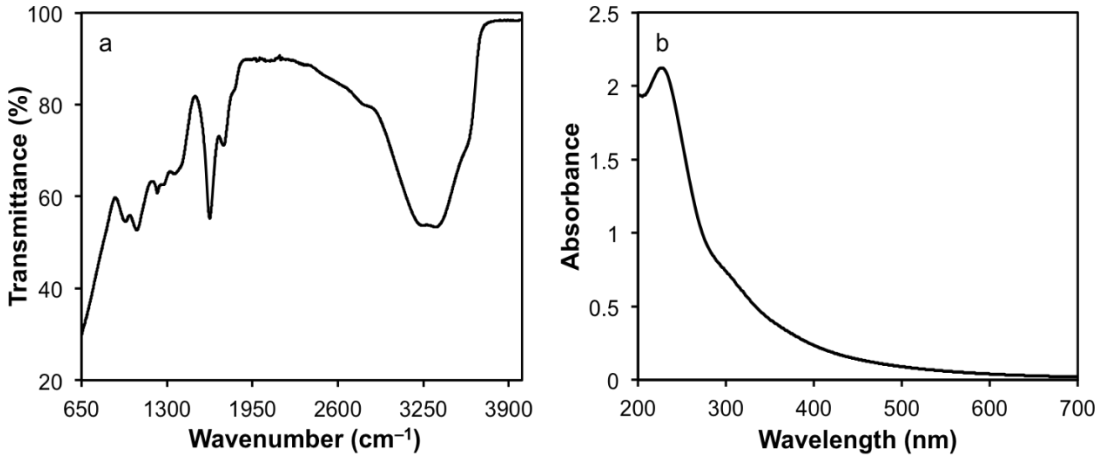

Figure 4.1 (a) FTIR and (b) UV-Vis spectra of synthesized GO.

4.3.2 Evaluation of electrode modification materials

In order to evaluate the effect of each nanomaterials selected for our immunosensor and therefore obtain the optimal electrode modification strategy, DPV scans were performed for

different materials processed electrodes and the results are shown in Fig. 4.2. Compared to bare SPE with a peak current of -14.59 μA (Fig. 4.2a), PPy coated SPE (Fig. 4.2b) shows a peak current of -42.17 μA with ~3-fold increase in current magnitude, which proves PPy is an effective conducting polymer to amplify the current signal. DPV peak current was further improved to -58.33 μA after AuNPs were deposited on PPy-SPE (Fig. 4.2c), which attributes to the superior electric conductivity of AuNPs. In this process, AuNPs are also employed as a necessary intermediate to form Au-S bond for antibody immobilization effectively. However, as mentioned previously, PPy- film itself may have instabilities in conductivity and mechanical strength and this could be improved by adding GO to form a PPy/GO nanocomposite film. Fig. 4.2d shows enhanced electron transfer (-80.2 μA) at AuNPs-PPy/GO-SPE surface in comparison to Fig. 4.2c, which verifies the PPy/GO coating has better performance than PPy film. Due to the lack of electric conductivity of GO material, it is expected that adding one step to electrochemically fully reduce the deposited GO on working electrode would achieved even higher current response. This agrees with the results shown in Fig. 4.2f (-109.4 μA). Fig. 4.2e shows the peak current obtained using AuNPs-PPy/chemically reduced GO (rGO)-SPE. In this process, rGO was used instead of GO and PPy/rGO film was electrochemically deposited on electrode. The current signal is not much different from that of Fig. 4.2d and is much lower than Fig. 4.2f, which suggests that ErGO is more capable of boosting the electron transfer at the modified electrode surface. The obtained results clearly indicate that electrode modification strategy used in Fig. 4.2f (AuNPs-PPy/ErGO-SPE) demonstrates the well improvement in electron transfer reactions compared to others. Therefore, eventually the AuNPs modified PPy/ErGO nanocomposite film on SPE working surface was selected in this work.

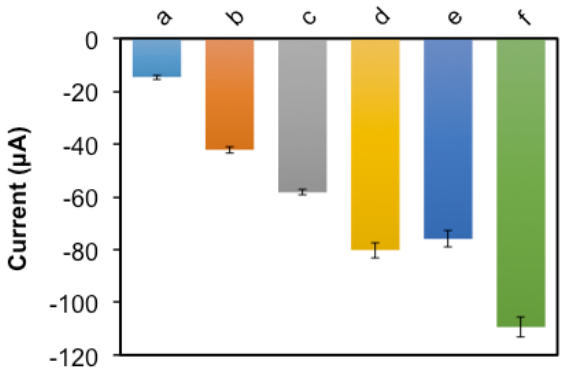

Figure 4.2 DPV responses of 5 mM [Fe(CN)6]3–/4– in 1M KCl at (a) bare SPE, (b) PPy-SPE, (c) AuNPs-PPy-SPE, (d) AuNPs-PPy/GO-SPE, (e) AuNPs-PPy/rGO-SPE and (f) AuNPs-PPy/ErGO-SPE. Error bars represent standard deviations of three independent measurements.

4.3.3 Electrochemical reduction of GO to ErGO

As shown in **Fig. 4.3**, CV was performed in N_2 saturated 0.05 M phosphate buffer (Na_2HPO_4/NaH_2PO_4) solution (pH 7.0) for 25 successive complete cycles in the potential range between 0 and −1.4 V at the scan rate of 50 mV/s. In this reduction step an irreversible peak at −1.1 V was observed during the first cycle with an onset potential of –0.65 V, which attributes to the reduction of oxygenated groups on GO surface (Guo et al., 2009; Unnikrishnan, Palanisamy, & Chen, 2013). The reduction current was greatly diminished in the subsequent cycles, and the peak entirely vanished after 25 cycles with stable current, which implies the complete reduction of GO.

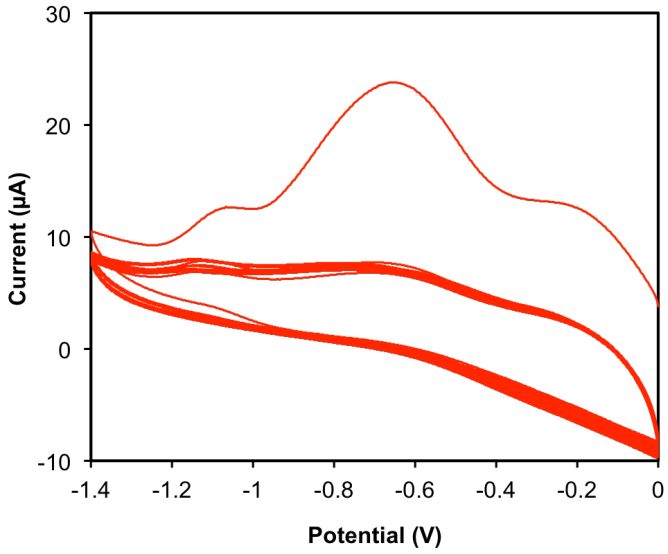

Figure 4.3 Electrochemical reduction of PPy/GO to PPy/ErGO in nitrogen-saturated 0.05 M, pH 7.0 phosphate buffer (Na2HPO4/NaH2PO4) solution.

4.3.4 Depositing AuNPs on the working electrode surface

We investigated the effective way to deposit AuNPs on the PPy/ErGO film surface via drop- and dip-coating methods using 5 mM $[Fe(CN)_6]^{3-/4-}$ in 1 M KCl. In **Fig. 4.4** (black curve) DPV result clearly shows good electron transfer with a sharper peak current of about 180 µA observed after drop-coating of AuNPs solution; the corresponding result for dip-coating was a very broad and small peak current (red curve), which indicates poor electron transfer between the electrolyte and the electrode surface. Thus, drop-coating of AuNPs yielded better electro-catalytic response may due to more uniform dispersion of AuNPs on the PPy/ErGO surface than with dip-coating. Hence, the drop-coating method was selected.

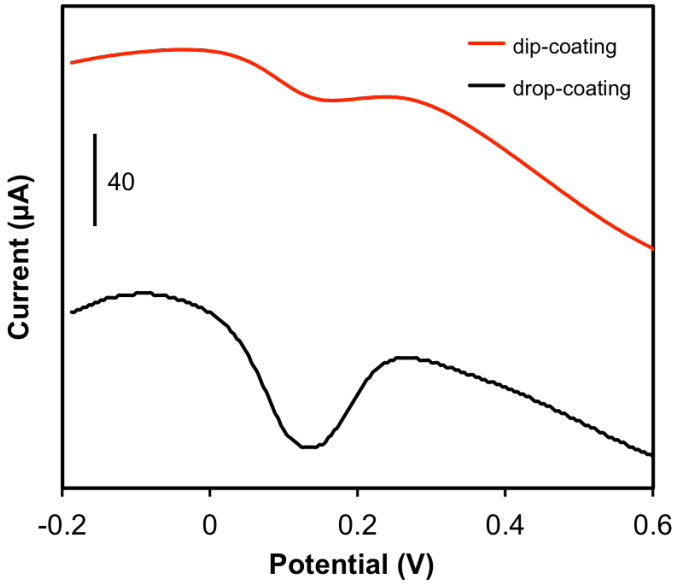

Figure 4.4 DPV responses of 5 mM [Fe(CN)6]3–/4– in 1M KCl at AuNPs-PPy/ErGO-SPE prepared by dip-coating and drop-coating methods.

4.3.5 Optimization of antibody concentration

We optimized the required anti-FB1/anti-DON antibody loading concentration on the immunosensor for effective detection of FB1 and DON. The DPV responses at different anti-toxin antibody loads on AuNPs-PPy/ErGO-SPE were evaluated in the presence and absence of corresponding toxins contains 5 mM $[Fe(CN)_6]^{3-/4-}$ in 1 M KCl. The DPV results of applying 40 µL of anti-FB1 antibody solution of different concentrations (2, 6, 10, 12 µg/mL) on four AuNPs-PPy/ErGO-SPE surfaces alone (black line) and after 40 min incubation with 1 µg/mL of FB1 (red line) are presented in **Fig. 4.5**a. The results clearly show the current magnitude decreased initially with increasing antibody loading and reached the lowest value at concentration of 10 µg/mL (black line). The red line further confirmed that the maximum current signal reduction after FB1 incubation occurs at 10 µg/mL antibody concentration, indicating the optimal formation of antibody-toxin complex and subsequent insulating effects. Therefore, 40 µL

of 10 µg/mL anti-FB1 antibody loading (i.e. 0.4 µg) was selected as the optimal for FB1 detection. Similar, DPV results obtained with applying 40 µL of different concentrations of anti-DON antibody solution (0.5, 1, 2, 3 µg/mL) are shown in **Fig. 4.5**b in the absence (black line) and presence (red line) of 1 µg/mL DON. These results indicate that an anti-DON antibody loading of 40 µL at 2 µg/mL is the optimal (i.e. 0.08 µg).

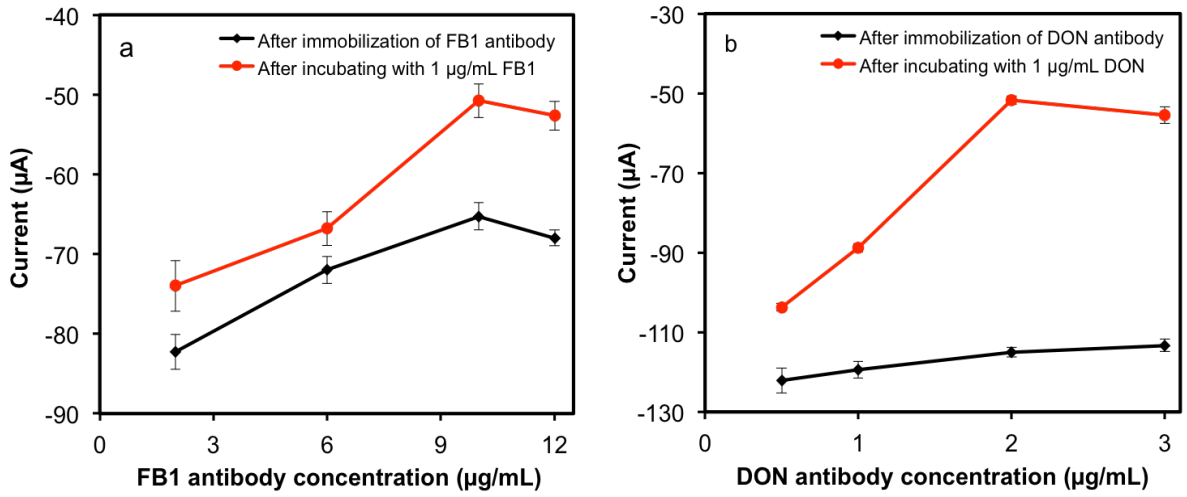

Figure 4.5 (a) DPV response to various FB1 antibody concentrations and peak reduction after 40 min incubation with 1 µg/mL FB1. (b) DPV peak current versus various DON antibody concentrations and peak reduction after 40 min incubation with 1 µg/mL DON. Values are mean of four independent measurements, and error bars are standard deviations.

4.3.6 Electrochemical and SEM characterization of fabricated SPE

Figure 4.6A shows the CV results of before and after each modification step on SPE working surface. The electrochemical response of 5 mM redox couple of $[Fe(CN)_6]^{3-/4-}$ at bare SPE (**Fig. 4.6A**, curve a) with a peak separation of 359 mV at 50 mV/s scan rate, reveals a quite slow electron transfer process. The redox peaks increased after the electrode was modified with PPy film (**Fig. 4.6A**, curve b). After depositing PPy/GO film (**Fig. 4.6A**, curve c), both cathodic and anodic peaks further increased and a much smaller peak separation of 160 mV was observed, implying an improved electron transfer. However, it has been reported that oxygenated groups on GO could have insulating effects to the electrode and thus hinder the electron transfer (Jung, Dikin, Piner, & Ruoff, 2008). This can be resolved by removing the oxygenated groups on GO, which has been confirmed by the CV result of PPy/ErGO-SPE (**Fig. 4.6A**, curve d). Given the large surface area, excellent electrical conductivity and catalytic properties of AuNPs, the electrochemical response was further improved after AuNPs deposition with cathodic peak of 135 μA (**Fig. 4.6A**, curve e), which indicates better catalytic ability than reported electrodes (Chen et al., 2013; Srivastava et al., 2013; Sunday et al., 2015). **Fig. 4.6A** (curve f), CV results show a decrease in cathodic and anodic peaks obtained with Ab-AuNPs-PPy/ErGO-SPE. This result confirms that antibody was immobilized on the AuNPs-PPy/ErGO film surface effectively without denaturation. The modified electrode was further characterized by electrochemical impedance spectroscopy (EIS). The Nyquist plots of impedance spectra in **Fig. 4.6B** clearly show that each step of modification on SPE working surfaces have different electron-transfer resistances R_{et} (a–f), which corresponds to the diameter of the semi-circles. These plots were fitted using a Randle's equivalent circuit shown in **Fig. 4.6B** and the R_{et} (a-f: 14 kΩ, 12.2 kΩ, 9.9 kΩ, 1827 Ω, 385 Ω and 3099 kΩ) were obtained. The magnitude of R_{et} relies on the dielectric

and insulating properties on the working electrode. A large R_{et} value indicates a poor electron transfer process at the modified working electrode. Change of R_{et} with each step demonstrates a similar trend to the above changes in CV responses.

SEM images of the working electrode of SPEs after different modification steps are presented in **Fig. 4.6C**. SEM image of electrochemically deposited PPy film shows the uniform and microporous structure of PPy (**Fig. 4.6C**, image a), as it has been reported in the literature (Seenivasan, Chang, et al., 2015). Similarly, the image of electrochemically grown PPy/GO film exhibits thin and wrapped GO sheet around PPy film with enhanced the surface roughness and area (**Fig. 4.6C**, image b) (Li, Xie, & Li, 2013; Zhu, Zhai, Wen, & Dong, 2012). It has been studied by many researchers that GO dispersed in water shows a negative zeta potential, which can be attributed to the oxygen containing groups on the surface(Raj & John, 2013; Yang & Gunasekaran, 2013). While after being reduced to ErGO, the zeta potential is close to zero due to the removal of oxygen species. After electrochemical reduction, the PPy/ErGO film shows more aggregated and rough surface of ErGO with occasional wrinkles and folds around PPy (**Fig. 4.6C**, image c) than reported methods (Si, Chen, Kannan, & Kim, 2011; M. Wang, Yuan, Yu, & Shi, 2014). This may be attributed to the increased van der Waals attraction between adjacent layers due to the removal of oxygen functional groups, which confirms the successful electrochemical reduction of GO (B & R, 2006; Yoo et al., 2015). **Fig. 4.6C**, image d shows well distributed AuNPs on the PPy/ErGO film after drop-coating of AuNPs solution. In this step, the negatively charged sodium citrate prepared AuNPs are attracted electrostatically by positive charged PPy film. These SEM images clearly indicate we have successfully fabricated well-integrated nanocomposite film with good orientation, conducting property and stability on working surface of SPE and also obtained more intensive AuNPs

deposition compared to published works (Qian, Yu, Zhou, Wu, & Shen, 2014; Y. Yang, Asiri, Du, & Lin, 2014).

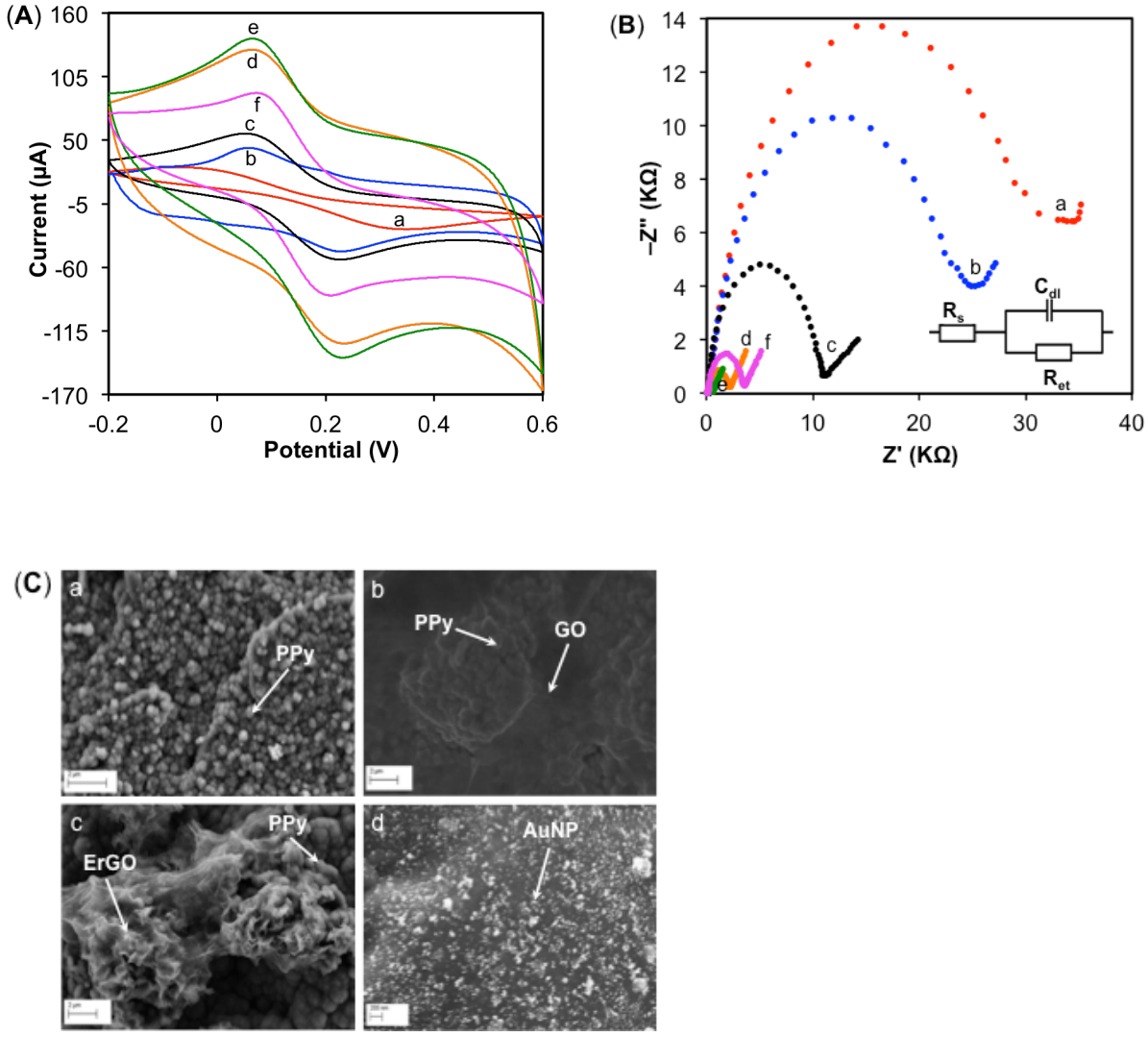

Figure 4.6 (A) CV and (B) EIS responses of 5 mM [Fe(CN)6]3–/4– in 1M KCl at (a) bare SPE, (b) PPy-SPE, (c) PPy/GO-SPE, (d) PPy/ErGO-SPE, (e) AuNPs-PPy/ErGO-SPE and (f) Ab-AuNPs-PPy/ErGO-SPE. CV scan rate = 50 mV/s and applied potential range = –0.2 to +0.6 V. In Randles' equivalent circuit (B inset), R_s, electrolyte resistance; R_{et}, electron-transfer resistance; C_{dl}, double layer capacitance. EIS frequency range was from 0.1 to 100,000 Hz and the amplitude was 5 mV. (C) **SEM images of working electrode surface of SPE modified with (a) PPy (b) PPy/GO (c) PPy/ErGO and (d) AuNPs-PPy/ErGO films.**

4.3.7 Sensitivity, specificity, reproducibility and stability

The DPV response of 5 mM redox couple $[Fe(CN)_6]^{3-/4-}$ at as-prepared immunosensor was examined over a wide range of FB1 and DON concentrations in 1X PBS (**Fig. 4.7A, B**, blue lines). It is observed that, for both FB1 and DON, the added toxin instantly reduces the magnitude of DPV peak current. The observed peak currents were inversely proportional to the total toxin concentrations for both FB1 and DON via antibody-toxin interaction (see **Scheme 4.1B**). The detection sensitivity for FB1 and DON are 0.010 and 0.075 μA/ppb, respectively.

The LOD of the developed sensing method was calculated using a linear regression curve based method reported in literature (Shrivastava & Gupta, 2011):

$$LOD=3*S_a/b,$$

Where, S_a is the standard deviation of intercept and b is the slope of the calibration curve. Thus, the LOD for FB1 was calculated to be 4.2 ppb, with a linear regression range of 0.2 to 4.5 ppm (R^2=0.992). LOD for DON was determined to be 8.6 ppb, with a linear regression range of 0.05 to 1 ppm (R^2=0.994). **Table 4.1** shows that our immunosensor achieved lower LOD and much broader linear working ranges for both FB1 and DON compared to reported sensing techniques (Dominguez et al., 2015; Ezquerra et al., 2015; Jodra, Lopez, & Escarpa, 2015; Kadir & Tothill, 2010; Ricci et al., 2009; Romanazzo et al., 2010; Sunday et al., 2015; X. Yang et al., 2015; Zhilei et al., 2011), which is more useful for toxin detection in real samples.

The specificity of the immunosensor was tested by incubating it in target toxin solutions containing interfering agent. As shown in **Fig. 4.7C**, when the immunoelectrode was immobilized with anti-FB1 antibody, the sensor responded only to 1 ppm of FB1 (c); the response for 1 ppm of DON (b) was the same as that obtained for blank 1X PBS solution (a). Furthermore, when equal amounts of DON (1 ppm) and FB1 (1 ppm) were mixed and tested, the

DPV peak signal (d) obtained was the same as that obtained for 1 ppm of FB1 alone (c). Similar results was obtained in terms of specificity towards DON using DON immunosensor (**Fig. 4.7D**), indicate that our sensors are highly specific to the target toxin as long as the specific antibody immobilized on the electrode surface.

The reproducibility of the immunosensor performance was evaluated by calculating relative standard deviation (%RSD) values of three measurements made using three different Ab-AuNPs-PPy/ErGO-SPEs for 1 μg/mL DON and 1 μg/mL FB1 respectively. The 5.7% RSD obtained for DON detection and 4.9% RSD obtained for FB1 detection demonstrate good reproducibility.

The stability of the fabricated immunosensor was determined by measuring DPV current responses to DON after storing the electrode in 1X PBS at 4 °C for up to 12 days. **Fig. 4.8.** shows the magnitude of current signal was fairly stable after the first 6 days (decreased from –82.1 to –79.3 μA, n=3), showing a slightly decline after 12 days (decreased from –79.3 to –72.9 μA, n=3). An RSD of 5.8% (n=3) indicated good stability over 12 days.

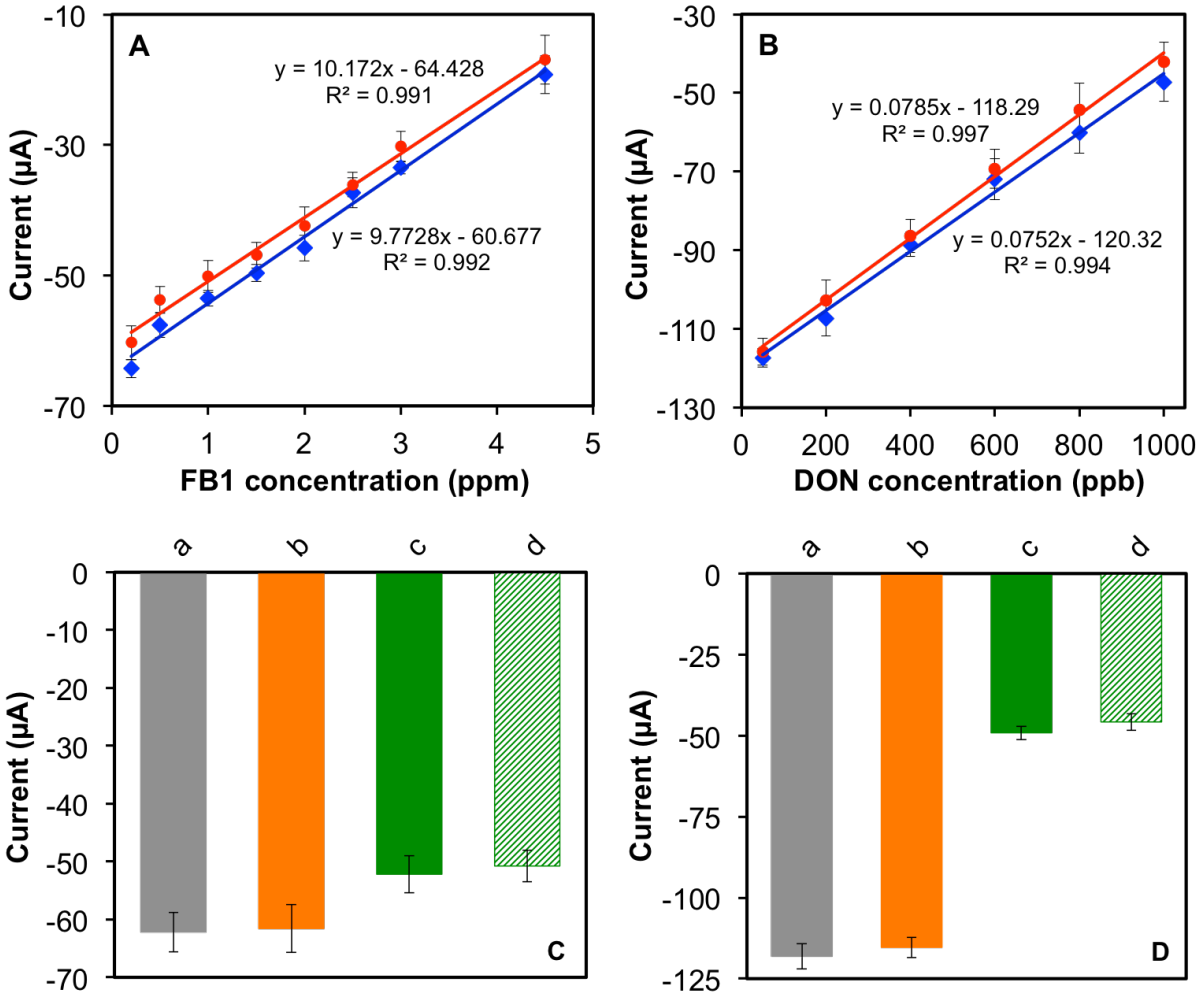

Figure 4.7 Linear calibration plots of DPV peak current versus (A) 0.2 to 4.5 ppm FB1 concentration with 0.4 µg FB1-antibody loaded AuNPs-PPy/ErGO-SPE in buffer (blue) and corn extract (red), and (B) 0.05 to 1 ppm DON concentration with 0.08 µg DON-antibody loaded AuNPs-PPy/ErGO-SPE in buffer (blue) and corn extract (red). DPV applied potential range: –0.2 to +0.3 V. Values are mean of three independent measurements, and error bars are standard deviations. Specificity of the (C) **FB1 immunosensor towards (a) PBS 0 ppm FB1, (b) 1 ppm DON, (c) 1 ppm FB1 and (d) 1 ppm FB1 + 1 ppm DON, and** (D) **DON immunosensor towards (a) PBS 0 ppm DON, (b) 1 ppm FB1, (c) 1 ppm DON and (d) 1 ppm DON + 1 ppm FB1 under optimal**

experimental conditions. Error bars represent standard deviations of three independent measurements.

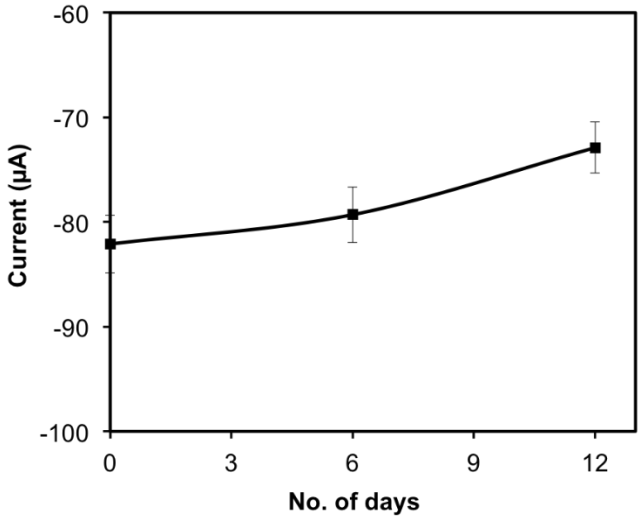

Figure 4.8 Stability of the immunosensor stored in 1X PBS at 4 °C over 12 days. Error bars represent standard deviations of three independent measurements.

4.3.8 Sensor performance in extracts from spiked corn samples

The calibration curves obtained for FB1 and DON in extracts obtained from spiked corn were plotted in **Fig. 4.7A, B** (red lines). The data from corn sample extracts are slightly lower than the corresponding results obtained when testing with buffer. However, both calibration curves showed similar trends, with even a slight increase in sensitivity, indicating negligible matrix effect. The recovery of spiked toxins in corn samples were in the range of 93.1 % to 104.3 % and their RSD values are less than 10% (**Table 4.2)**. These results indicate very high acceptability of our sensor for detecting mycotoxin contamination in real food matrices.

Table 4.1 Comparison of the sensing characteristics of Ab-AuNPs-PPy/ErGO electrode with those reported in literature

Mycotoxin	Sensor format	Linear range	Limit of detection	Reference
DON	ELIME assay	100–4500 ng/mL	63 ng/mL	(Romanazzo et al., 2010)
DON	Label-free inhibition based electrochemical immunosensor	6–30 ng/mL	0.3 μg/mL	(Sunday et al., 2015)
DON	96-well SPE plate	2–20 μg/g	1.1 μg/g	(Ricci et al., 2009)
DON	AuNPs/p-aminothiophenol/folic acid/GC	0.1–20 μg/mL	0.03 μg/mL	(Gu et al., 2015)
DON	Ab-AuNPs-PPy/ErGO-SPE	0.05–1 ppm	8.6 ppb	present work
FB1+FB2 + FB3	Electrochemical magnetoimmunosensor		0.33 μg/L	(Jodra et al., 2015)
FB1+FB2	Direct competitive/Amperometry	1–1000 ng/mL	5 ng/mL	(Kadir & Tothill, 2010)
FB1	Multi-channel electrochemical sensor	0–54 μg/L	0.58 μg/L	(Ezquerra et al., 2015)
FB1	Electrochemical immunosensor	0.01–1000 ng/mL	0.002 ng/mL	(X. Yang et al., 2015)
FB1	Ab-AuNPs-PPy/ErGO-SPE	0.2–4.5 ppm	4.2 ppb	present work

4.3.9 Reliability of the linear regression

To investigate the reliability of the linear regression curve, random samples containing a certain amount of target DON/FB1 was tested for validation purpose. First, the immunosensor was incubated with the random sample, a DPV scan was performed and recorded the change in peak current. The measured DPV peak current signal was used to calculate the amount of toxin concentration present in the tested random sample by linear regression equation. The

corresponding data in **Table 4.3** indicated that our calibrations are fairly robust and suitable for practical measurement of mycotoxin concentration

Table 4.3**.** Comparison of actual and measured concentrations predicted by calibration curves* performed in buffer for DON and FB1.

Toxin	Spiked (µg/kg)	Measured (µg/kg)	RSD (%)	Error (%)	Recovery (%)
FB1	100	90.7	9.9	9.3	90.7
	2000	1840	4.9	8.0	92.0
	4000	4210	3.1	5.25	105.3
DON	20	18.1	11.2	9.5	90.5
	500	511	1.0	2.2	102.2
	900	881	1.2	2.1	97.9

*Data are based on four measurements each.

4.4 Conclusions

We have demonstrated the fabrication of an electrochemical immunosensor for rapid and sensitive detection of two mycotoxins (FB1 and DON). The working electrode surface was modified with PPy, ErGO and AuNPs, which significantly improves electrochemical conductivity, good orientation and offers the ability for reliable antibody immobilization on the working electrode. The immunosensor was able to detect FB1 and DON with a limit of 4.2 ppb and 8.6 ppb, and has good reproducibility (%RSD<6% for both FB1 and DON). The linear regression relations have been validated by blind sample tests. The present immunosensor can

specifically detect the target toxins in co-existing toxin environments. Hence using specific antibodies, this sensing scheme would allow us to detect multiple co-contaminant mycotoxins simultaneously. The sensor performance was also tested in extracted corn samples and demonstrated high sensitivity and low matrix interference. In future, the current sensing platform can easily integrated with automated microfluidic system potential to allow not only simultaneous detection of multiple mycotoxins with low detection limit and also screening mycotoxins contaminant level in foods & feeds with low-cost.

References

Anderson, G. P., Kowtha, V. A., & Taitt, C. R. (2010). Detection of fumonisin b1 and ochratoxin a in grain products using microsphere-based fluid array immunoassays. *Toxins (Basel), 2*(2), 297-309. doi:10.3390/toxins2020297

Arino, A., Herrera, M., Juan, T., & Estopanan, G. (2009). Comparison of deoxynivalenol, ochratoxin A and aflatoxin B1 levels in conventional and organic durum semolina and the effect of milling. *J. Food Nutr. Res., 48*(2), 92–99.

B, P., & R, D. M. (2006). Impedance spectroscopy: over 35 years of electrochemical sensor optimization. *Electrochim. Acta, 51*, 6217.

Bagci, P. O., Wang, Y. C., & Gunasekaran, S. (2015). A simple and green route for room-temperature synthesis of gold nanoparticles and selective colorimetric detection of cysteine. *J. Food Sci., 80*(9), N2071–N2078. doi:10.1111/1750-3841.12974

Birzele, B., Prange, A., & Kramer, J. (2000). Deoxynivalenol and ochratoxin A in German wheat and changes of level in relation to storage parameters. *Food Addit. Contam., 17*(12), 1027–1035.

Cahill, L. M., Kruger, S. C., McAlice, B. T., Ramsey, C. S., Prioli, R., & Kohn, B. (1999). Quantification of deoxynivalenol in wheat using an immunoaffinity column and liquid chromatography. *J. Chromatogr. A, 859*, 23–28.

Carlson, D. B., Williams, D. E., Spitsbergen, J. M., Ross, P. F., Bacon, C. W., Meredith, F. I., & Riley, R. T. (2001). Fumonisin B1 promotes aflatoxin B1 and N-methyl-N'-nitro-nitrosoguanidine-initiated liver tumors in rainbow trout. *Toxicol. Appl. Pharmacol., 172*(1), 29–36.

CAST. (2003). *Mycotoxins: Risks in plant, animal, and human systems. Task Force Report No. 139. Council for Agricultural Science and Technology (CAST), Ames, Iowa, USA*

Castells, M., Marin, S., Sanchis, V., & Ramos, A. J. (2008). Distribution of fumonisins and aflatoxins in corn fractions during industrial cornflake processing. *Int. J. Food Microbiol., 123*(1-2), 81–87. doi:DOI 10.1016/j.ijfoodmicro.2007.12.001

Chen, M., Zhao, C., Chen, W., Weng, S., Liu, A., Liu, Q., . . . Lin, X. (2013). Sensitive electrochemical immunoassay of metallothionein-3 based on K3[Fe(CN)6] as a redox-active signal and C-dots/Nafion film for antibody immobilization. *Analyst, 138*(24), 7341-7346. doi:10.1039/c3an01351k

Chu, F. S., & Li, G. Y. (1994). Simultaneous occurrence of fumonisin B1 and other mycotoxins in moldy corn collected from the people's republic of china in regionswith high incidences of esophageal cancer. *Appl. Environ. Microbiol., 60*(3), 847–852.

Dominguez, C. X., Amezquita, R. A., Guan, T. X., Marshall, H. D., Joshi, N. S., Kleinstein, S. H., & Kaech, S. M. (2015). The transcription factors ZEB2 and T-bet cooperate to program cytotoxic T cell terminal differentiation in response to LCMV viral infection. *J. Exp. Med., 212*(12), 2041–2056. doi:10.1084/jem.20150186

Dugan, E. A. (2005). The detection of aflatoxins by TLC. *LC-GC North America, 23*, 51.

Ezquerra, A., Vidal, J. C., Bonel, L., & Castillo, J. R. (2015). A validated multi-channel electrochemical immunoassay for rapid fumonisin B1 determination in cereal samples. *Anal. Methods, 7*(9), 3742–3749. doi:10.1039/c4ay02897j

Frisvad, J. C., & Thrane, U. (1987). Standardized high-performance liquid chromatography of 182 mycotoxins and other fungal metabolites based on alkylphenone retention indices and UV-VIS spectra (diode array detection). *J. Chromatogr., 404*(1), 195–214.

German, N., Voronovic, J., Ramanavicius, A., & Ramanaviciene, A. (2012). Gold Nanoparticles and Polypyrrole for Glucose Biosensor Design. *Procedia Eng., 47*, 482–485. doi:10.1016/j.proeng.2012.09.189

Gu, W., Zhu, P., Jiang, D., He, X., Li, Y., Ji, J., . . . Sun, X. (2015). A novel and simple cell-based electrochemical impedance biosensor for evaluating the combined toxicity of DON and ZEN. *Biosens. Bioelectron., 70*, 447–454. doi:10.1016/j.bios.2015.03.074

Guan, J., Wang, Y. C., & Gunasekaran, S. (2015). Using l-arginine-functionalized gold nanorods for visible detection of mercury(II) ions. *J. Food Sci., 80*(4), N828–N833. doi:10.1111/1750-3841.12811

Guo, H. L., Wang, X. F., Qian, Q. Y., Wang, F. B., & Xia, X. H. (2009). A Green Approach to the Synthesis of Graphene Nanosheets. *ACS Nano, 3*(9), 2653–2659.

Hajjaji, A., El Otmani, M., Bouya, D., Bouseta, A., Mathieu, F., Collin, S., & Lebrihi, A. (2006). Occurrence of mycotoxins (ochratoxin A, deoxynivalenol) and toxigenic fungi in Moroccan wheat grains: impact of ecological factors on the growth and ochratoxin A production. *Mol. Nutr. Food Res., 50*(6), 494–499. doi:10.1002/mnfr.200500196

Jodra, A., Lopez, M. A., & Escarpa, A. (2015). Disposable and reliable electrochemical magnetoimmunosensor for Fumonisins simplified determination in maize-based foodstuffs. *Biosens. Bioelectron., 64*, 633–638. doi:10.1016/j.bios.2014.09.054

Jung, I., Dikin, D. A., Piner, R. D., & Ruoff, R. S. (2008). Tunable electrical conductivity of individual graphene oxide sheets reduced at "low" temperatures. *Nano Lett., 8*(12), 4283–4287.

Kadir, M. K., & Tothill, I. E. (2010). Development of an electrochemical immunosensor for fumonisins detection in foods. *Toxins (Basel), 2*(4), 382-398. doi:10.3390/toxins2040382

Kolosova, A. Y., Shim, W. B., Yang, Z. Y., Eremin, S. A., & Chung, D. H. (2005). Direct competitive ELISA based on a monoclonal antibody for detection of aflatoxin B1. Stabilization of ELISA kit components and application to grain samples. *Anal. Bioanal. Chem., 384*(1), 286–294. doi:10.1007/s00216-005-0103-9

Kuila, T., Bose, S., Khanra, P., Mishra, A. K., Kim, N. H., & Lee, J. H. (2011). Recent advances in graphene-based biosensors. *Biosens. Bioelectron., 26*(12), 4637–4648. doi:10.1016/j.bios.2011.05.039

Lee, N. A., Wang, S., Allan, R. D., & Kennedy, I. R. (2004). A rapid aflatoxin B-1 ELISA: Development and validation with reduced matrix effects for peanuts, corn, pistachio, and soybeans. *J. Agric. Food Chem., 52*(10), 2746–2755. doi:10.1021/jf0354038

Li, J., Xie, H., & Li, Y. (2013). Fabrication of graphene oxide/polypyrrole nanowire composite for high performance supercapacitor electrodes. *J. Power Sources, 241*, 388–395. doi:10.1016/j.jpowsour.2013.04.144

Liu, X., Xu, Y., He, Q. H., He, Z. Y., & Xiong, Z. P. (2013). Application of mimotope peptides of fumonisin b1 in Peptide ELISA. *J. Agric. Food Chem., 61*(20), 4765–4770. doi:10.1021/jf400056p

Luo, Z., Lu, Y., Somers, L. A., & Johnson, A. T. (2009). High yield preparation of macroscopic graphene oxide membranes. *J. Am. Chem. Soc., 131*(3), 898–899. doi:10.1021/ja807934n

Marcano, D. C., Kosynkin, D. V., Berlin, J. M., Sinitskii, A., Sun, Z., Slesarev, A., . . . Tour, J. M. (2010). Improved Synthesis of Graphene Oxide. *ACS Nano, 4*(8), 4806–4814. doi:10.1021/nn1006368

Monbaliu, S., Van Poucke, C., Detavernier, C., Dumoulin, F., Van De Velde, M., Schoeters, E., . . . De Saeger, S. (2009). Occurrence of mycotoxins in feed as analyzed by a multi-

mycotoxin LC-MS/MS method. *J. Agric. Food Chem., 58*(1), 66–71. doi:10.1021/jf903859z

NGFA. (2011). *National Grain and Feed Association. FDA Mycotoxin Regulatory Guidance.* https://www.ngfa.org/wp-content/uploads/NGFAComplianceGuide-FDARegulatoryGuidanceforMycotoxins8-2011.pdf *(Accessed March 28, 2016)*.

Pietri, A., Zanetti, M., & Bertuzzi, T. (2009). Distribution of aflatoxins and fumonisins in dry-milled maize fractions. *Food Addit. Contam. A, 26*(3), 372–380. doi:Doi 10.1080/02652030802441513

Pii 908706643

Pumera, M. (2011). Graphene in biosensing. *Mater. Today, 14*(7-8), 308–315. doi:10.1016/s1369-7021(11)70160-2

Qian, T., Yu, C., Zhou, X., Wu, S., & Shen, J. (2014). Au nanoparticles decorated polypyrrole/reduced graphene oxide hybrid sheets for ultrasensitive dopamine detection. *Sensor Actuat. B–Chem., 193*, 759–763. doi:10.1016/j.snb.2013.12.055

Ran, R., Wang, C., Han, Z., Wu, A., Zhang, D., & Shi, J. (2013). Determination of deoxynivalenol (DON) and its derivatives: Current status of analytical methods. *Food Control, 34*(1), 138–148. doi:10.1016/j.foodcont.2013.04.026

Ricci, F., Flavio, P., Abagnale, M., Messia, M., Marconi, E., Volpe, G., . . . Palleschi, G. (2009). Direct electrochemical detection of trichothecenes in wheat samples using a 96-well electrochemical plate coupled with microwave hydrolysis. *World Mycotoxin J., 2*(2), 239–245. doi:doi:10.3920/WMJ2008.1133

Romanazzo, D., Ricci, F., Volpe, G., Elliott, C. T., Vesco, S., Kroeger, K., . . . Palleschi, G. (2010). Development of a recombinant Fab-fragment based electrochemical immunosensor for deoxynivalenol detection in food samples. *Biosens. Bioelectron., 25*(12), 2615–2621. doi:10.1016/j.bios.2010.04.029

Seenivasan, R., Chang, W. J., & Gunasekaran, S. (2015). Highly sensitive detection and removal of lead ions in water using cysteine-functionalized graphene oxide/polypyrrole nanocomposite film electrode. *Acs Appl. Mater. Inter., 7*(29), 15935–15943. doi:10.1021/acsami.5b03904

Seenivasan, R., Maddodi, N., Setaluri, V., & Gunasekaran, S. (2015). An electrochemical immunosensing method for detecting melanoma cells. *Biosens. Bioelectron., 68*, 508–515. doi:10.1016/j.bios.2015.01.022

Shrivastava, A., & Gupta, V. B. (2011). Methods for the determination of limit of detection and limit of quantitation of the analytical methods. *Chron. Young Sci., 2*(1), 21–25 doi:10.4103/2229-5186.79345

Si, P., Chen, H., Kannan, P., & Kim, D.-H. (2011). Selective and sensitive determination of dopamine by composites of polypyrrole and graphene modified electrodes. *Analyst, 136*(24), 5134–5138. doi:10.1039/C1AN15772H

Soares, C., Rodrigues, P., Freitas-Silva, O., Abrunhosa, L., & Venancio, A. (2010). HPLC method for simultaneous detection of aflatoxins and cyclopiazonic acid. *World Mycotoxin J., 3*(3), 225–231. doi:Doi 10.3920/Wmj2010.1216

Srivastava, S., Kumar, V., Ali, M. A., Solanki, P. R., Srivastava, A., Sumana, G., . . . Malhotra, B. D. (2013). Electrophoretically deposited reduced graphene oxide platform for food toxin detection. *Nanoscale, 5*(7), 3043-3051. doi:10.1039/c3nr32242d

Sun, G., Wang, S., Hu, X., Su, J., Zhang, Y., Xie, Y., . . . Wang, J. S. (2011). Co-contamination of aflatoxin B-1 and fumonisin B-1 in food and human dietary exposure in three areas of China. *Food Addit. Contam. A, 28*(4), 461–470. doi:Doi 10.1080/19440049.2010.544678

Sunday, C. E., Masikini, M., Wilson, L., Rassie, C., Waryo, T., Baker, P. G., & Iwuoha, E. I. (2015). Application on gold nanoparticles-dotted 4-nitrophenylazo graphene in a label-free impedimetric deoxynivalenol immunosensor. *Sensors (Basel), 15*(2), 3854-3871. doi:10.3390/s150203854

Theumer, M. G., Lopez, A. G., Aoki, M. P., Canepa, M. C., & Rubinstein, H. R. (2008). Subehronic mycotoxicoses in rats. Histopathological changes and modulation of the sphinganine to sphingosine (Sa/So) ratio imbalance induced by Fusarium verticillioides culture material, due to the coexistence of aflatoxin B1 in the diet. *Food. Chem. Toxicol., 46*(3), 967–977. doi:DOI 10.1016/j.fct.2007.10.041

Turkevich, J., Stevenson, P. C., & Hillier, J. (1951). A study of the nucleation and growth processes in the synthesis of colloidal gold. *Discuss. Faraday Soc., 11*, 55–75.

Unnikrishnan, B., Palanisamy, S., & Chen, S. M. (2013). A simple electrochemical approach to fabricate a glucose biosensor based on graphene-glucose oxidase biocomposite. *Biosens. Bioelectron., 39*(1), 70–75. doi:10.1016/j.bios.2012.06.045

Wang, F., Wang, J., Chen, H., & Dong, S. (2007). Assembly process of CuHCF/MPA multilayers on gold nanoparticles modified electrode and characterization by electrochemical SPR. *J. Electroanal. Chem., 600*(2), 265–274. doi:http://dx.doi.org/10.1016/j.jelechem.2006.10.008

Wang, M., Yuan, W., Yu, X., & Shi, G. (2014). Picomolar detection of mercury (II) using a three-dimensional porous graphene/polypyrrole composite electrode. *Anal. Bioanal. Chem., 406*(27), 6953–6956. doi:10.1007/s00216-014-7871-z

Wang, X., Xing, W., Yu, B., Feng, X., Song, L., & Hu, Y. (2013). A facile and cost-effective approach to the reduction of exfoliated graphite oxide using sodium hypophosphite under acidic conditions. *J. Mater. Chem. C, 1*(4), 690–694. doi:10.1039/c2tc00259k

Wang, Y.-C., Cokeliler, D., & Gunasekaran, S. (2015). Reduced Graphene Oxide/Carbon Nanotube/Gold Nanoparticles Nanocomposite Functionalized Screen-Printed Electrode for Sensitive Electrochemical Detection of Endocrine Disruptor Bisphenol A. *Electroanalysis*, n/a-n/a. doi:10.1002/elan.201500120

Wang, Y. C., & Gunasekaran, S. (2012). Spectroscopic and microscopic investigation of gold nanoparticle nucleation and growth mechanisms using gelatin as a stabilizer. *J. Nanopart. Res., 14*(10), 1–11. doi:10.1007/s11051-012-1200-2

Xu, X., Huang, D., Cao, K., Wang, M., Zakeeruddin, S. M., & Gratzel, M. (2013). Electrochemically reduced graphene oxide multilayer films as efficient counter electrode for dye-sensitized solar cells. *Sci. Rep., 3*, 1489. doi:10.1038/srep01489

Yang, X., Zhou, X., Zhang, X., Qing, Y., Luo, M., Liu, X., . . . Qiu, J. (2015). A Highly Sensitive Electrochemical Immunosensor for Fumonisin B1Detection in Corn Using Single-Walled Carbon Nanotubes/Chitosan. *Electroanal., 27*(11), 2679–2687. doi:10.1002/elan.201500169

Yang, Y., Asiri, A. M., Du, D., & Lin, Y. (2014). Acetylcholinesterase biosensor based on a gold nanoparticle-polypyrrole-reduced graphene oxide nanocomposite modified electrode for the amperometric detection of organophosphorus pesticides. *Analyst, 139*(12), 3055-3060. doi:10.1039/c4an00068d

Yi, C., Qi, S., Zhang, D., & Yang, M. (2010). Covalent conjugation of multi-walled carbon nanotubes with proteins. *Methods Mol. Biol., 625*, 9–17. doi:10.1007/978-1-60761-579-8_2

Yoo, H. D., Jang, J. H., Cho, K., Zheng, Y., Park, Y., Ryu, J. H., & Oh, S. M. (2015). Effects of Interlayer Distance and van der Waals Energy on Electrochemical Activation of Partially Reduced Graphite Oxide. *Electrochim. Acta, 173*, 827–833. doi:http://dx.doi.org/10.1016/j.electacta.2015.05.113

Zhilei, W., Xiulan, S., Zaijun, L., Yinjun, F., Guoxiao, R., Yaru, H., & Junkang, L. (2011). Highly sensitive deoxynivalenol immunosensor based on a glassy carbon electrode modified with a fullerene/ferrocene/ionic liquid composite. *Microchim. Acta, 172*(3), 365–371.

Zhong, J., Gao, S., Xue, G., & Wang, B. (2015). Study on Enhancement Mechanism of Conductivity Induced by Graphene Oxide for Polypyrrole Nanocomposites. *Macromolecules, 48*, 1592–1597. doi:10.1021/ma502449k

Zhu, C., Zhai, J., Wen, D., & Dong, S. (2012). Graphene oxide/polypyrrole nanocomposites: one-step electrochemical doping, coating and synergistic effect for energy storage. *J. Mater. Chem., 22*(13), 6300–6306. doi:10.1039/C2JM16699B

CHAPTER 5 Electrochemical Immunosensor Incorporated with Microfluidic Devices on ITO Microelectrode for Simultaneous Detection of Mycotoxins

Abstract

Due to the widely occurring co-contamination of mycotoxins in raw food materials, the simultaneous monitoring of multiple mycotoxins is needed. Herein, we report an electrochemical biosensor fabricated on ITO-coated glass, based on antibody-toxin specific recognition, and microfluidic technology for the detection of mycotoxins FB1 and DON in a single test. A slightly modified three-electrode electrochemical pattern with two working electrodes were designed and printed on an ITO-coated glass slide using photolithography. The working electrodes were functionalized with AuNPs and toxin-specific antibodies, and a drop of sample solution was incubated with both working electrodes in a PDMS microfluidic channel. In presence of target toxins, the antibodies tend to form toxin-antibody complexes on the working electrode surface and thus change the electrochemical signal responses, which is recorded and compared with control signal to quantify the toxin concentrations. The dual-channel electrochemical immunosensor demonstrated detection limits for FB1 and DON were 97 pg/mL and 35 pg/mL respectively, and the corresponding detection range were 0.3 to 140 ppb and 0.2 to 60 ppb. This method also shows good performance in real food matrix such as corn, and was proved to be stable for 2 weeks under proper storage. The developed biosensors provide a promising way to closely screen multiple mycotoxins in a single assay.

5.1 Introduction

Some fungi produce more than one toxins and more than one fungal species can infect plants with synergistic effects, variable patterns of contamination have been observed, and when contamination occurs, often multiple toxins are detectable (Miller, 1992). For example, AF and FUM are co-contaminants often found in corn (Castells, Marin, Sanchis, & Ramos, 2008; Sun et al., 2011; Theumer, Lopez, Aoki, Canepa, & Rubinstein, 2008; Theumer, Lopez, Masih, Chulze, & Rubinstein, 2003), milled corn fractions (Castells et al., 2008; Pietri, Bertuzzi, Agosti, & Donadini, 2010; Pietri, Zanetti, & Bertuzzi, 2009), rice and wheat flour (Sun et al., 2011), and malted barley (Pietri et al., 2010); DON, ZEA, and nivalenol in wheat (Muthomi, Ndung'u, Gathumbi, Mutitu, & Wagacha, 2008); patulin, cyclopiazonic acid, penicillic acid, diacetoxyscirpenol (WAREING, 1998) and AF (Eboku, 2010) in cassava; and AF, FUM, OTA, and ZEA in sows/sow feeds (Carina Maricel Pereyra, 2010). DON and OTA are also common co-contaminants in wheat (Arino, Herrera, Juan, & Estopanan, 2009; Birzele, Prange, & Kramer, 2000; Conkova, Laciakova, Styriak, Czerwiecki, & Wilczynska, 2006; Hajjaji et al., 2006). In a study, when the occurrence of mycotoxins in agricultural commodities, including corn, compound animal feeds, silage, cornmeal, puffed corn, wheat, bran, soybean meal, rapeseed meal, distillers dried grains with solubles, total mixed ration, concentrate supplement, cottonseed meal and whole cottonseed, was tested for major mycotoxins namely aflatoxin B_1 (AFB_1), ZEA, DON, FUM, fusariotoxin T-2 and OTA, almost all (98%) samples were contaminated with more than one mycotoxins (Yin et al., 2011). Therefore, techniques that are capable of detecting only one mycotoxin is far away from satisfying the urgent need in the food industry to effectively address the mycotoxin-related health issues to humans and animals. More efforts should be put into developing sensors for multiple mycotoxins detection.

For simultaneous monitoring of mycotoxins co-contamination in grain, the following techniques have been investigated by researchers in the past, including suspension array in corn and peanut (Ying Wang, 2013; Yue Sun 2014), liquid chromatography (Kong, 2013), immunochromatographic array (Li Xin, 2013), immunoassay lateral flow (Song 2014), optical sensor (Zhang Jing 2016). Large amount of studies were found using HPLC/GC-MS, then immunoassay, and some optical, especially fluorescence method. The instrumental analytical methods and ELISA require expensive equipment and skilled operators, as well as large sample volume and complicated sample pretreatment.

Electrochemical biosensors incorporated with nanomaterials have been extensively studied in the medical and clinical fields, for simultaneous detection of multiple viruses, cancer biomarkers, cancer cells, and chemicals. However, due to the different chemical and biological properties of medical specimens and mycotoxins, these detection methods may not be directly applied to the detection of mycotoxins. To the best of our knowledge, there is very limited literature focused on electrochemical biosensing for simultaneous detection of mycotoxins. Muhammad et al. (Ref?) reported some preliminary data claiming that mycotoxins zearalenonoe (ZEA) and citrinin (CIT) can be well distinguished by two separated oxidation peaks on a DPV curve, on pyrolytic graphite electrode. The authors tested the mixture of CIT and ZEA solution with four different electrode materials including edge-plane pyrolytic graphite (EPPG), basal plane pyrolytic graphite (BPPG), glassy carbon (GC) and boron-doped diamond (BDD), and the results showed that only some of these electrodes were able to show different DPV peaks assigned to ZEA and CIT, among which EPPG performs the best. However, the authors failed to explain the reasons for this detection behavior, which provided little information to peer researchers. The authors then tested a serial concentrations of the toxins mixture on EPPG

electrode, by fixing one toxin concentration and varying the other, and so on. The recorded DPV peak heights did decrease with decreased toxin concentrations; however, the peak heights for the unchanged toxin also decreased in a relative apparent manner, which made the data less convincing in terms of specificity. In summary, the study presented in Muhanmud et al. paper serves as a preliminary research that proves the possibility of simultaneous electrochemical detection of multiple mycotoxins based on choice of proper electrode. Very recently, Wang et al., 2017 reported an electrochemical aptasensor for simultaneous detection of FB1 and OTA, based on magnetic beads and metal sulfide quantum dots. The sensing mechanism is similar to a competitive ELISA, given that the toxin-specific aptamer immobilized on metal quantum dots (resembles the toxin-specific antibody in ELISA) prefer to bind with target toxins rather than cDNA fragments immobilized on the magnetic beads, leading to the release of preloaded quantum dots labels from magnetic beads. The amount of quantum dots labels remained on magnetic beads is reversely proportional to the toxin concentration in sample. These remained labels are easily collected by an external magnetic field and dissolved to be metal ions, which are ready to be measured by square wave voltammetry stripping technique. The sensor has achieved a detection limit of 20 pg/mL and 5 pg/mL for FB1 and OTA respectively, and proved effective in maize sample. However, it takes few hours and multiple steps to prepare quantum dots coated SiO2 label and cDNA conjugated magnetic beads. Also, unlike well-developed antibody-based immunosensors, the appropriate aptamer selection and determination for each desired mycotoxin requires tremendous work and could be an obstacle for wide application of this type of sensor.

This situation and the successful electrochemical biosensor developed in our lab in previous studies have motivated us to expand the biosensor platform from single working electrode to multi-electrode for the detection of multiple toxins at the same time.

Herein, we report a dual-working electrode electrochemical immunosensor on ITO with capillary driven microfluidic system for simultaneous detection of FB1 and DON in corn.

5.2 Experimental

5.2.1 Materials and reagents

SPEs (TE100) were purchased from CH Instruments, Inc. (Bee Cave, TX, USA). ITO-coated glass slides (2.54 cm×7.62 cm) were purchased from Nanocs Inc., USA. Positive photoresist (MICROPOSIT S1813) and developer MF-321 were purchased from Shipley Company, USA. Gold (III) chloride trihydrate (HAuCl4·3H2O) (99.9+%) and 3-mercaptopropionic acid (MPA, 99+%) were purchased from Acros Organics. FB1, DON and bovine serum albumin (BSA) were purchased from Sigma-Aldrich (St. Louis, MO, USA). Monoclonal anti-DON mouse antibody (1 mg/mL) and monoclonal anti-FB1 mouse antibody (1 mg/mL) were purchased from Antibodies-online.com (Atlanta, GA, USA). Immobilization of antibodies onto the electrode surface was performed using 1-ethyl-3-(3-dimethylaminopropyl) carbodiimide (EDC) and N-hydroxysuccinimide (NHS) chemistry with a minimum purity of 98% or higher (Bioworld, Dublin, OH, USA and Acros Organics). Phosphate buffered saline (PBS) 10X, methanol (99.8%), sulfuric acid (96 %), hydrogen peroxide (50 %), and hydrochloric acid (36.5–38 %) were from Fisher Scientific (Rockford, IL, USA). Potassium ferrocyanide trihydrate (reagent grade) and potassium chloride were acquired from Fisher Science Education (Hanover Park, IL, USA). Potassium ferricyanide, sodium phosphate monobasic (NaH_2PO_4) and sodium phosphate dibasic (Na_2HPO_4) were certified A.C.S. reagents from Thermo Fisher Scientific (Fair Lawn, NJ, USA). All chemicals were used as received without any purification,

and deionized (DI) water of resistivity ⩾18.2 MΩ.cm (Ultrapure water system, Millipore, Billerica, MA, USA) used for solution preparation and all experiments.

5.2.2 Photolithographic fabrication of patterned ITO electrode

Four identical 3-electrode sensor arrays were patterned on an ITO-coated glass slide using photolithographic method as depicted in Scheme 5.1. A customized photomask was used to facilitate each of the 3-electrode sensors (1.2 x 1.5 mm working electrode (WE), 0.5 x 1.5 mm counter electrode (CE), and 0.5- x 1.5-mm reference electrode (RE)) along with three 3 x 3 mm connection sites. Positive photoresist lithography followed by wet-etching was performed according to Seenivasan's method (Seenivasan, Singh, Warrick, Ahmad, & Gunasekaran, 2017). Briefly, ITO–coated glass slide was first pretreated with acetone, isopropanol, ethanol and DI water step-wisely for three times each, and air-dried prior to positive photoresist patterning. After chemical pretreatment, the ITO glass slide was taped down in a spin-coater and the positive photoresist was spin-coated on the slide surface at 500 rpm for 5 s followed by 2500 rpm for 60 s to form a thin and even PR film. Then, the positive photoresist –coated slide was soft-baked on a hot plate at 110 °C for 60 s, exposed to UV light (energy density 300 W/cm^2) through the photomask for 60 s, developed in MF-321 developer solution under slow shaking motion for 60 s to remove exposed positive photoresist, washed with DI water twice to remove any residual developing solution, and finally air dried. Next, the ITO slide was soaked in an etchant solution containing 8 mL concentrated hydrochloric acid (HCl), 2 mL DI water, and 4 mL concentrated nitric acid (HNO_3) for about 3 min at room temperature. After etching, the remaining positive photoresist was removed with acetone and isopropanol under slow shaking motion followed by washing with DI water and air drying. The resulting patterned ITO electrode was examined

under an optical microscope to ensure there is no open or short circuit using a multimeter before further use.

In order to make a three-electrode system for electrochemical detection, an Ag/AgCl pseudo-reference electrode is needed. This can be done by placing a silver paint (Tedpella, USA) on one ITO electrode (dimension 0.5 x1.5 mm) and air dried. Then the ITO slide is subjected to a linear sweep voltammetric scanning from 0 to +0.3 V at 300 mV/s scan rate for 1 cycle to form Ag/AgCl in 0.1 M HCl deposition solution (Almeida et al. 2008; Polk et al. 2006). Thus, a fully functional basic three-electrode electrochemical system is completed.

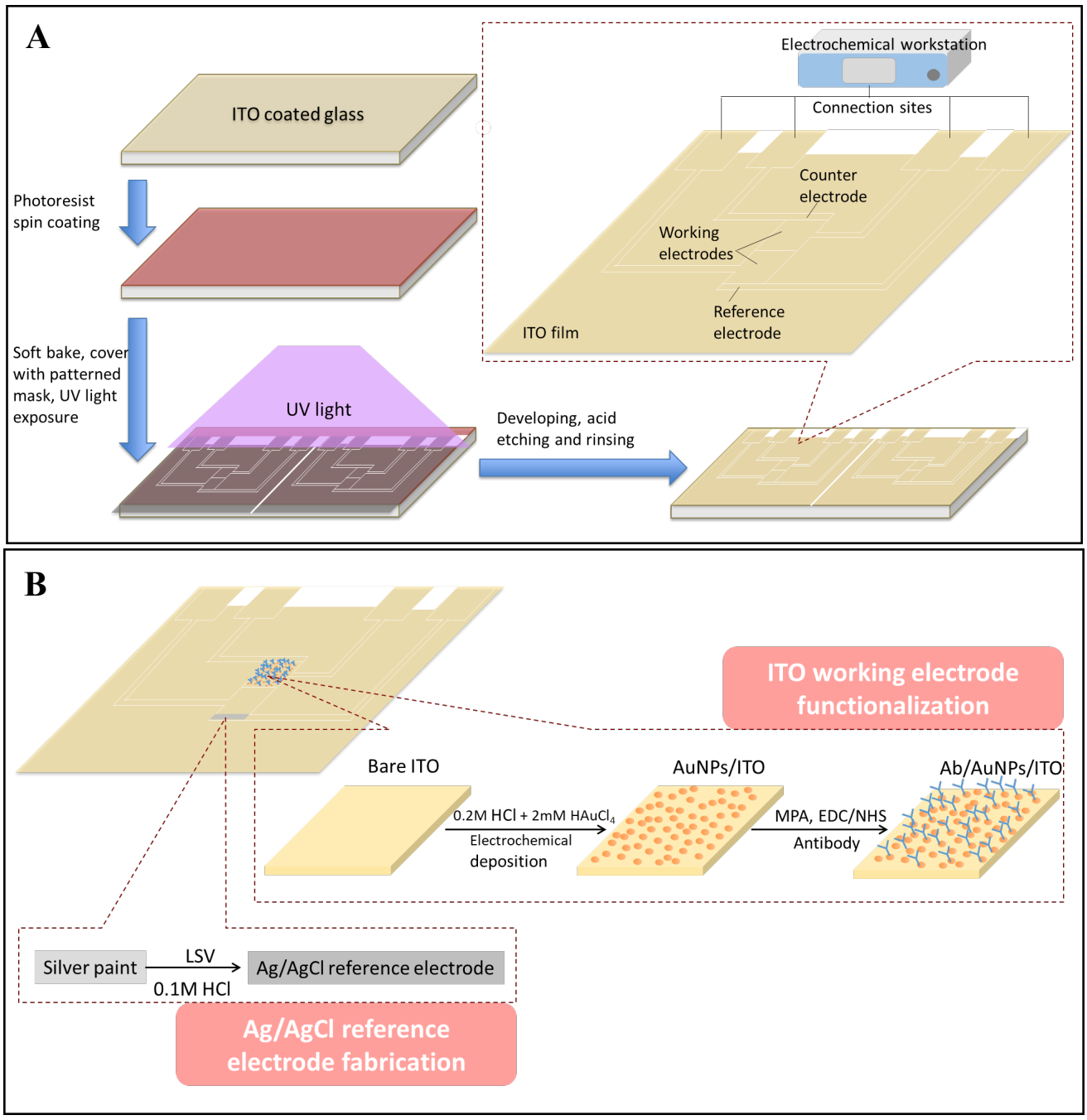

Scheme 5.1 (A) Fabrication of ITO electrode array using photolithography and enlarged view of one ITO three-electrode unit with double working electrodes. (B) Pseudo Ag/AgCl reference electrode fabrication and working electrode modification steps

5.2.3 Functionalization of the ITO immunosensor

As shown in Scheme 5.1B, after electrochemical deposition of AuNPs on working electrodes, specific anti-toxin antibodies were immobilized on the electrode surface via the well-known EDC/NHS mechanism. Briefly, the AuNPs-ITO electrode was first incubated in 20 µL of 10 mM MPA solution and left for 6 h at room temperature to allow the formation of Au-S bond. After rinsing with DI water three times, the MPA-functionalized electrode was incubated for one hour at room temperature in an activation solution of EDC/NHS (2 mM/5 mM in 1X PBS, pH 6.0) to activate the carboxyl groups for effective immobilization of antibodies on the electrode surface (Yi, Qi, Zhang, & Yang, 2010). The electrode was washed three times with DI water to remove any excess EDC/NHS and by-products followed by incubated with 20 µL of anti-FB1 or anti-DON antibody solution (pH 9.0) at 4 °C overnight to allow effective antibody immobilization. Finally, the electrode was incubated with 1% BSA for 30 min to block unoccupied sites and washed with 1X PBS.

5.2.4 Incorporation of microfluidic devices

A polydimethylsiloxane (PDMS) microfluidic device is produced using soft lithography, with circled inlet and outlet located at two ends of microfluidic channel. The channel dimension is designed to match the 3 electrode system dimension. The channel is closed from PDMS-air interface, but open at the PDMS-electrode interface. The mycotoxin samples as well as other reagents were injected at the inlet and distributed by a capillary force driven microfluidic PDMS device, which eliminates the use of additional power source, such as a pump. The difference in size of the inlet and outlet ports provides a capillary pressure difference, which drives the sample runs through the channel towards the outlet in a laminar flow mold. The working electrode area

then is able to be fully covered by the sample solution for the antibody-antigen reaction to take place.

5.2.5 Characterization of fabricated ITO sensor

An electrochemical workstation (CHI660D, CH Instruments Inc.) was used for all electrochemical measurements. CV techniques with applied potential range from –0.2 to +0.6 V at a scan rate of 50 mV/s was used for electrochemical characterization of each modified and unmodified electrode in microfluidic channels filled with 20 μL of 1x PBS solution containing 5mM redox probe ferricyanide/ferrocyanide $[Fe(CN)_6]^{3-}/[Fe(CN)_6]^{4-}$ and 0.1 M KCl.

The ITO electrode surface after each modification step was examined using a LEO 1530 scanning electron microscope (SEM).

5.3 Results and discussion

5.3.1 AuNPs deposition on ITO electrode

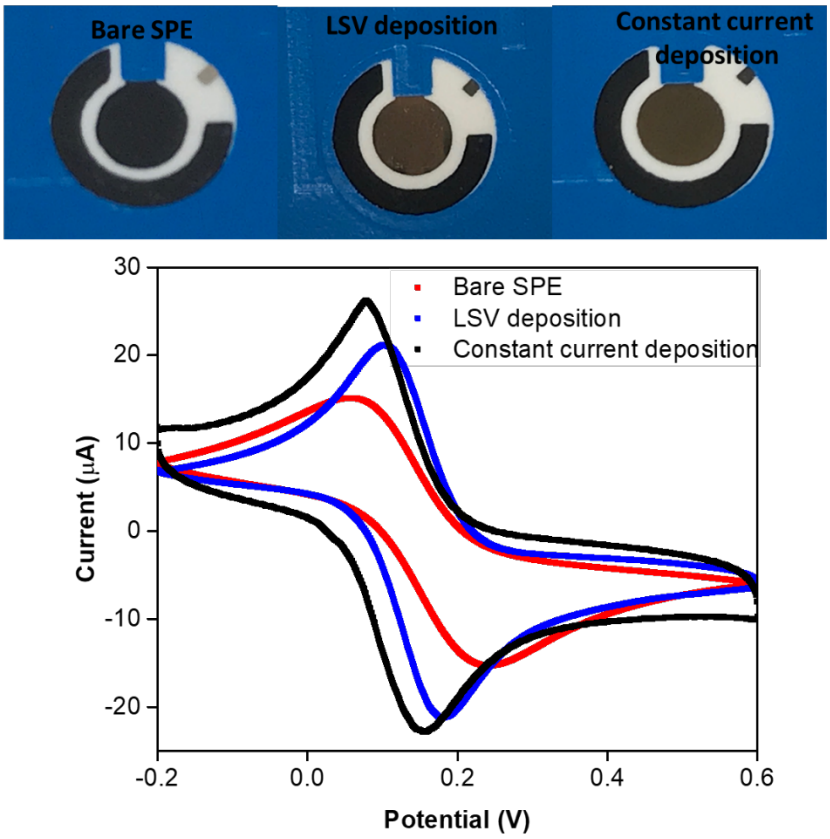

Figure 5.1 1 CV responses of 5 mM [Fe(CN)6]3–/4– in 1M KCl at bare SPE and after electrochemical AuNPs deposition using linear sweep voltammetry (LSV) and constant current method respectively. CV scan rate = 50 mV/s and applied potential range = –0.2 to +0.6 V.

Before modifying the ITO electrode with AuNPs, SPEs were used to optimize the electrochemical deposition method. There are many different electrochemical techniques to deposit AuNPs on the electrode surface, among which linear sweep voltammetry (LSV) and constant current methods are two widely used approaches due to their rapidness and simplicity.

The two methods were both tested using SPEs, with 4 mL of 0.2 M HCl solution containing 2 mM $HAuCl_4$. Figure 5.1 shows the CV response of a bare SPE and two SPEs with AuNPs electrochemically coated using LSV and constant current method respectively. Compared to the broad redox peaks of bare SPE, the increased and sharper redox peaks and smaller peak potential separations after AuNPs coating indicate a more efficient electron transfer process at the working electrode and electrolyte interface. This is due to the excellent electric conductivity of AuNPs. By further looking at the actual AuNPs film coated on the SPE, it is obvious that the SPE subjected to constant current (11 mA/cm^2, 60 s) achieves a more uniform AuNPs film with smooth edges. The one went through LSV (0.3~-0.7 V, 100 mV/s) has unevenly coated edges and some defects on surface. Thus, constant current method was selected as the AuNPs deposition method on ITO.

5.3.2 Characterization of functionalized working electrode surface

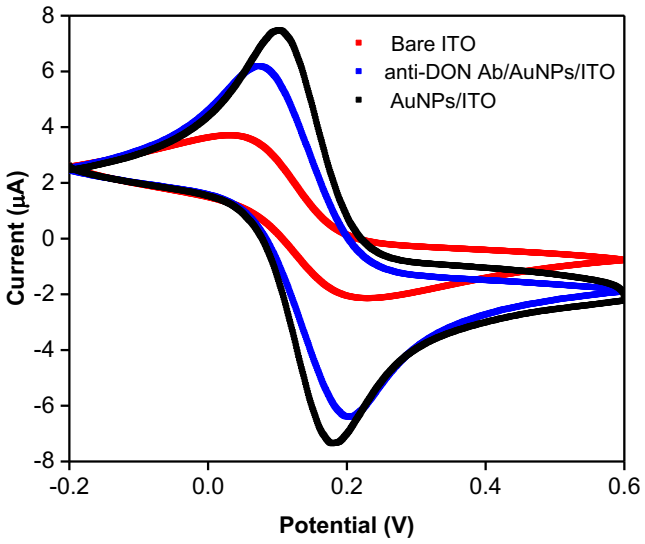

Figure 5.2 CV responses of 5 mM [Fe(CN)6]3–/4– in 1M KCl at bare ITO (red), AuNPs/ITO (black), and anti-DON ab/AuNPs/ITO (blue).

Figure 5.2 shows the CV results of bare ITO electrode without any modification, and after AuNPs deposition and anti-DON antibody immobilization on the working electrode. The CV reponse at bare ITO (Fig. 5.2 red curve) shows broad cathodic and anodic peaks with a large peak separation of 172 mV at 50 mV/s scan rate, indicating a very low electron transfer efficiency. After attaching a densely distributed AuNPs film, the redox peak currents increased drastically while the peak potential separation significantly reduced to 77 mV (Fig. 5.2, black curve), demonstrating a greatly improved electron transfer process due to the increased specific surface area and superior electrical conductivity of AuNPs. Fig. 5.2, blue curve shows that the peak currents dropped slightly after immobilization of an electrical inert anti-DON antibody layer, and the peak separation was also increased to 126 mV (decreased by 26.74% compared to bare ITO). This is due to the insulating effect of the non-conductive antibodies, however the electron transfer efficiency is still significantly enhanced in comparison of bare ITO.

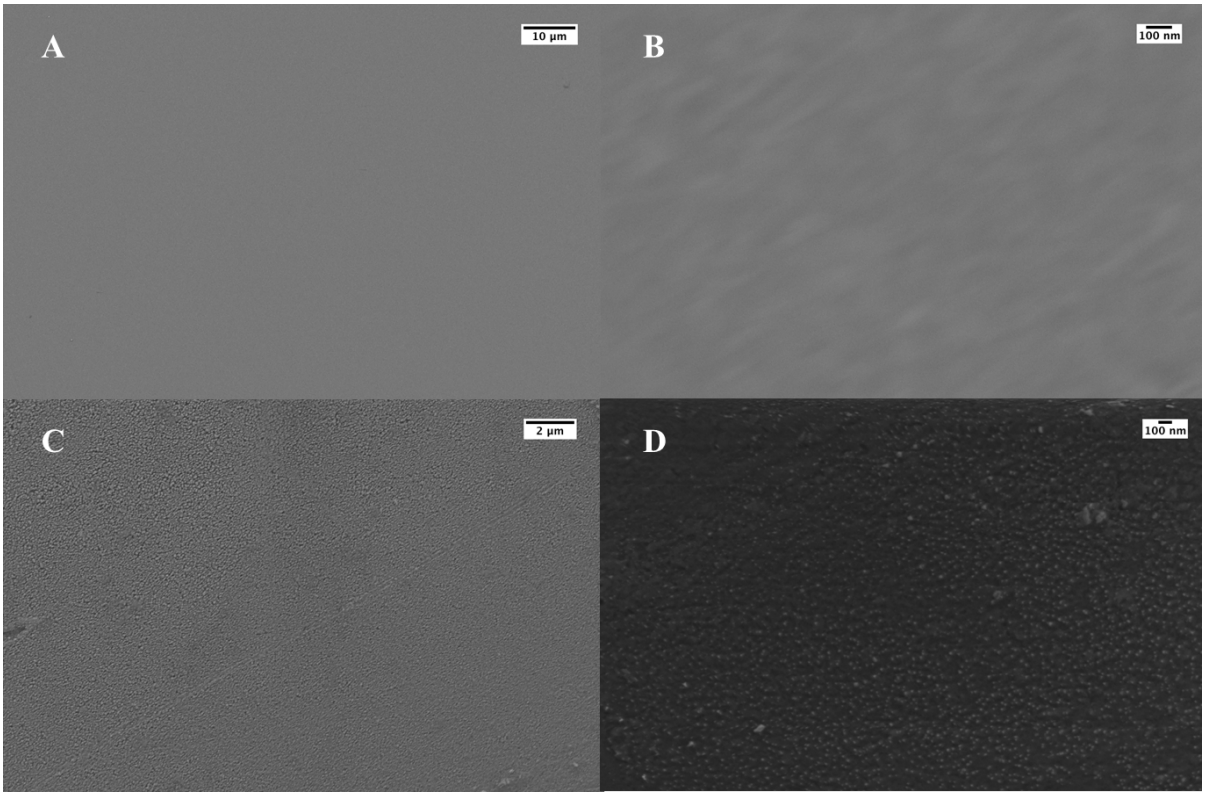

Figure 5.3 SEM images of working electrode surface of (A) bare ITO, (B) enlarged bare ITO, (C) AuNPs/ITO and (D) enlarged AuNPs/ITO.

Fig. 5.3A shows a typical SEM image of bare ITO surface with no modification, and fig.5.3B is the enlarged view of the ITO surface at 100 nm scale. Both figures demonstrate a quite smooth morphology of the bare ITO electrode. Fig. 5.3 C shows the AuNPs modified ITO electrode and fig. 5.3D is the closer view of these AuNPs. From the figures we can see, gold nanoparticles have been successfully deposited on the surface of ITO substrate using direct electrochemical deposition. As can be seen in fig.5.3 C& D, the electrode surface becomes rougher than that of the bare ITO due to the addition of AuNPs, and the average diameter of deposited AuNPs is about 20 nm and they are densely and uniformly distributed on top of the ITO surface. Compared to physically adsorbed AuNPs film by drop coating, the size of electrochemically deposited AuNPs are more uniform with less clusters. In addition, the AuNPs film produced by this method is more stable on working electrode and has no other functional groups on surface. The SEM results further confirms the increased CV redox current and decreased peak potential separation after AuNPs deposition.

5.3.3 Optimization of antibody concentration

In our previous study we optimized the antibody loadings for both FB1 and DON at SPE working electrode. Since the change of working electrode material and surface area, the antibody concentration needs to be optimized again. The DPV responses to different anti-toxin antibody concentrations immobilized on the AuNPs-ITO electrode were recorded after incubation the working electrode with 10 μL antibody solution at 0, 2, 4, 6, 8 μg/mL

respectively. It is clearly shown in Fig. 5.4 that the peak current amplitude drastically decreases with the increase of antibody concentration from 0 to 4 µg/mL, while starts to slightly increase when antibody concentration continues to increase. This trend was observed in both FB1 and DON tests. This indicates that there is no more binding sites for more antibodies on the working electrode surface when the antibody concentration goes beyond 4 µg/mL for both antibodies, and further increasing the antibody concentration may adversely affect the efficient immobilization of these antibodies. Thus, the optimized concentration was selected as 4 µg/mL for both FB1 and DON antibodies.

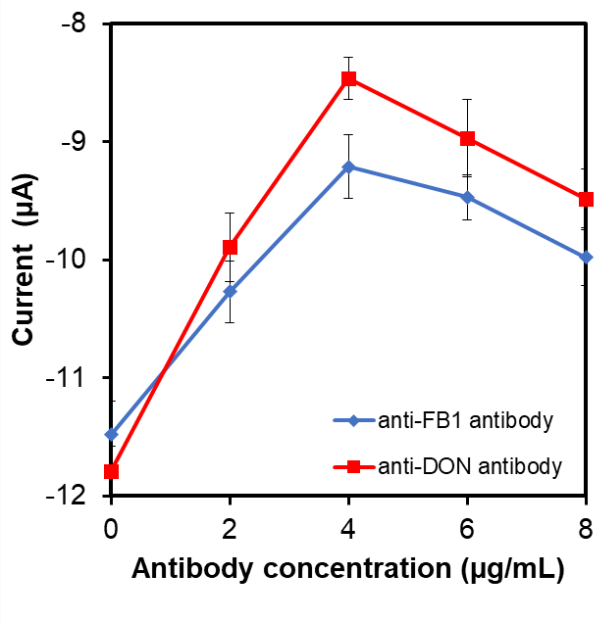

Figure 5.4 Effect of antibody concentration on peak current response of the ITO immunosensor.

5.3.4 Optimization of pH

pH of the antibody-toxin binding buffer is a critical factor to determine the efficiency of the interaction between antibody and toxin. The pH effect on the DPV current

response of the ITO immunosensor was evaluated from pH 5.0 to pH 9.0. The applied antibody concentration was 4 µg/mL for both DON and FB1, and the incubation time was 60 min. Fig. 5.5 summarizes the DPV peak currents obtained at pH 5, 6, 7, 7.4, 8 and 9 in the presence of 1ppm FB1 and 1 ppm DON, respectively. Given the initial peak current (not shown in fig. 5.5) of anti-FB1 ab/AuNPs/ITO electrode at pH 7.4 in the absence of FB1 was -9.72 mV and the initial peak current of anti-FB1 ab/AuNPs/ITO electrode at pH 7.4 in the absence of FB1 was -7.13 mV, both curves in fig. 5.5 clearly indicate that the antibody-antigen binding was greatly suppressed in acidic pH environment and slightly inhibited at pH 8 and pH 9. The maximum current reduction compared to initial current occurs at pH 7.4 for both FB1 and DON, thus pH 7.4 was selected as the optimal pH value for antibody-toxin interaction.

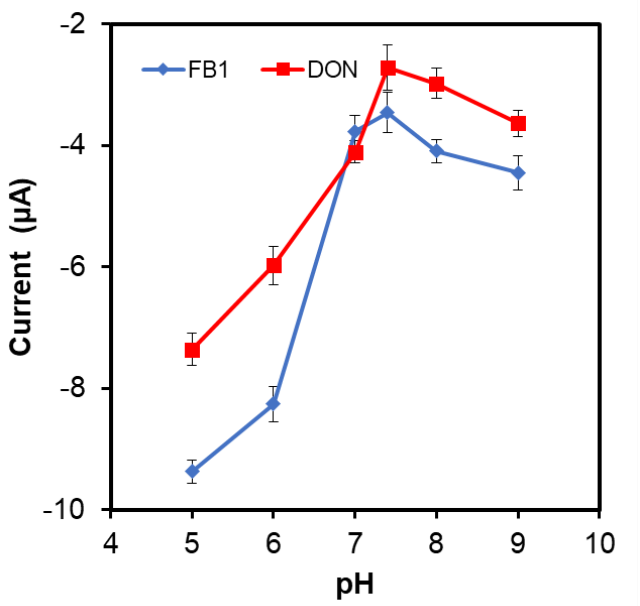

Figure 5.5 Effect of pH of the antibody-toxin interaction buffer on peak current response of the ITO immunosensor.

5.3.5 Optimization of incubation time

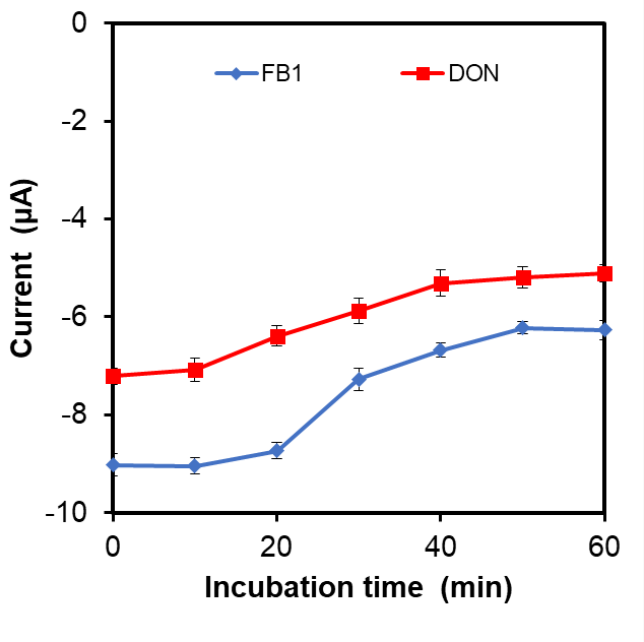

Figure 5.6 Dependence of the DPV peak current on the incubation time in the presence of DON and FB1.

The incubation time of the antibody-immobilized ITO electrode in the presence of 1 ppm of each toxin was investigated respectively and is shown in Fig. 5.6 At the initial 10 min of incubation for both FB1 and DON, the peak current signal shows negligible change, and after 10 min, the magnitude of peak currents of both analytes starts to decrease with the increase of incubation time. Finally, the signal reaches its plateaus at 50 min for FB1 and at 40 min for DON. Considering the simultaneous detection demand, 50 min was selected as the optimized incubation time for both toxins.

5.3.6 Sensitivity, specificity, reproducibility and stability

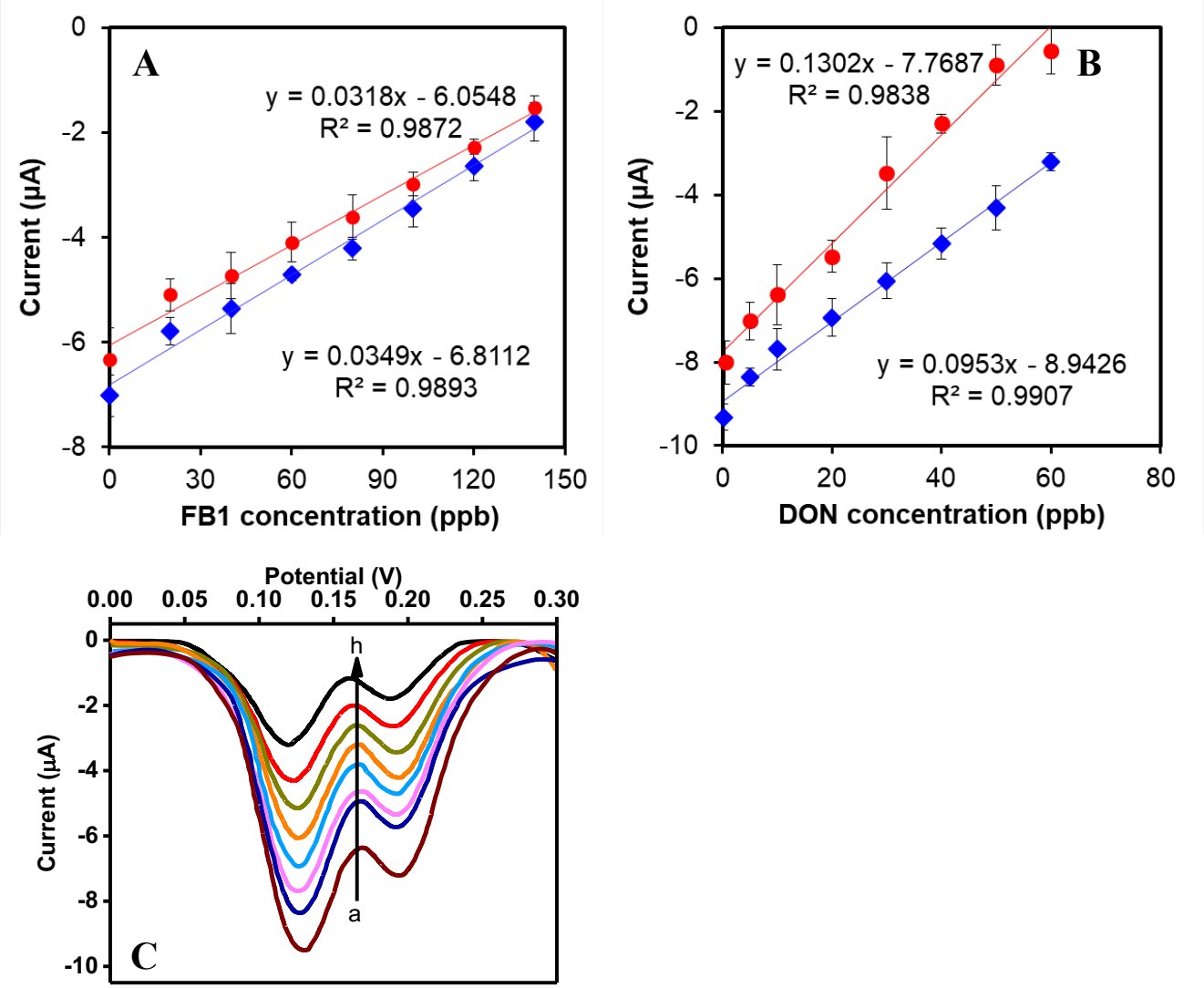

Figure 5.7 Linear calibration of DPV peak current measured at applied potential of 0-0.3 V using the double working electrodes immunosensor for (A) 0.3 to 140 ppb FB1 in buffer (blue) and corn extract (red), and (B) 0.2 to 60 ppb DON in buffer (blue) and corn extract (red). Values are mean of three independent measurements and error bars are standard deviations. (C) DPV results of simultaneous detection of FB1 (left peak series) and DON (right peak series) after incubating the ITO electrodes with toxin mixture.

Figure 5.7C shows the serial of dual-peak DPV curves obtained using the double-working electrode ITO immunosensor in the presence of both DON and FB1 at different concentrations. The left side peaks occurred at potentials between 0.12 and 0.13 V in accordance with FB1, and the right side peaks occurred at potentials around 0.19 V represents DON (The peak potential range for each toxin generally agrees with the peak potentials when being tested individually either using ITO immunosensor in present chapter or using Ab-AuNPs-PPy/ErGO-SPE immunosensor in chapter 4.).

The DPV peak currents obtained using spiked DON and FB1 in PBS buffer (blue calibration curves in fig. 5.7 A & B) show well-defined linear calibration curve in the range of 0.2 to 60 ppb (DON, R^2=0.9907) and 0.3 to 140 ppb (FB1, R^2=0.9893) respectively. According to the calibration curves, the limit of detection (LOD=3*standard deviation of blank/slope) for DON and FB1 were 35 pg/mL and 97 pg/mL respectively. The detection sensitivity for DON and FB1 and DON are 0.095 and 0.035 μA/ppb, respectively Therefore, the microfluidic incorporated ITO immunosensor was able to detect two mycotoxins at the same time with good sensitivity and working range.

The calibration curves (red curves in fig. 5.7 A & B) for DON and FB1 spiked into the corn extracts show generally similar trend to that of toxin spiked buffer samples, which is confirmed by the similar linear regression equations. This means the sensing method maintained its performance in food complex with negligible matrix effect, which is of great importance to a successful biosensor.

AFB1 was used as the interfering agent to evaluate the specificity of this ITO immunosensor. Fig. 5.8 demonstrates that in comparison of the blank sample, the peak current

dramatically decreased in the presence of target toxins DON and FB1, while was only slightly affected in the presence of AFB1. Such results indicate that the immobilized DON and FB1 antibodies have successfully captured their target in the presence of non-target AFB1. This confirms that the sensor is capable of specifically recognizing only target toxins in a mixture of multiple analytes.

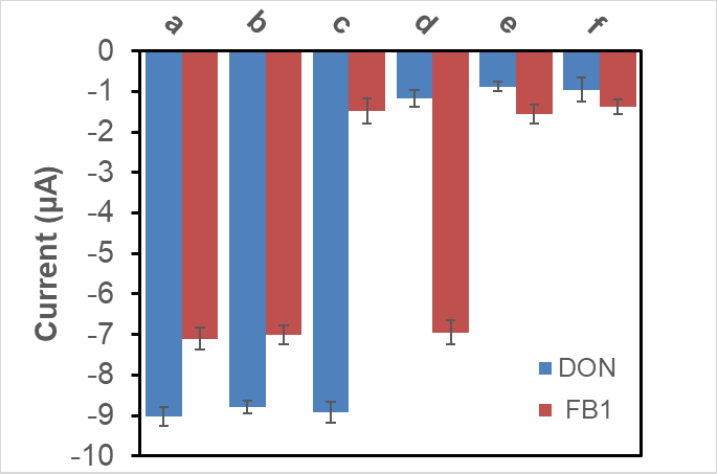

Figure 5.8 Specificity of the ITO immunosensor in toxin mixtures of (a) 1X PBS, no toxin, (b) 500 ppb AFB1 in 1X PBS, (c) 500 ppb AFB1 and 500 ppb FB1 in 1X PBS, (d) 500 ppb AFB1 and 500 ppb DON in 1X PBS, (e) 500 ppb AFB1, 500 ppb FB1 and 500 ppb DON in 1X PBS, (f) 500 ppb FB1 and 500 ppb DON in 1X PBS.

To examine the reproducibility of the microfluidic incorporated double-working electrode ITO immunosensor, relative standard deviation (%RSD) of three independent DPV measurements against a toxin mixture containing 1 ppm of each toxin was calculated. The values

were 4.3% for DON and 6.2% for FB1, which were reasonable values indicating reliable sensing performance.

The stability of the fabricated ITO immunosensor was determined by measuring DPV responses of the antibody/AuNPs/ITO electrode with anti-FB1 and anti-DON antibodies immobilized respectively on each working electrode under the optimized conditions. After storing the electrode in 1X PBS at 4 °C for up to two weeks, the peak current signals were similar to that of day one, with an average of 7.31% change in magnitude, showing good stability over two weeks under proper storage condition.

Table 5.1 summarizes recent (2010 to present) literatures with a focus on simultaneous detection of at least two types of mycotoxins using various sensing methods. Besides DON and FB1, other mycotoxins such as OTA, FB2, NIV, AFB1 and ZON have also been investigated in different combinations in grain and cereals. However, none of these literatures studied DON and FB1 co-contamination in grain. Our research provides a reliable sensing method for investigating these two mycotoxins in one grain sample simultaneously, and the application could be expanded to other mycotoxins/analytes.

5.1 Comparison of the performance of referenced and the present simultaneous detection methods for mycotoxins

Target mycotoxins	Sensor scheme	Working range	LOD	Food matrix	Reference
OTA, FB1	Magneto-controlled aptasensor	10 pg/mL-10 ng/Ml (OTA), 50 pg/mL-50 ng/Ml (FB1)	5 pg/mL (OTA), 20 pg/mL (FB1)	Maize	(Wang et al., 2017)
OTA, DON, AFB1	Metal sulfide quantum dots coated silica microfluidic + photoconductors coupled with fluorescence microscopy	-	100 ng/mL (OTA & DON), 3 ng/mL (AFB1)	-	(Soares et al., 2017)
FB1,FB2	Antibody modified gold electrode with chronoamperometry	1-1000 ng/mL	5 ng/mL	Corn	(Kadir & Tothill, 2010)
FB1, OTA	Microsphere linked indirect competitive fluid array		10-100 ng/g	Grains	(Anderson, Kowtha, & Taitt, 2010)
DON, ZON	Competitive inhibition immunoassay	-	10-17 ng/mL	Maize and wheat	(Dorokhin, Haasnoot, Franssen, Zuilhof, & Nielen, 2011)
DON, nivalenol (NIV)	Indirect competitive immunoassay, SPR	0.1 and 0.05mg/kg for NIV and DON	0.2 mg/kg (NIV), 0.1 mg/kg (DON)	wheat	(Kadota et al., 2010)
OTA, FB1	Competitive removal of DNA from photonic crystal array	0.01-1 ng/mL for OTA and 0.001-1 ng/mL for FB1	0.25 pg/mL for OTA and 0.16 pg/mL for FB1	Cereals	(Yue et al., 2014)
DON, FB1	Microfluidic and AuNPs enhanced ITO-based electrochemical immunosensor	0.2 to 60 ppb for DON and 0.3 to 140 ppb for FB1	35 pg/mL (DON) and 97 pg/mL (FB1)	Corn	Present work

5.3.7 Sensor application in spiked corn samples

After optimization of the detection methods in toxin-spiked buffer, this double working electrodes immunosensor was applied to toxin spiked ground corn samples to investigate the food matrix effects on sensor performance. The preparation of corn extract samples was slightly modified from previous methods used in Chapter 4.

The biggest challenge in simultaneously extracting multiple mycotoxins from spiked corn samples, is the incomplete extraction of these toxins, due to their very different chemical structures and properties. In addition, the extraction solvents themselves, and the extraction of various matrix components may seriously affect the sensing results. Compared to spiked corn samples in the lab, the real contaminated field corns may contain even more interfering components, which needs special attention during the extraction process. In our case, DON has a very polar chemical structure with three –OH substituents, thus very soluble in aqueous solutions. Water or phosphate buffer solutions are usually used for extracting DON from the food samples (Pascale, 2009). However, FB1 has a linear chemical structure containing an amino group and a few -COOH groups, requiring an organic solvent for extraction. A common extraction method is using a methanol and water mixture at 70:30 or 80:20 (v/v)(Ezquerra, Vidal, Bonel, & Castillo, 2015) Therefore, the extraction solvent of methanol/water (80:20 v/v) mixture was employed for FB1and DON extraction (Kolosova, Shim, Yang, Eremin, & Chung, 2005). Ground corn samples were first spiked with mycotoxins FB1 and DON mixtures (1:1 w/w) at different concentrations (each toxin at 50, 100, 200, 300 µg/kg respectively) and 5 g of the spiked sample was extracted in 25 mL extraction solution at room temperature with stirring for 15 min. The extraction was then centrifuged at 10,000 rpm for 5 min. The supernatant was carefully collected and 0.2 mL of the supernatant was taken and diluted for 10-fold using 1X

PBS buffer for antibody-toxin incubation. Table 5.2 shows the recovery rates of DON and FB1 from corn extracts tested by the immunosensor. The results demonstrate that the recovery rates fall in a range of 88.6-95.83% for FB1 and 82.4-95.75% for DON, which shows the feasibility of potential practical application of this sensor in complex food matrix.

Table 5.2 Recovery of FB1 and DON in spiked corn samples when tested using extracts.

Toxin	Spiked (µg/kg)	Measured (µg/kg)	RSD (%)	Recovery (%)
FB1, DON	50, 50	44.3, 41.2	5.42, 6.77	88.6, 82.4
	100, 100	89.9, 92.1	8.33, 4.27	89.9, 92.1
	200, 200	189.6, 191.5	5.12, 7.20	94.8, 95.75
	300, 300	287.5, 266.1	4.78, 6.29	95.83, 88.7

5.4 Conclusions

The goal for this study was to design a rapid and sensitive biosensor for simultaneous detection of multiple mycotoxins in one run, given the high co-occurrence rate of mycotoxins in food and feed materials. Towards this goal, this chapter describes the fabrication and evaluation of an electrochemical immunosensor on ITO-coated glass platform, with the aid of a microfluidic device for ultrasensitive, fast and simultaneous detection of mycotoxins FB1 and DON. Compared to the biosensor developed in previous chapters, we have further simplified the

working electrode functionalization procedure for the ITO-based electrodes while still maintaining high electrical conductivity (i.e., deposited only AuNPs and toxin-specific antibodies on the working electrode), which saves sensor preparation time as well as eliminates human errors during multiple preparation steps. Introduction of the microfluidic channel has provided a closed and controllable micro-environment for sample incubation and electrochemical detection, resulting in improved sensitivity and reproducibility of the biosensor. The microfluidic-integrated ITO electrochemical biosensor demonstrated excellent sensitivity and reproducibility for both mycotoxins being studied, as well as stability over two weeks of appropriate storage. Hence the developed biosensor has the potential to be applied in food safety monitoring, environmental hazards detection and even medical fields.

References

A Guide for Grain Elevators, Feed Manufacturers, Grain Processors and Exporters National Grain and Feed Association FDA Regulatory Guidance for Mycotoxins A Guide for Grain Elevators, Feed Manufacturers, Grain Processors and Exporters by National Grain and Feed Association. (2011).

Anderson, G. P., Kowtha, V. A., & Taitt, C. R. (2010). Detection of fumonisin b1 and ochratoxin a in grain products using microsphere-based fluid array immunoassays. *Toxins (Basel)*, *2*(2), 297–309. https://doi.org/10.3390/toxins2020297

Dorokhin, D., Haasnoot, W., Franssen, M. C. R., Zuilhof, H., & Nielen, M. W. F. (2011). Imaging surface plasmon resonance for multiplex microassay sensing of mycotoxins. *Analytical and Bioanalytical Chemistry*, *400*(9), 3005–3011. https://doi.org/10.1007/s00216-011-4973-8

Dors, G., Caldas, S., … V. F.-A., & 2011, undefined. (n.d.). Aflatoxins: Contamination, analysis and control. *Intechopen.com*. Retrieved from https://www.intechopen.com/download/pdf/20401

Eivazzadeh-Keihan, R., Pashazadeh, P., Hejazi, M., de la Guardia, M., & Mokhtarzadeh, A. (2017). Recent advances in Nanomaterial-mediated Bio and immune sensors for detection of aflatoxin in food products. *TrAC Trends in Analytical Chemistry*, *87*, 112–128. https://doi.org/10.1016/j.trac.2016.12.003

Fazekas, B., Tar, A., Kovács, M., & Kovacs, M. (2005). Aflatoxin and ochratoxin A content of spices in Hungary. *Food Addit Contam*, *22*(9), 856–863. https://doi.org/10.1080/02652030500198027

Foroud, N. A., & Eudes, F. (2009). Trichothecenes in Cereal Grains. *International Journal of Molecular Sciences*, *10*(1), 147–173. https://doi.org/10.3390/ijms10010147

Gelderblom, W. C., Marasas Wf Fau - Lebepe-Mazur, S., Lebepe-Mazur S Fau - Swanevelder, S., Swanevelder S Fau - Vessey, C. J., Vessey Cj Fau - Hall, P. de la M., Hall Pde, L., & Toxicology. (n.d.). Interaction of fumonisin B(1) and aflatoxin B(1) in a short-term carcinogenesis model in rat liver, (0300–483X (Print)).

Kadir, M. K. A., & Tothill, I. E. (2010). Development of an electrochemical immunosensor for fumonisins detection in foods. *Toxins*. https://doi.org/10.3390/toxins2040382

Kadota, T., Takezawa, Y., Hirano, S., Tajima, O., Maragos, C. M., Nakajima, T., … Sugita-Konishi, Y. (2010). Rapid detection of nivalenol and deoxynivalenol in wheat using surface plasmon resonance immunoassay. *Analytica Chimica Acta*, *673*(2), 173–178. https://doi.org/10.1016/J.ACA.2010.05.028

Li, Z. Z., Yu, Y., Li, Z. Z., & Wu, T. (2015). A review of biosensing techniques for detection of trace carcinogen contamination in food products. *Anal Bioanal Chem*, *407*(10), 2711–2726. https://doi.org/10.1007/s00216-015-8530-8

Marroquin-Cardona, A. G., Johnson, N. M., Phillips, T. D., & Hayes, A. W. (2014). Mycotoxins in a changing global environment--a review. *Food Chem Toxicol*, *69*, 220–230. https://doi.org/10.1016/j.fct.2014.04.025

Pohanka, M., Malir, F., Roubal, T., & Kuca, K. (2008). Detection of Aflatoxins in Capsicum Spice Using an Electrochemical Immunosensor. *Analytical Letters*, *41*(13), 2344–2353. https://doi.org/10.1080/00032710802350518

Raj, M. A., & John, S. A. (2013). Fabrication of Electrochemically Reduced Graphene Oxide Films on Glassy Carbon Electrode by Self-Assembly Method and Their Electrocatalytic Application. *The Journal of Physical Chemistry C*, *117*(8), 4326–4335. https://doi.org/10.1021/jp400066z

Ran, R., Wang, C., Han, Z., Wu, A., Zhang, D., & Shi, J. (2013). Determination of deoxynivalenol (DON) and its derivatives: Current status of analytical methods. *Food Control*, *34*(1), 138–148. https://doi.org/10.1016/j.foodcont.2013.04.026

Rhouati, A., Catanante, G., Nunes, G., Hayat, A., & Marty, J. L. (2016). Label-Free Aptasensors for the Detection of Mycotoxins. *Sensors (Basel)*, *16*(12). https://doi.org/10.3390/s16122178

Seenivasan, R., Singh, C. K., Warrick, J. W., Ahmad, N., & Gunasekaran, S. (2017). Microfluidic-integrated patterned ITO immunosensor for rapid detection of prostate-specific membrane antigen biomarker in prostate cancer. *Biosensors and Bioelectronics*. https://doi.org/10.1016/j.bios.2017.04.004

Sun, D.-D., Gu, X., Li, J.-G., Yao, T., & Dong, Y.-C. (2015). Quality evaluation of five commercial enzyme linked immunosorbent assay kits for detecting aflatoxin b1 in feedstuffs. *Asian-Australasian Journal of Animal Sciences*, *28*(5), 691–6. https://doi.org/10.5713/ajas.14.0868

Wang, C., Qian, J., An, K., Huang, X., Zhao, L., Liu, Q., … Wang, K. (2017). Magneto-controlled aptasensor for simultaneous electrochemical detection of dual mycotoxins in maize using metal sulfide quantum dots coated silica as labels. *Biosens Bioelectron*, *89*(Pt 2), 802–809. https://doi.org/10.1016/j.bios.2016.10.010

Yang, J., & Gunasekaran, S. (2013). Electrochemically reduced graphene oxide sheets for use in high performance supercapacitors. *Carbon*, *51*, 36–44. https://doi.org/10.1016/j.carbon.2012.08.003

Yi, C., Qi, S., Zhang, D., & Yang, M. (2010). Covalent conjugation of multi-walled carbon nanotubes with proteins. *Methods Mol Biol*, *625*, 9–17. https://doi.org/10.1007/978-1-60761-579-8_2

Yue, S., Jie, X., Wei, L., Bin, C., Dou Dou, W., Yi, Y., … Tiesong, Z. (2014). Simultaneous detection of ochratoxin a and fumonisin b1 in cereal samples using an aptamer-photonic crystal encoded suspension array. *Analytical Chemistry*, *86*(23), 11797–11802. https://doi.org/10.1021/ac503355n

Arino, A., Herrera, M., Juan, T., & Estopanan, G. (2009). Comparison of deoxynivalenol, ochratoxin A and aflatoxin B1 levels in conventional and organic durum semolina and the effect of milling. Journal of Food and Nutrition Research, 48(2), 92-99.

Birzele, B., Prange, A., & Kramer, J. (2000). Deoxynivalenol and ochratoxin A in German wheat and changes of level in relation to storage parameters. Food Additives and Contaminants, 17(12), 1027-1035.

Carina Maricel Pereyra, L. R. C., Stella Maris Chiacchiera, and Ana María Dalcero. (2010). Fungi and Mycotoxins in Feed Intended for Sows at Different Reproductive Stages in Argentina. Vet Med Int., 2010, 569108-569115. doi:10.4061/2010/569108

Castells, M., Marin, S., Sanchis, V., & Ramos, A. J. (2008). Distribution of fumonisins and aflatoxins in corn fractions during industrial cornflake processing. International Journal of Food Microbiology, 123(1-2), 81-87. doi:DOI 10.1016/j.ijfoodmicro.2007.12.001

Conkova, E., Laciakova, A., Styriak, I., Czerwiecki, L., & Wilczynska, G. (2006). Fungal contamination and the levels of mycotoxins (DON and OTA) in cereal samples from Poland and East Slovakia. Czech Journal of Food Sciences, 24(1), 33-40.

Eboku, A. N. K. a. D. (2010). Mould and Aflatoxin Contamination of Dried Cassava Chips in Eastern Uganda: Association with Traditional Processing and Storage Practices. Journal of Biological Sciences, 10(8), 718-729.

Hajjaji, A., El Otmani, M., Bouya, D., Bouseta, A., Mathieu, F., Collin, S., & Lebrihi, A. (2006). Occurrence of mycotoxins (ochratoxin A, deoxynivalenol) and toxigenic fungi in Moroccan wheat grains: impact of ecological factors on the growth and ochratoxin A production. Molecular Nutrition & Food Research, 50(6), 494-499. doi:10.1002/mnfr.200500196

Miller, J. D. (1992). Fungi as Contaminants in Indoor Air. Atmospheric Environment Part a-General Topics, 26(12), 2163-2172.

Muthomi, J. W., Ndung'u, J. K., Gathumbi, J. K., Mutitu, E. W., & Wagacha, J. M. (2008). The occurrence of Fusarium species and mycotoxins in Kenyan wheat. Crop Protection, 27(8), 1215-1219. doi:10.1016/j.cropro.2008.03.001

Pietri, A., Bertuzzi, T., Agosti, B., & Donadini, G. (2010). Transfer of aflatoxin B1 and fumonisin B1 from naturally contaminated raw materials to beer during an industrial brewing process. Food Additives and Contaminants Part a-Chemistry Analysis Control Exposure & Risk Assessment, 27(10), 1431-1439. doi:Doi 10.1080/19440049.2010.489912

Pii 923380521

Pietri, A., Zanetti, M., & Bertuzzi, T. (2009). Distribution of aflatoxins and fumonisins in dry-milled maize fractions. Food Additives and Contaminants Part a-Chemistry Analysis Control Exposure & Risk Assessment, 26(3), 372-380. doi:Doi 10.1080/02652030802441513

Pii 908706643

Soares, R. R., Santos, D. R., Chu, V., Azevedo, A. M., Aires-Barros, M. R., & Conde, J. P. (2017). A point-of-use microfluidic device with integrated photodetector array for immunoassay multiplexing: Detection of a panel of mycotoxins in multiple samples. Biosens Bioelectron, 87, 823-831. doi:10.1016/j.bios.2016.09.041

Sun, G., Wang, S., Hu, X., Su, J., Zhang, Y., Xie, Y., . . . Wang, J. S. (2011). Co-contamination of aflatoxin B-1 and fumonisin B-1 in food and human dietary exposure in three areas of China. Food Additives and Contaminants Part a-Chemistry Analysis Control Exposure & Risk Assessment, 28(4), 461-470. doi:Doi 10.1080/19440049.2010.544678

Theumer, M. G., Lopez, A. G., Aoki, M. P., Canepa, M. C., & Rubinstein, H. R. (2008). Subehronic mycotoxicoses in rats. Histopathological changes and modulation of the sphinganine to sphingosine (Sa/So) ratio imbalance induced by Fusarium verticillioides culture material, due to the coexistence of aflatoxin B1 in the diet. Food and Chemical Toxicology, 46(3), 967-977. doi:DOI 10.1016/j.fct.2007.10.041

Theumer, M. G., Lopez, A. G., Masih, D. T., Chulze, S. N., & Rubinstein, H. R. (2003). Immunobiological effects of AFB1 and AFB1-FB1 mixture in experimental subchronic mycotoxicoses in rats. Toxicology, 186(1-2), 159-170. doi:Pii S0300-483x(02)00603-0

WAREING, P. W., WESTBY, A., GIBBS, J.A., ALLOTEY, L.T. and HALM, M. (1998). Fungal and mycotoxin contamination of kokonte, a dried cassava product in Ghana. International Journal of Food Science and Technology, 34, 5082.

Yin, Y. L., Guan, S., Gong, M., Huang, R. L., Ruan, Z., Zhou, T., & Xie, M. Y. (2011). Occurrence of mycotoxins in feeds and feed ingredients in China. Journal of Food Agriculture & Environment, 9(2), 163-167.

CHAPTER 6 Conclusions and Future Work

6.1 Conclusions

In this dissertation, we have stated the need for effective sensing method for mycotoxins, followed by a detailed review with special focus on electrochemical immunosensors for the detection of mycotoxins. The general goal of the PhD work is to develop a rapid, sensitive, selective and affordable detection method for accurate monitoring of mycotoxins concentration in grain. Thus, we have investigated several designs of electrochemical immunosensors with the aid of nanomaterials and microfabrication. Three different electrochemical immunosensors incorporated with nanomaterials and microfluidic system were proposed and evaluated in terms of limit of detection, specificity, and stability when being applied to mycotoxin detection.

Various nanomaterials, including multiwalled CNT, GO and AuNPs were applied either individually or together onto the working electrode surface in order to create a 3D nanostructure surface with larger surface-to-volume ratio, as well as to improve the electrical conductivity.

Target-specific antibodies were used as binding agents to recognize and capture desired mycotoxins present in samples. These biosensors parameters were optimized to achieve good sensitivity.

In Chapter 3, we demonstrated a novel electrochemical immunosensor based on multiwall CNTs modified SPE for the detection of AFB1. The carbon nanomaterial modified working electrode demonstrated significantly improved surface characteristics and electron transferring ability, providing the basis for a good electrochemical biosensor. However, we discovered that the stability of the proposed sensor was poor.

In Chapter 4, to improve the stability and repeatability of the biosensor, we proposed a new working electrode surface modification strategy, the combination of a conducting polymer ppy and a nanomaterial GO. The pyrrole was electrochemically polymerized onto the electrode surface and GO was reduced electrochemically as well to turn it into a more conductive form. AuNPs were then drop-coated on the ppy-ErGO layers as the anchor sites for antibody immobilization. According to the results, electrode surface modified with this method has offered great repeatability and stability over two weeks.

In Chapter 5, we developed a sensor for multiple mycotoxins detection, while the single working electrode SPE used in previous chapters could not satisfy this need. Therefore, we proposed a new sensor platform, ITO-coated glass slide to serve as the sensing platform, which allows us to design our own multi-electrode pattern and print the design onto the ITO slide using photolithography technique. As ITO itself is an excellent electric conductive material, we simplified the electrode modification by using only AuNPs to produce the 3D nanostructure and to initiate the antibody immobilization step. The experimental outcome shows improved sensitivity and requires less reagent consumption, as well as a smaller amount of sample. The dual working electrode biosensor performed successfully in detecting FB1 and DON simultaneously, with little interference.

In summary, the results of this work have successfully fulfilled the goal of this dissertation, and could be used as reference for further developing and optimizing other biosensors targeting various analytes. This dissertation has also shown that electrochemical immunosensor incorporated with microfluidic devices can provide a noteworthy improvement toward the development of ultra- sensitive, selective and time effective sensing approaches that can be applied to multiple mycotoxins detection, as well as other potential chemical and

biological hazards. In addition, the knowledge obtained from the functionalization of the working electrodes provides some new insight into nanomaterial/biomolecule interactions.

6.2 Future research

Based on the results of this study, the suggested future work are as follows:

1. In this study, only two mycotoxins (FB1 and DON) were tested simultaneously with the dual working electrodes ITO sensor. In the future, more working electrodes could be added to the proposed ITO sensor platform, allowing for the detection of a large panel of multiple mycotoxins at the same time. This sensor could also be applied to a wide range of analytes with necessary parameter optimization, such as proteins, bacterial cells, cancer cells, biohazard molecules.
2. Based on our experience, the morphology and surface properties of the working electrode plays a significant role in determining the sensor performance. The interaction between nanomaterials, antibodies, analytes and possible interfering agents at the electrode-liquid interface in the tiny microfluidic channel could be more thoroughly investigated to gain a better understanding and control of the micro-environment, possibly bring the sensor performance to an advanced level.
3. Another future direction is to incorporate the proposed sensor into an automated system controlled by computer programs to minimize human operation, as well as eliminate human errors. One possible example is a smartphone-based portable sensing device for onsite detection and instant readout.

Appendix A

The following figures and table are supplementary data as described in the captions. They are related to the experiments and discussion, but are not essential to understanding of the main ideas of the research.

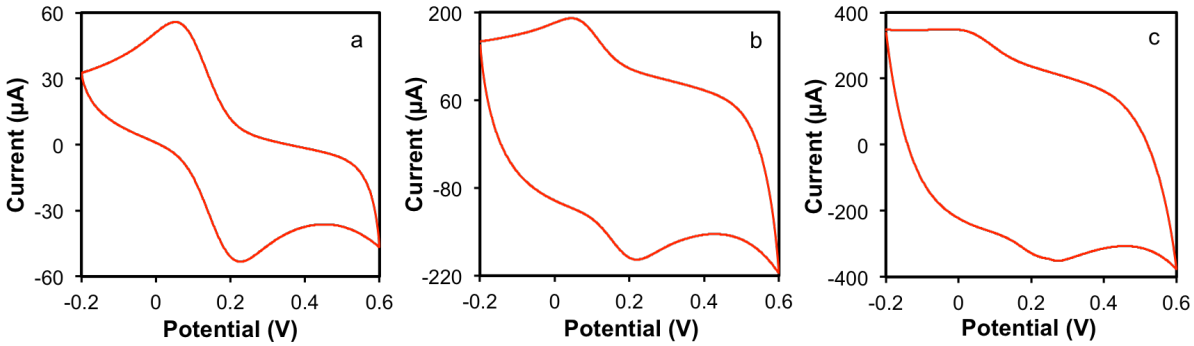

Figure A 1 CV responses of 5 mM $[Fe(CN)_6]^{3-/4-}$ in 1 M KCl at PPy/GO electrochemically deposited on SPE at pyrrole concentrations of (a) 0.025 M, (b) 0.05 M and (c) 0.1 M. GO concentration=0.33 mg/mL; KCl concentration =0.1 M

. Figure A1 is related to Chapter 4. It shows the CV responses of 5 mM $[Fe(CN)_6]^{3-/4-}$ in 1 M KCl at SPEs after PPy/GO electrochemical deposition using three different pyrrole concentrations (0.025, 0.05, 0.1 M) with fixed concentration of 0.33 mg/mL GO and 0.1 M KCl. In Figure A1 (a), CV results clearly show PPy/GO film modified SPE with 0.025 M pyrrole concentration gives the characteristic well-defined sharp cathodic and anodic peaks with 160 mV peak separations, which indicates very efficient electron transfer reaction between the electrolyte and the electrode surface. But, with increased pyrrole concentration 0.05 M and 0.1 M, the CV shows less sharp peaks and greater peak separation of 170 mV in 0.05 M pyrrole (Figure A1 (b)) and broad peaks in 0.1 M pyrrole (Figure A1 (c)), which demonstrates poor electron transfer

between the electrolyte and the electrode surface. Hence, the 0.025 M pyrrole was determined as optimal level.

Figure A 2 Photo of carboxylated CNT dispersed in water

Figure A2 is realted to Chapter 3, it shows the actual photo of well dispersed CNT after carboxylation.

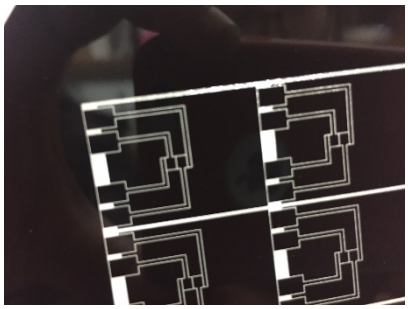

Figure A 3 Photo of patterned double -working electrode system on ITO coated glass

Figure A3 is related to Chapter 5, it shows the actual photo of four identical fabricated ITO electrode system with double –working electrode.

Table A 1. Zeta potential of PDDA solution and Citrate reduced AuNPs solution. The zeta potential value is mean of five runs.

	Zeta potential (mV)	Standard error
PDDA	23.79	3.75
Citrate-AuNPs	-37.36	8.14

Table A1 is related to the electrode modification section in Chapter 3. The conducting polymer PDDA is positively charged in solution, while the sodium citrate reduced AuNPs solution is negatively charged. The modified materials are electrostatically attracted by each other on electrode surface.